PNNL-26631

Pacific Northwest
National Laboratory
Operated by Battelle for the
U.S. Department of Energy

Technical Letter Report

Low-Frequency/SAFT-UT Data Fusion: Development and Evaluation of the Multi-Parameter Analysis Tool Set (MPATS)

PNNL Project No. 43565
JCN Y6604

A. A. Diaz
G. J. Schuster
S. L. Crawford
K. M. Judd
S. R. Doctor

December 2003

Prepared for the U.S. Department of Energy
under Contract DE-AC05-76RL01830

DISCLAIMER

PACIFIC NORTHWEST NATIONAL LABORATORY
operated by
BATTELLE
for the
UNITED STATES DEPARTMENT OF ENERGY
under Contract DE-AC05-76RL01830

Printed in the United States of America

Available to DOE and DOE contractors from the
Office of Scientific and Technical Information,
P.O. Box 62, Oak Ridge, TN 37831-0062;
ph: (865) 576-8401
fax: (865) 576-5728
email: reports@adonis.osti.gov

Available to the public from the National Technical Information Service,
U.S. Department of Commerce, 5285 Port Royal Rd., Springfield, VA 22161
ph: (800) 553-6847
fax: (703) 605-6900
email: orders@ntis.fedworld.gov
online ordering: http://www.ntis.gov/ordering.htm


This document was printed on recycled paper.
(9/2003)

PNNL-26631

Technical Letter Report

Low-Frequency/SAFT-UT Data Fusion: Development and Evaluation of the Multi-Parameter Analysis Tool Set (MPATS)

PNNL Project No. 43565
JCN Y6604

A. A. Diaz
G. J. Schuster
S. L. Crawford
K. M. Judd
S. R. Doctor

December 2003

Prepared for
the U.S. Department of Energy
under Contract DE-AC05-76RL01830

Pacific Northwest National Laboratory
Richland, Washington 99352

Abstract

This technical letter report documents work performed at the Pacific Northwest National Laboratory (PNNL) in Richland, Washington, for development and evaluation of a data fusion methodology for enhancement of data analysis procedures when using a multi-angle, multi-frequency inspection protocol for coarse-grained steel components.

The data acquisition technique uses a zone-focused, multi-incident angle, low-frequency (250–450 kHz) inspection protocol coupled with the synthetic aperture focusing technique (SAFT). The primary focus for development of this inspection technique is to provide information to the United States Nuclear Regulatory Commission on the utility, effectiveness, and reliability of the low-frequency/SAFT method as related to the in-service ultrasonic inspection of coarse-grained primary piping components in light water reactors. Acquisition of ultrasonic data from both sides of a weld, using multiple inspection angles and a variety of examination frequencies, results in the production of multiple data sets for post-processing, analysis, and determination of a final-call assessment from the data. Prior to the work described here, the analysis protocol was very time-consuming, costly, and technically challenging for the operator. PNNL has focused on obtaining improved consistency in results from data analysis and enhancing the ability to more effectively and reliably discriminate between the ultrasonic responses from grain boundaries versus cracks by using advanced analysis software based on interactive tools.

The work described here addresses an NRC Operating Plan (OP) Milestone that is defined as:

> Using the existing expertise with SAFT-UT and other work to date at PNNL to enhance techniques and methods that would allow for consistent and reliable discrimination between coherent ultrasonic energy scattered from grain boundaries versus that from cracks in coarse-grained steel components and further enhance the SAFT-UT software so that its data analysis is both timely and economical.

This report describes PNNL's multi-phased approach to meet this deliverable by focusing on development/testing of software analysis tools, and quantifying the performance of the software tools on actual low-frequency/SAFT data acquired from coarse-grained cast stainless steel components. This report describes the Multi-Parameter Analysis Tool Set (MPATS), its capabilities and functionality, and illustrates the software's flexibility, utility, time savings, and ease-of-use for addressing the challenges associated with the previous analysis protocol. The interactive capabilities and enhanced functionality of the MPATS is based on PV-Wave™ software for data analysis and fusion operations. PV-Wave is a 3D data analysis platform and has many signal and imaging processing functions built in. It is well-suited for the analysis operations required, and is shown here to provide a streamlined and powerful foundation for the development of MPATS for enhanced discrimination and crack identification in coarse-grained material.

As a result of this early work, PNNL identified the interactive capabilities of a PV-Wave software platform for building the software data analysis and fusion tools. PV-Wave is a 3D data analysis tool and has many signal and imaging processing functions built in. It was deemed better suited for data processing than Excel. Data from previous field work at EPRI was used to evaluate and refine the crack identification criteria, and were used for testing and developing the software and analysis tools. A working version of the enhanced data analysis software package was completed in early December 2003, and subsequently tested in a semi-blind fashion.

The scope of this activity focused on five primary tasks:

1. Literature review and development of software requirements document

2. Development and testing of software and analysis tools
3. Identification and utilization of previously acquired ultrasonic data from EPRI field tests for development and testing purposes
4. Quantification and software performance evaluation activities
5. Final documentation and technical letter report to NRC on status and progress.

For this effort, the PNNL team ranked and prioritized the work described here in order to focus on the most significant tools and criteria for applying the software in a meaningful way and for quantification of the MPATS software performance to meet the objectives of the OP milestone.

Acknowledgments

The work reported here was conducted and written under JCN Y6604, with technical guidance provided by Ms. Deborah Jackson, the NRC Project Monitor. Ms. Jackson's technical support and guidance in the direction of this development effort are very much appreciated. The quantification activities for this work were generated using low-frequency/SAFT data acquired at the EPRI NDE Center in 1997, and our thanks again are directed to Ms. Jackson and Mr. Harold Gray (U.S. NRC) for their participation in these activities.

PNNL staff would also like to thank the EPRI NDE Center in Charlotte, North Carolina, for the opportunity to work with EPRI staff members who demonstrated their hospitality and technical support throughout data acquisition activities in 1997. We thank Mr. Stan Walker, Mr. Steve Kenefick, Mr. Jeff Landrum, Mr. F. Larry Becker, and Dr. Doug MacDonald.

At PNNL, the authors wish to thank Mrs. Earlene Prickett and Mrs. Pamela Kinsey for their secretarial and clerical support, advice, and assistance in producing this technical letter report.

Acronyms, Abbreviations, and Glossary

A/D	analog-to-digital
CCSS	centrifugally cast stainless steel
CSS	cast stainless steel
dB	decibel
DMW	dissimilar metal weld
EPRI	Electric Power Research Institute
FY	fiscal year
GHz	gigohertz
Hz	hertz
ID	inner diameter
ISI	in-service inspection
kHz	kilohertz
LF/SAFT	low-frequency/SAFT
LF	low frequency
L-wave	longitudinal wave
LWRs	light water reactors
MHz	megahertz
MPATS	Multi-Parameter Analysis Tool Set
NRC	U.S. Nuclear Regulatory Commission
OD	outer diameter
OP	Operating Plan
PC	personal computer
PNNL	Pacific Northwest National Laboratory
POD	probability of detection
PWRs	pressurized water reactors
RF	radio frequency
SAA	signal amplitude anomaly
SAFT	synthetic aperture focusing technique
SCSS	statically cast stainless steel
SR	software requirements
UT	ultrasonic testing
WOG	Westinghouse Owner's Group

Hanning window: The Hanning window is the first half of a cosine – in other words, only the positive cosine values.

radio buttons: A computer science term that identifies a standard type of windows control. A set of radio buttons provides a mutually exclusive selection of pre-established options.

skeleton: An image processing term that is defined as a line along the points that are equi-distant from the edges of a region in the image.

vertical kernel: An image processing term that is defined as a small matrix used to transform an input image by convolution into an output image.

Contents

Figures

Tables

1.0 Introduction

In order to address a U.S. Nuclear Regulatory Commission (NRC) Operating Plan (OP) milestone, the Pacific Northwest National Laboratory (PNNL) is submitting this technical letter report documenting work conducted in fiscal year (FY) 03. The work reported here directly addresses the scope and deliverable as defined in the OP milestone below:

> Using the existing expertise with SAFT-UT and other work to date at PNNL to enhance techniques and methods that would allow for consistent and reliable discrimination between coherent ultrasonic energy scattered from grain boundaries versus that from cracks in coarse-grained steel components and further enhance the SAFT-UT software so that its data analysis is both timely and economical.
> Milestone Due: December 31, 2003

This technical letter report documents work performed by PNNL in Richland, Washington, for development and evaluation of a data fusion methodology to enhance data analysis procedures when using a multi-angle, multi-frequency inspection protocol for coarse-grained steel components. In particular, PNNL is developing and evaluating a low-frequency ultrasonic inspection method coupled with an advanced signal processing technique for improved detection, localization, and sizing of cracks in primary loop reactor piping components fabricated from centrifugally cast and statically cast stainless steels. This inspection and analysis process should work equally well for addressing other coarse-grained inspection problems.

The underlying inspection problem is multi-faceted. The low cost and relative corrosion resistance of cast stainless steels (CSS) have resulted in extensive use of this material in the primary piping systems of light water reactors (LWRs). In-service inspection (ISI) requirements dictate that piping welds in the primary pressure boundary of LWRs be subject to a volumetric examination based on the requirements of Section XI of the ASME Boiler and Pressure Vessel Code. The volumetric examination may be either radiographic or ultrasonic. For in-service examinations, background radiation and access limitations generally prevent the use of radiography. Hence, cast austenitic welds in primary piping loops of LWRs are subject to ultrasonic ISI. The purpose of ultrasonic in-service inspection (UT/ISI) of nuclear reactor piping and pressure vessels is the reliable detection and accurate sizing of any material degradation. Before defects can be sized, they must first be detected. This is typically accomplished by analyzing ultrasonic echo waveforms from material anomalies. Due to the coarse microstructure of CSS material, many inspection problems exist and are common to structures such as corrosion-resistant cladded pipe, statically cast elbows, statically cast pump bowls, centrifugally cast stainless steel (CCSS) piping, dissimilar metal welds (DMWs), and weld-overlay-repaired pipe joints. Far-side weld inspection of stainless steels is an inspection technique included in the work scope since the ultrasonic field passes through weld material.

Because CCSS piping is used in the primary reactor coolant loop piping of 27 pressurized water reactors (PWRs) manufactured by the Westinghouse Electric Corporation, there exists a need to develop effective and reliable inspection techniques for these components. CCSS inspection procedures continue to perform unsatisfactorily due to the coarse microstructure that characterizes these materials. The major microstructural classifications are columnar, equiaxed, and a mixed columnar-equiaxed microstructure of which the majority of field material is believed to be the latter.

CCSS is an anisotropic and nonhomogeneous material. The manufacturing process can result in the formation of a long columnar grain structure (approximately normal to the surface) with grain growth oriented along the direction of heat dissipation, often several centimeters in length. During the

solidification of the material, columnar, equiaxed (randomly speckled microstructure), or a mixed or layered structure can result depending on chemical content and control of the cooling process (Diaz et al. 1998, NUREG/CR-6594).

The large size of the anisotropic grains, relative to the acoustic pulse wavelength, strongly affects the propagation of ultrasound by causing severe attenuation, changes in velocity, and scattering of ultrasonic energy. Refraction and reflection of the sound beam occurs at the grain boundaries resulting in defects being incorrectly reported, specific volumes of material not being examined, or both. When coherent reflection and scattering of the sound beam occurs at grain boundaries, ultrasonic indications occur which are difficult to distinguish from signals originating from flaws. When inspecting pipe sections, where the signal-to-noise ratio is relatively low, ultrasonic examinations can be confusing, unpredictable, and unreliable.

Over the past 8 years, PNNL has embarked on the development of a more direct inspection approach that is inherently less sensitive to the effects of the material structure and weldment geometry, and more effective at discriminating cracks from other signal responses. The inspection technique uses a zone-focused low-frequency (250–450 kHz) inspection protocol coupled with the synthetic aperture focusing technique (SAFT). Although laboratory and field trials have provided promising results with regard to localization and detection capabilities in these materials, the procedures required for effective analysis of the data are very time-consuming and labor-intensive. The inspection procedures result in the acquisition of multiple ultrasonic data sets as a function of inspection angle, examination frequency, and the scan direction relative to the weld. The large volume of data is difficult to manage and challenging to analyze, as the various steps required to SAFT process the data files, study the ultrasonic responses, and determine the comprehensive meaning between the various data sets can be very challenging. Hence, there is a need to develop and test a set of software tools for effective data fusion and improved analytical capabilities that reduce the time for analysis, improves consistency of the process, and enhances the ability to discriminate between ultrasonic responses from material structure (grain boundaries, etc.) and cracks.

In a general sense, the data analysis protocol utilizes multiple data sets for crack identification, localization, and sizing. The analysis technique is based on redundancy of the ultrasonic indications as a function of the various inspection parameters. Scans are performed at various angles and frequencies and, when possible, from both sides of the weld. Data sets are then post-processed using the synthetic aperture focusing technique. SAFT-processed data sets are then properly projected and the resultant full-volume focused image provides a visual platform for ultrasonic characterization or mapping of the inspected area.

Prior to the present effort, each scan was separately analyzed for indications. Each indication was given a start and stop pair of (x, y) coordinates related to outer diameter (OD) positional data on the component under test. These coordinates were manually entered into an Excel™ spreadsheet. The different scans were placed in different columns so that Excel could automatically assign colors and symbols to the respective data sets (scans). The multiple indications from these data sets (scans) were then manually superimposed (essentially overlaid) on top of one another in Excel, and the plots were examined visually to determine what indications appeared to recur most often, which (if any) were geometrical features, and which seem to be attributed to grain noise or other irrelevant indications, based on a well-defined set of criteria (discussed later in more detail). The most likely cluster (using elementary positional averaging and redundancy) was used to determine the crack location. In some cases an arithmetic average of the endpoints and distance from the weld centerline were used; in other cases, a visual estimate was used; this had the advantage of allowing the inspector to assign (implicit) weights to the data sets. Finally, a single composite data set was formulated from the data acquired from the multiple scans, and a call was made on the component under examination.

1.1 General Objectives, Scope, and Technical Challenges

The work conducted to date using the low-frequency/SAFT (LF/SAFT) inspection technique demonstrated the potential for useful crack detection in CSS and DMW materials. Results have demonstrated an improved probability of detection (POD) for fatigue cracking (of larger dimensions) in coarse-grained stainless steels. Utilization of this technique in the field has provided positive results with respect to detection, localization, and length sizing. However, these results do not represent data from a statistically large number of field-representative CSS specimens. To date, approximately 20 CSS specimens (PNNL and EPRI-WOG [Electric Power Research Institute-Westinghouse Owner's Group] specimens) have been examined using this inspection protocol.

Presently, the LF/SAFT technique allows for discrimination of cracks from other features based on a set of crack identification and detection criteria. In order to test and validate this criteria, there still exists a need for additional baseline measurements on coarse-grained specimens with large areas of uncracked weld material. This baseline data is necessary due to the extreme variability in sound transmission through different microstructures, making it difficult to establish amplitude-based criteria. Testing and validation of this criteria will require inspection of many more specimens, including base material with no cracking present, and recording amplitudes and indication characteristics from geometric and crack-like reflectors. Target motion criteria are difficult to use because of the low resolution at sub-megahertz (MHz) frequencies. The implementation to date for the analysis method for combining data from different angles, frequencies, and directions is relatively crude. The current effort reported here focuses on implementing a semi-automated analysis method for combining these data sets in a reliable and consistent fashion. The new software and interactive toolset developed here provides a means for more effectively combining data sets taken at multiple angles and frequencies and is called a multi-parameter analysis tool set (MPATS). The interactive toolset developed during FY03 and described here illustrates the advantages of using PNNL's existing data acquisition and analysis software, and also addresses the difficult challenges of proper registration between multiple data sets. Further testing and refinement of the crack identification criteria for eliminating the geometric reflections (based on variation of amplitude as a function of angle and frequency) so that cracks can be more reliably detected, is planned for future work.

The previous data fusion analysis process is too time-intensive and requires automation in order to provide an analysis that is reliable, less time-consuming, and easier to use. Issues of accurate registration (positionally) between data sets, overlaying and fusion of multiple data sets, and interactive application of specific criteria have been addressed as part of this effort. The crack identification criteria needs to be refined and validated through testing, which can only happen if the technique is applied to a wider array of CSS and DMW components where large areas of welded material and parent material (preferably without cracking) are scanned and the criteria is applied for testing its robustness. In this manner, the criteria can be evaluated and evolved to more effectively discriminate the indications that arise solely due to the microstructures encountered and geometrical reflectors associated with typical weldment structure.

Precise transducer positioning and geometric analysis are very important in a successful multi-scan analysis. The PNNL analysis protocol uses OD distances (not inner diameter [ID]) to match up positions from the two sides of the weld for localization of responses in the specimen. Although beam skew may contribute to alignment and positional error, the application of lower frequencies (longer wavelengths) should help reduce these effects. One key element for improving the efficiency of the data analysis protocol is the need to improve the ease of use of the data fusion analysis tools.

The scope of the current effort was addressed through a multi-phased approach, where staff focused on defining the software requirements, developing and testing MPATS software and analysis tools, and quantifying the performance of the tools using data acquired at the EPRI NDE Center during field exercises in 1997. This in turn allowed staff to review and test the crack identification criteria from a

semi-automated perspective through the use of interactive software tools, and to compare and contrast the detection, localization, and sizing results with manually derived results from 1997 and true-state data. In order to provide an analysis platform that is more flexible, powerful, less time-consuming, and easier to use, PNNL staff reviewed the literature to identify the most effective methods for multi-parameter data analysis. A software requirements (SR) document that defines the present state and future enhancements of the software, capabilities, functionality, and user requirements for the end-product was generated. The SR document defined specific performance features and characteristics of the software and analysis tools, and was presented to the NRC for agreement/concurrence prior to the start of the MPATS software development tasks. This document was used as the guide for conducting the developmental software work for the past year.

The primary objective of the MPATS software and data fusion effort was to develop a set of software tools that simplifies the analysis process and enhances the inspector's ability to apply the composite approach inherent in the multi-scan-angle-frequency analyses.

This technical letter report is organized in the following fashion. Section 2.0 describes the low-frequency/SAFT inspection technique and includes information about the detection system used for data acquisition and analysis. This section also describes the analytical approach used for discrimination of signal responses from cracks versus microstructure or weld geometry, including a detailed description of the crack identification and detection criteria. Section 3.0 describes the software development approach and discusses the technical roadmap for development of the MPATS software. Section 4.0 provides a physical description of the piping specimens used for development, testing, and evaluation of the MPATS software, including true-state data for each. Section 5.0 provides a detailed description of the MPATS functionality and capabilities and defines the various tools that comprise the MPATS software. Section 6.0 describes the evaluation and assessment phase of the MPATS software, and includes results of a quantification activity for assessment of the MPATS software performance. Section 7.0 contains the conclusions resulting from this effort, and Section 8.0 provides a discussion of recommendations for future work. Section 9.0 lists the references cited in this report.

2.0 Low-Frequency/SAFT Ultrasonic Inspection Methodology

2.1 LF/SAFT Inspection System

The low-frequency/SAFT mobile inspection system is an automated, computerized, ultrasonic imaging system designed and developed by PNNL for inspecting thick section, coarse-grained steel components in nuclear reactors (Diaz et al. 1998). This system, shown in Figure 2.1 and developed for the NRC, is a field-tested system, consisting of several subsystems and components.

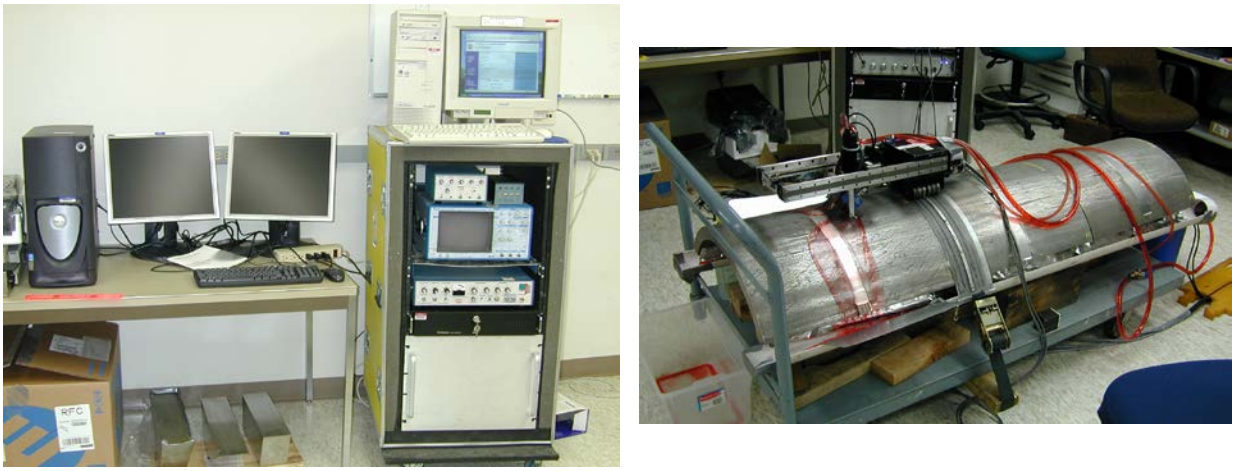

Figure 2.1. The Low-Frequency/SAFT Ultrasonic Data Acquisition System

The Panametrics pulser module is a high-voltage model 5058 pulser-receiver unit that produces high-voltage spike pulses for broadband excitation of the transducer. This unit provides damping control, step attenuation and gain control, high-pass and low-pass filtering options, and a variable pulse voltage control of up to 900 volts. This unit provides the capability to exploit the high bandwidth of custom-designed transducers and allow utility of examination frequencies in the range of 250 kHz to 450 kHz. This unit also includes an embedded dual-stage receiver that consists of a low-frequency, low-noise preamplifier in series with a high-performance, 60 decibel (dB) low-noise amplifier for conditioning and amplification of the received ultrasonic testing (UT) signal responses. A stand-alone 866 MHz personal computer (PC) contained in this subsystem takes on the role of data acquisition control, where the operator invokes the LF/SAFT scanning software menus and adjusts the scanning parameters prior to initiating a scan. The analog-to-digital (A/D) converter resides on this PC, which also controls the motor drivers and pipe scanner. This computer is directly connected to the data analysis PC. Unprocessed ultrasonic data streams from the control PC to the data analysis PC where it resides for SAFT post-processing, analysis, and archival. The data processing and storage subsystem performs SAFT processing of the raw (unprocessed) UT data using a Dell Precision 650 high-performance PC with dual high-speed processors (2.4 GHz each). This PC platform contains both read/write CD and DVD drives for storage of digital data. This PC also contains two flat-panel 19-inch monitors for displaying the SAFT-UT processed data (A-scans, B-scans, C-scans, and D-scans). The photographs in Figure 2.1 illustrate the LF /SAFT inspection system in its present configuration.

The LF/SAFT inspection system is equipped to acquire ultrasonic data efficiently and rapidly, under low noise conditions, for sectioned pipe segments or in-field piping components using a field-ready automated pipe scanner. The automated pipe scanner is employed for accurate and smooth continuous scanning of the search unit through a specified number of points in the X-Y plane, while maintaining low noise

conditions and a constant couple of the transducer to the surface. The pipe scanner is configured with tailored gimbals for transducer attachment and translation over the surface of the component. A network of specially fabricated drip lines attached to a couplant reservoir with a peristaltic pump is used to provide a constant stream of water on the specimen surface for improved coupling and transducer motion.

The LF/SAFT system's 866 MHz control PC contains the A/D converter used to sample (digitize) the data. The motor controller electronics initialize a trigger output to the A/D and pulser-receiver unit, which in turn, was used to sync the remaining instrumentation. The received signal responses (echoes) are initially amplified by a low noise, LF, ultrasonic preamplifier, and then bandpass filtered using the Panametrics 5058 in order to allow suitable amplification while reducing extraneous LF noise components under 100 kHz and higher frequency noise components over 500 kHz.

The preamplified and conditioned signal responses are then amplified by the second stage wideband Panametrics 5058 amplifier and sent to the control PC's A/D for sampling. All signals (excitation pulses and received signal responses) are monitored using a LeCroy 9450 digital oscilloscope, providing the capability to view the trigger and sync pulses, the excitation pulse before and after amplification, and the received signal response just prior to digitization. The LeCroy oscilloscope also provides linear averaging, and the capability to analyze the frequency characteristics of the A-scan data. A linear averaging scheme can be implemented with the radio frequency (RF) ultrasonic A-scan data using the SAFT acquisition software to minimize the effects of motor noise and random electronic noise, and increase the unprocessed signal-to-noise ratio. The data acquisition system is capable of acquiring low-frequency, low noise, ultrasonic data with a total system gain ranging from 0 dB to 100 dB.

After storage of the RF ultrasonic data sets to CD media, the data is signal processed using SAFT. The raw data sets are post-processed using a variety of beam processing angles, ranging from 6° to 24°. The SAFT software provides the user the capability to view the entire ultrasonic data set (3D array of points) in two-dimensional slices, by viewing color enhanced composite images that depict slices of the three-dimensional array in the X-Y plane (C-scan view), the Y-Z plane (B-scan end-view or D-scan view) and X-Z plane (B-scan side view). The X-axis defines the axis of motion for translation of the transducer, perpendicular to the circumferential weld axis. The Y-axis defines the translation of the transducer in the circumferential direction, parallel to the centerline of the weld. The Z-axis defines the depth into the specimen from the contacting top surface of the specimen, and is correlated to the time-of-flight data.

2.2 Data Analysis and Crack Detection Process

The analytical protocol for crack detection and discrimination is based on the premise that there exist sufficient differences between the characteristics of coherently scattered ultrasonic energy from grain boundaries and geometrical reflectors and the scattered ultrasonic energy from ID surface-breaking thermal and mechanical fatigue cracks in coarse-grained steels. PNNL's empirical approach relies on the physical acoustics that acoustic impedance variations at the grain boundaries can be reduced by using lower frequencies (longer wavelengths), and the degree of coherent energy scattered from these grain boundaries should be different as a function of frequency, insonification angle, scan direction, and the amplitude of returning signals. The LF/SAFT approach is directed toward detecting the corner-trap response from the surface-breaking crack as a function of time and spatial position. If the frequency is low enough, the examination is less sensitive to the effects of the microstructure and the POD increases for surface-breaking cracks. The tradeoff is resolution. However, with the addition of SAFT signal processing, the examination can be performed at low frequencies while maintaining the capability to detect cracks approximately 35% deep or greater in typical CSS piping components. Therefore, by utilizing multiple examination frequencies and incident angles, and inspecting from both sides of a weld,

the low-frequency/SAFT technique invokes a composite approach for detection, localization, and sizing of cracks in CSS material.

The examination process is further enhanced by the addition of a low-frequency, variable angle, high bandwidth search unit which enables the inspector to compensate for acoustic velocity variations due to the microstructure by selecting the optimal incident angle in the material under test. The high bandwidth allows the inspector to utilize a wide range of examination frequencies centered about 350 kHz. The zone-focal characteristics of the dual-element search unit provide optimal insonification of the inner surface (ID) over a specified range of incident angles.

The inspection system is configured to accommodate data acquisition for a variety of component geometries and sizes, including:

- Pipe to pipe sections
- Pipe to elbow sections
- Outlet nozzle to safe end to elbow sections
- Outlet nozzle to pipe
- Inlet nozzle to elbow
- Inlet nozzle to pipe
- Pipe to safe end to reactor pressure vessel outlet nozzle sections
- Pipe to safe end to reactor pressure vessel inlet nozzle sections
- DMW sections
- Calibration standards

Each weld is examined using the following orientations (where access permits):

- 0° longitudinal wave (L-wave), 350 kHz for back surface profiling over the entire weld area
- 30° L-wave, 250, 350, and 450 kHz both near and far-side scanning
- 45° L-wave, 250, 350, and 450 kHz both near and far-side scanning
- 60° L-wave, 250, 350, and 450 kHz both near and far-side scanning

Therefore, assuming the full complement of scans can be achieved, 19 full scans may be conducted per weld, unless the component geometry, weld crown, or surface area precludes the use of specific incident angles.

The analysis is focused on detailed criteria for identifying or rejecting regions as cracked in the material, where ultrasonic signal amplitude anomalies (SAAs) occur. These criteria are based on acquiring some combination of redundancy in the ultrasonic data as a function of the various inspection parameters which include: examination incident angle, driving frequency of the transducer, and scan direction. Based on the PNNL research to date, there are nine specific criteria that the data analyst or automated software platform must consider during the evaluation process, and these are described below. The diagram in Figure 2.2 illustrates the examination volume of interest for crack identification as it relates to component geometry.

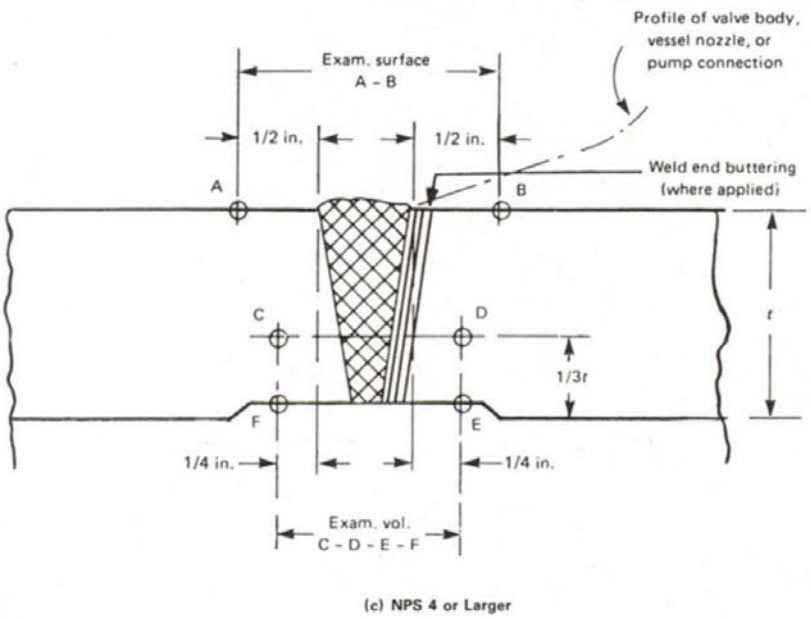

Figure 2.2. Illustration Defining the Examination Volume. Reprinted from ASME 2001 Edition, Section XI, by permission of The American Society of Mechanical Engineers. All rights reserved..

1. SAAs occurring in the volumetric space between the top edges of the two counterbore slopes will be fully examined. SAAs occurring outside of this region will not be examined. This is due primarily to the high-amplitude signal returns scattered from counterbore geometry effectively masking any cracking that may exist in this area.
2. If the full complement of inspection angles were used in the examination (0°, 30°, 45°, and 60°), coinciding SAAs ***should*** occur from at least one inspection angle from both sides of the weld, in order for the indication to be further considered as evidence of cracking. Exceptions may be made to this, if for instance strong SAAs are evident from only one side due to unusual material or surface conditions on the adjacent side precluding the acquisition of useable data.
3. If the full complement of inspection angles were used in the examination, coinciding SAAs ***must*** occur at more than one examination frequency, or more than one examination incident angle, or more than one scan direction (from data acquired from the other side of the weld), or some combination thereof, in order to establish a degree of redundancy that allows the inspection analyst to determine whether or not the SAA is evidence of cracking.
4. SAAs may occur above, on, or below the back-surface line appearing on the SAFT images. Differences in position of ±1.27 cm (±0.5 in.) above or below this line are not significant, and SAA position will be measured from the peak amplitude point. When a SAA occurs in this region, its tail will be included in the boxed examination region of the image. When the back-surface line is positioned accurately, corner trap signal returns from cracking in the material will result in SAAs that lie just on the back-surface line, with the majority of the SAA below the line. The accuracy of the back-surface line is a function of the material velocity and transducer delay, and the actual position of a SAA relative to this line is a function of incident angle, acoustic velocity, frequency, wavelength, and zone focal dimensions of the transducer. Due to the fact that material velocity varies with spatial position and incident angle in the material, inaccuracies must be allowed for. The 0° data acquired from both sides of the weld is used to determine ID surface contouring, and nominal wall thickness data is used to substantiate the ultrasonic data on the SAFT images. Depending on the differences

between the nominal wall thickness data and the 0° ultrasonic profiling data, the actual z-axis dimension of the volume boxed for examination can range up to 3.81cm (1.5 in.) in total length.

5. SAAs ***should*** have some degree of characteristic shape (either circular or elliptical) to them, with somewhat smooth contours on their edges, as opposed to random, blotchy, scattered amplitude blips that appear with little symmetry and rough contours. Also, SAAs ***should*** have reasonable and proper orientation with respect to the examination incident angle of the insonifying beam. A perpendicular orientation is normal.
6. SAAs occurring very near the edge of the material under test (especially in the case of curved pipe sections) will be discounted due to edge scattering effects. The side wall of the pipe section acts as a mirror to reflect more energy back to the receive element than would normally occur if no edge existed. This can be minimized by starting the transducer at a point on the pipe OD surface where no overlap exists between the transducer face and the edge of the pipe, but this effectively decreases the width of the scan on the ID surface.
7. Differences in lateral position of ±1.27 cm (±0.5 in.) or less are not significant, except at a single examination incident angle with multiple frequencies.
8. Length and depth sizing will be performed from the most continuous SAFT processed image where the signal-to-noise ratio is high, if a data file of this nature exists; however, in most cases, the composite data will be plotted using spreadsheet analysis and data resolution of 2.54 mm (0.1 in.) in the x- and y-axes. If tip signal returns exist, depth measurements will be made using the most continuous SAFT processed image. In the case of length sizing and localization (positioning), the −3 dB points will be used to “clip” the data from the background noise, and the data points will be extracted from the SAFT images and plotted on a spreadsheet. Generally, the accuracy of length sizing and crack positioning will be ±1.27 cm (±0.5 in.) in both circumferential and axial directions. If one data file exhibits a strong signal-to-noise ratio, and the SAA of interest is coincident in other scans, this data file may be used for location and sizing; however, in general when no single data file can be judged to exhibit these characteristics, the composite data will be plotted, and the data will be averaged graphically in order to determine location and size.
9. The analysis protocol will provide sizing and location data that is referenced to the OD surface dimensions, and will compensate for transducer overlap and nominal beam position in the material.

These criteria were used in manual analysis procedures during the field trials of the low-frequency/SAFT during early November 1997 at the EPRI NDE Center in Charlotte, North Carolina. A select number of the most impactful criteria were used in development of the MPATS software for this effort.

3.0 Software Development Approach

The purpose of MPATS is to develop tools which will allow the discovery of image processing sequences that can automatically distinguish cracks from grain boundaries. A suite of small image processing and data fusion utility software programs were proposed for the multi-parameter analysis tool set. This section describes the proposed collection of software programs. Section 5.0 discusses the portion of the tool set that was constructed and how they function.

In MPATS, small, single-purpose PV-Wave applications for use on SAFT-UT files perform image processing or data fusion. The applications are organized into five categories: image enhancement (SAA filters), registration, segmentation, data fusion, and quantification. Data fusion is defined as the process of combining data or information to estimate or predict entity state, such as the characterization of material as cracked or blank (Hall and Llinas 2001). The other four categories of image processing are taken from the medical imaging literature (Bankman 2000).

3.1 Image Enhancement and SAA Filters

The basic idea here is to remove the extraneous responses in an image based on an SAA parameter or a combination of SAA parameters. The SAA parameters should be specific to the inspection angle and frequency. The algorithms must be able to find all of the responses associated with the SAA and measure their statistics. Five small, single purpose, SAA filters are considered.

Brightness Filter – If the brightest voxel or a portion of the brightest voxels in an SAA is less than a selected amount, remove all energy from the SAA from the image.

Size Filter – If the length or other dimension of the SAA is less than a selected amount, then remove the SAA from the image.

Shape Filter – SAAs should have some degree of characteristic shape. Create a shape metric and filter SAA based on the metric. If the shape parameter is less than some set value, then make the SAA disappear/reappear with the push of a button.

Orientation filter – SAAs should have a reasonable and proper orientation with respect to the examination's beam angle. A perpendicular orientation is expected. Measure the angle of the SAA with respect to the beam angle and remove SAAs that are not properly oriented.

Smoothness Filter – SAAs should have somewhat smooth contours on their edges, as opposed to random, blotchy, scattered amplitude blips that appear with little symmetry and rough contours. Measure smoothness and remove SAAs without this property.

3.2 Registration

The ultrasonic response volume should be registered with respect to the weld centerline, counterbore, weld profile, and process and product forms established using overlay drawing of the inside surface of the part and other important geometrical quantities. The part geometry should be extracted from the normal beam data image or part drawings. The overlay application applies geometrical position information to display the back surface and weld on a B-scan side view image. Controls for back surface and weld placement adjustments will allow fine-tuning of the data registration.

ReverseBoth – Low-frequency/SAFT data are acquired in scanner coordinates. The first registration step in MPATS is to reverse the X-axis, the Y-axis, or both to transform the scanner coordinates into component coordinates.

ShiftBoth – Small location errors can occur as the relatively large low-frequency transducer is placed on the inspection surface. Remove the location error in the X-axis, the Y-axis, or both.

DrawPart – Generate an overlay drawing of weld geometry with process and product forms.

3.3 Segmentation

After the volumetric responses are registered with respect to the part geometry, the inspection volume can be divided into meaningful pieces. For example, the edges of the inspection volume contain artifacts that need to be suppressed while the back-surface indications within the inspection volume are most relevant to surface-connected cracks.

EdgeFilter – As occurring near the edges (in the circumferential or Y-axis of the data set) of the material should be discounted due to edge scattering effects. Automatic filtering should be applied to the inspection volume to suppress bright edge effects. A push button or slider is used to increase/remove edge effect filtering.

BackSurface – SAAs that originate from an inside surface-connected crack should be distinguished from those that do not.

ProductForm – SAAs occurring in the volumetric space between the two counterbore slopes and including weld root should be analyzed while the SAAs occurring outside this volumetric space should not.

3.4 Data Fusion

A full complement of inspections includes up to 19 SAFT processed files. Coinciding SAAs must occur at more than one examination frequency, examination angle, or scan direction. The separate inspection files are fused into one.

View All Data – Provide a method of reviewing the available data quickly and consistently. The format of the inspection set should be entered into the system. Blank images can be used to show missing inspections.

Fuse Two Image Files into One – Coinciding SAAs should occur from at least one inspection angle from both sides of the weld. Fuse two images from opposite sides of the weld into a single image. Consider logical AND to detect a redundancy on a per voxel basis then for detected voxels use maximum or average response from separate voxels. Assign non-detected voxels a zero or baseline value.

Fuse All Files into One – Combinations of the 19 images should be used, in an automated, rule-based system to reliably distinguish cracks from coarse-grain signal responses.

3.5 Quantification

The objective and OP milestone can be met by the automated or semi-automated generation of a final call image for a detected flaw. The 19 LF/SAFT inspections are reduced in a timely and economical way to the final call image. This image contains confidence and uncertainty visual cues. The effects of redundancy on confidence are displayed on the final call image.

DetectionCall – The pitfall of rule-based systems is that they are over-trained and as such work only on the test data. A means should be provided to show why the rules should work and that they do on at least one independent data set. An independent data set is one that is not used in establishing the rules.

LengthCall – Provide algorithms for length sizing and measuring its uncertainty.

DepthCall – Provide algorithms for depth sizing and measuring its uncertainty.

4.0 Piping Specimens Used for MPATS Software Evaluation

Data acquired from four specimens (sectioned and welded components) were used for quantification activities and performance evaluation of the MPATS software during the course of this effort. These specimens were WOG specimens, in particular, CSS pipe sections. All WOG specimens described in this study will be identified only by a capital letter (e.g., WOG Specimen A) and this nomenclature will be used throughout the report, in order to disguise the true identification of any specimen examined. This section contains a detailed description of the specimens examined during the exercise at the EPRI NDE Center in 1997 and subsequently used for evaluation and quantification activities with the MPATS software.

The cracks in the WOG pipe sections were created using methods that have proven useful in producing realistic surface-connected mechanical and thermal fatigue cracks. The flaws in the WOG specimens are basically considered to be planar cracks, parallel to the weld centerline, and perpendicular to and connected to the inner diameter. However, the fabrication process has also created some transverse cracking in some of these specimens.

WOG Specimens A through D (used in this study) were all statically cast elbow sections welded to centrifugally cast pipe sections. The OD contours were significantly sloped across the crown of the welds, and there existed surface “lips” on the elbow sides of each component that quite often precluded the implementation of 30° and/or 60° incident scans from one or both sides of the weld due to transducer decoupling effects. The ID contours exhibited significant counterbore geometry and variations in thickness as a function of axial position on the specimens. Due to the fact that the weld centerline varied positionally between the two counterbores and the crown of the weld was often quite sloped, the 0° data did not always provide useful profiling information. Also, due to decoupling effects, transducer positioning relative to the weld centerline was difficult to establish on an accurate and consistent basis.

Specimen A was 24.13 cm (9.5 in.) wide (circumferential direction), 54.0 cm (21.25 in.) long (axial direction), and 5.46 cm (2.15 in.) thick at the weld centerline. With conventional examinations performed at EPRI, severe beam splitting and distortion was exhibited from the pipe side with less attenuation occurring from the elbow side using a 1 MHz longitudinal wave examination. This block contained a crack (the cracking mechanism was unknown to PNNL) located directly on the weld root.

Specimen B was 24.13 cm (9.5 in.) wide (circumferential direction), 60.33 cm (23.75 in.) long (axial direction), and 6.21 cm (2.445 in.) thick at the weld centerline. There was significant thickness variation as a function of axial position along this specimen. The joint configuration of this specimen consisted of a manual field-welded centrifugally cast pipe-to-statically cast elbow. The pipe side contained a mixed structure, with a coarse columnar-grained microstructure near the OD which phased into a coarse-grained randomly oriented (equiaxed) microstructure near the ID. The elbow side contained statically cast stainless steel (SCSS) with intermediate-sized grains. This joint was manually field welded using stainless steel 308 weld material. It exhibited a slightly tapered contour up toward the elbow side, and a wavy ground weld crown. The ID surface contour of the elbow side was irregular. The weld root, with respect to the counterbore, was considerably shifted toward the pipe side. This block contained a thermal fatigue crack on the elbow side.

Specimen C was 25.4 cm (10.0 in.) wide (circumferential direction), 60.96 cm (24.0 in.) long (axial direction), and 7.19 cm (2.832 in.) thick at the weld centerline. This specimen exhibited significant thickness variation as a function of axial position. The joint configuration of this specimen consisted of an automatic shop-welded centrifugally cast pipe-to-statically cast elbow. The pipe side contained a randomly oriented (equiaxed) coarse-grained microstructure. The elbow side contained SCSS with

intermediate-sized grains. The ID contour of the elbow side was extremely irregular, and this specimen exhibited a severely tapered weld crown (tapered up toward the elbow). The weld root was considerably shifted in position toward the pipe side with respect to the counterbore. This block contained a mechanical fatigue crack on the elbow side.

Specimen D was 24.13 cm (9.5 in.) wide (circumferential direction) across the weld crown, 60.96 cm (24.0 in.) long (axial direction), and 7.13 cm (2.807 in.) thick at the weld centerline. This specimen exhibited significant thickness variation as a function of axial position. The joint configuration of this specimen consisted of an automated shop-welded centrifugally cast pipe-to-statically cast elbow. The pipe side contained a randomly oriented (equiaxed) coarse-grained microstructure, and the elbow side exhibited SCSS with intermediate-sized grains. The ID contour of the elbow side was very irregular, and this specimen exhibited a severely tapered weld crown (tapered up toward the elbow). The weld root of this specimen was considerably shifted in position toward the pipe side, with respect to the counterbore. This block contained a mechanical fatigue crack located on the pipe side.

The true-state crack dimensions and positional data are illustrated in Table 4.1.

Table 4.1. True-State Crack Dimensions and Positional Data for CSS Samples Used in This Study

Specimen ID	Nominal Crack Depth (%TW)	Nominal Crack Length (cm)	Axial Offset from Weld Centerline (cm)	Circumferential Start Point from Edge of Sample (cm)	Circumferential End Point from Edge of Sample (cm)	Pipe (P) or Elbow (E) side
A	Unknown	4.32	0.51	9.40	13.72	E
B	Unknown	9.39	0.33	7.37	16.76	E
C	30-35%	7.62	0.97	9.40	17.02	E
D	30%	7.36	0.15	8.64	16.00	P

TW = through-wall

5.0 Description of Multi-Parameter Analysis Tool Set

The purpose of MPATS is to facilitate discovering the image processing sequences that can automatically distinguish cracks from grain boundaries. Section 3.0 described the proposed collection of small image processing and data fusion utility software for the MPATS. This section discusses the portion of the tool set that was constructed and how it functions. The next section shows how well these tools assisted in the evaluation of the CSS specimens.

The tools are organized into five categories: image enhancement (SAA filters), registration, segmentation, data fusion, and quantification. The first tool is a response volume enhancement tool that filters out small SAAs. The second tool is a data registration tool, *ReverseBoth*, which transforms a LF/SAFT inspection from scanner coordinates to material coordinates. One segmentation tool was constructed, *EdgeFilter*, that was extensively used in the evaluation of the LF/SAFT data in the next section. All three data fusion tools were built. The remainder are considered in the recommendations section.

5.1 Enhancement – SAA Size Filter

In MPATS, image enhancement removes the extraneous responses in an image based on an SAA parameter or a combination of SAA parameters. The SAA size filter was completed and tested. The testing showed that if the length or other dimension of an SAA is less than a selected amount that SAA can be removed from the response volume.

The graphical user interface of the SAA size filter is shown in Figure 5.1. This application is controlled by the user-selected parameters in the control box on the left. The “Open” and “Write SAFT file” buttons access a dialog box that allows the user to browse for and select or enter a file name. This dialog box is shown in Figure 5.2. The “Open” mode requires an “*.mpats” type of text file for its input. This file contains parameter information about the data and the way it has been filtered. The “Write SAFT file” command creates a binary SAFT style data file of the filtered data. The SAA filter application first displays the composite C-scan in the upper left corner of the window. A low-pass Butterworth filter is applied to the image. The filter cutoff and order values are controlled via the slider bars and the filtered image is shown in the lower left corner.

Next an amplitude threshold is applied to the data with the results shown in the upper right corner. The user-controlled slider bar sets the threshold level.

Finally the data values greater than the threshold level are screened on the basis of size. The sizing filter is implemented in two steps. First the thresholded data are divided into regions. These regions are made up of the SAAs of interest as determined by the user-selected threshold in this application. For example, in Figure 5.1 (upper right corner), there are six SAA regions. These regions are then measured based on the selected rule (area, width, length, skeleton, and vertical kernel) and on the size determined from the slider bar. In Figure 5.1, a length sizing rule with the limit set to eleven samples produces one SAA of interest as shown in the lower right image. This SAA was found to have a length greater than eleven. All other SAAa were shorter and do not appear in the image.

The analysis parameters are saved to the “*.mpats” file via the “Save” button. On rerunning the SAA size filter application, the same state would be restored as was shown on exiting the previously run SAA application.

The “Write SAFT file” button saves the filtered data in a SAFT formatted file. The file is compatible with the SAFT analysis and display code that produces the standard composite C-scan and B-scan images.

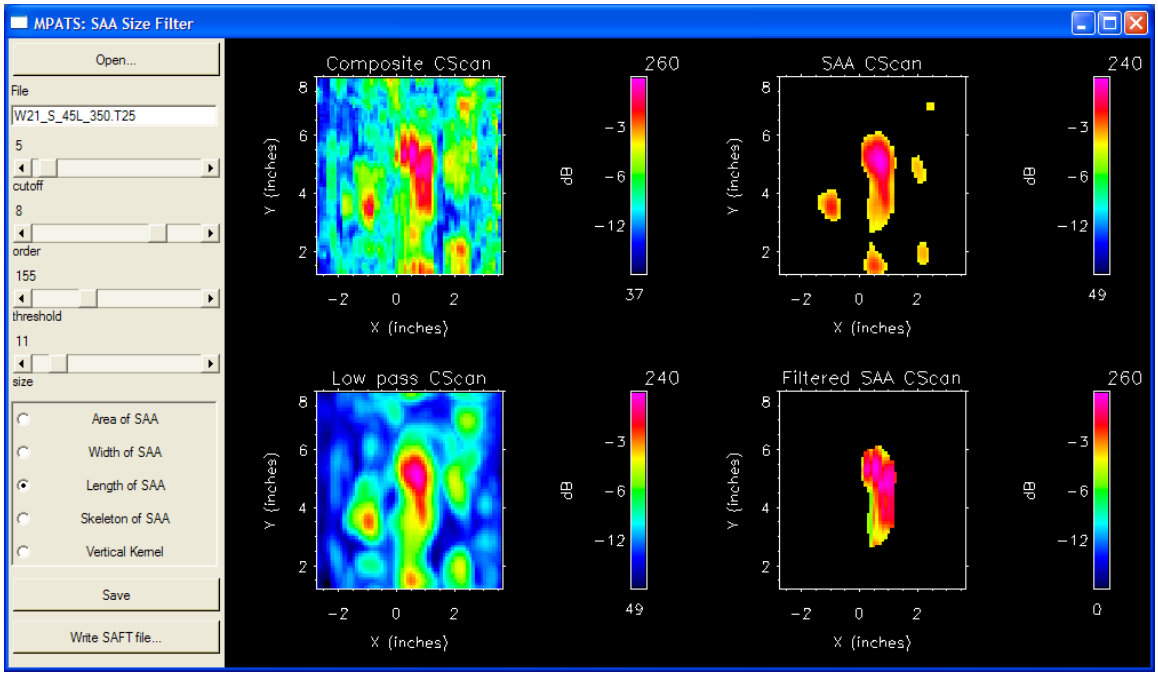

Figure 5.1. Application Window and Controls for the SAA Size Filter

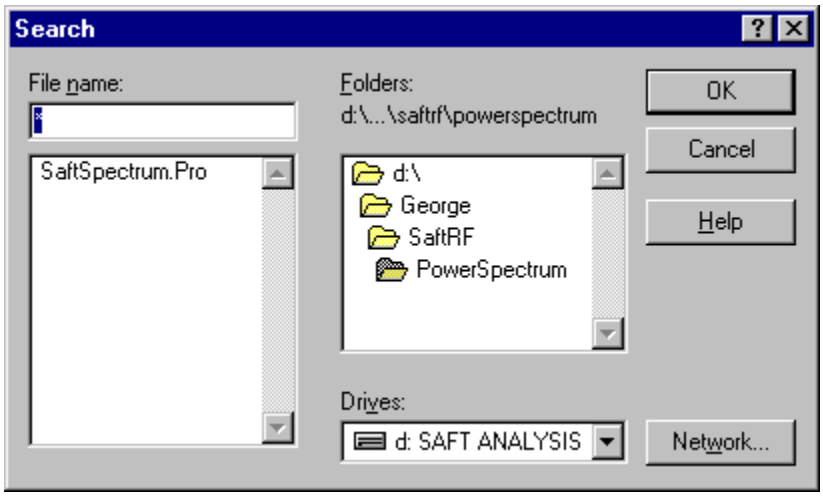

Figure 5.2. The Open File Dialog that Pops Up when the Open File Button is Pushed

5.2 Registration – *ReverseBoth*

The ultrasonic response volume should be registered with respect to the weld centerline, counterbore, weld profile, and process and product forms. LF/SAFT data are acquired in scanner coordinates. The first registration step in MPATS is to reverse the X-axis, the Y-axis, or both to transform the scanner coordinates into component coordinates. The *ReverseBoth* MPATS tool was constructed to do this.

The application window of *ReverseBoth* is shown in Figure 5.3. On the left are the user controls. The "Open" button accesses a dialog box that allows the user to browse for and select or enter the file name for an "*.mpats" type of text file that contains parameter information about the LF/SAFT data including its directory path. The first set of user controls are the radio buttons that allow the user to select to reverse the X-axis or leave it as scanned. The second set is for the Y-axis. The left column of images illustrates the input data while the right column of data shows the output or reversed data.

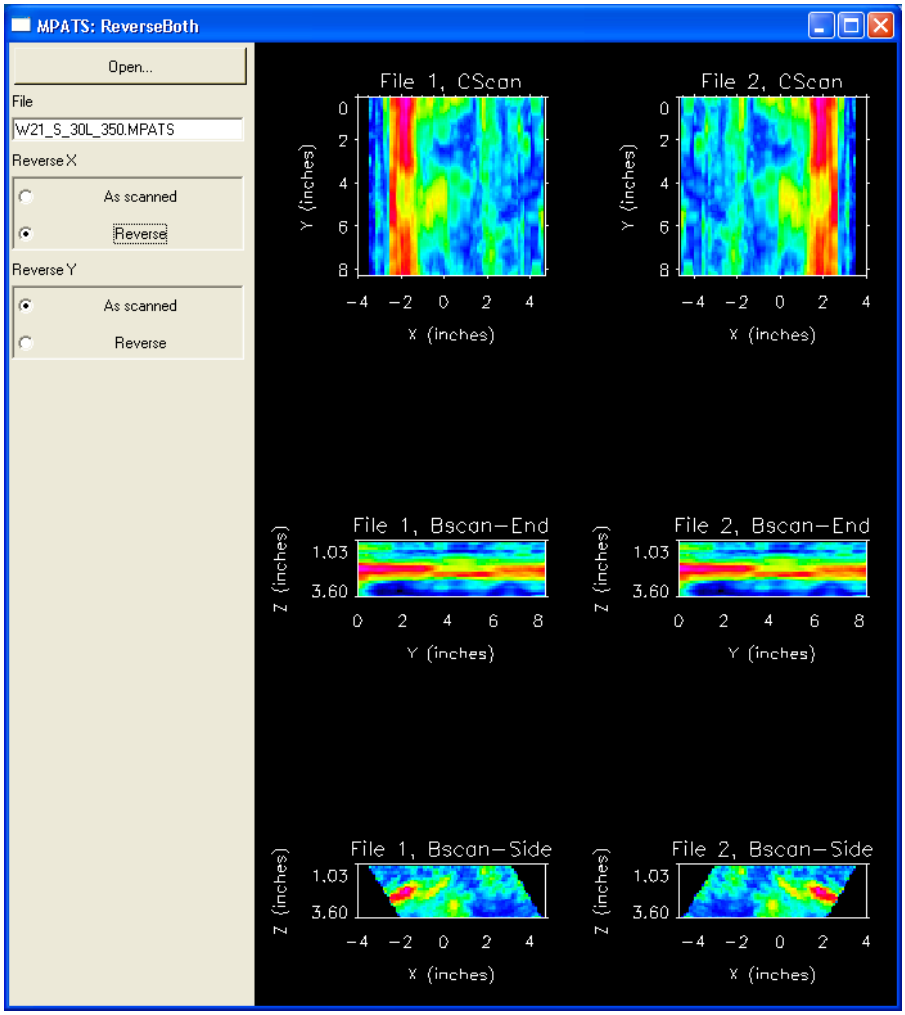

Figure 5.3. Application Window and Controls for the MPATS *ReverseBoth* Tool

5.3 Segmentation – *EdgeFilter*

An edge filter tool allows the user to window LF/SAFT data to select responses of interest. The application window and controls for the MPATS *EdgeFilter* tool is shown in Figure 5.4. The tool allows the user to open a LF/SAFT file and display it in top, end, and side views. The process of opening the file includes reading previously established settings for a 3D Hanning window. This is the only filter choice currently employed for this application. The Hanning window is applied to the LF/SAFT data and the result is displayed in top, end, and side views to the right of the un-windowed data.

The Hanning window controls are shown in the gray control pane on the left hand side of the tool. There are six slider bars that show the material coordinates (in English units only, in order to match the MPATS

and SAFT scaling in the illustrations) for the Hanning window settings. The X axis is windowed at −2.0 inches (xStartWin value) and +2.0 inches (xEndWin value). This selects the responses from the weld metal and surrounding base metal. The Y-axis is windowed at 1.7 and 7.5 inches to remove the edge effects caused by the partial SAFT aperture at the start and end of the scan. The Z-axis is windowed at 2.5 inches in both directions in order to select the energy returned from the back surface of the part.

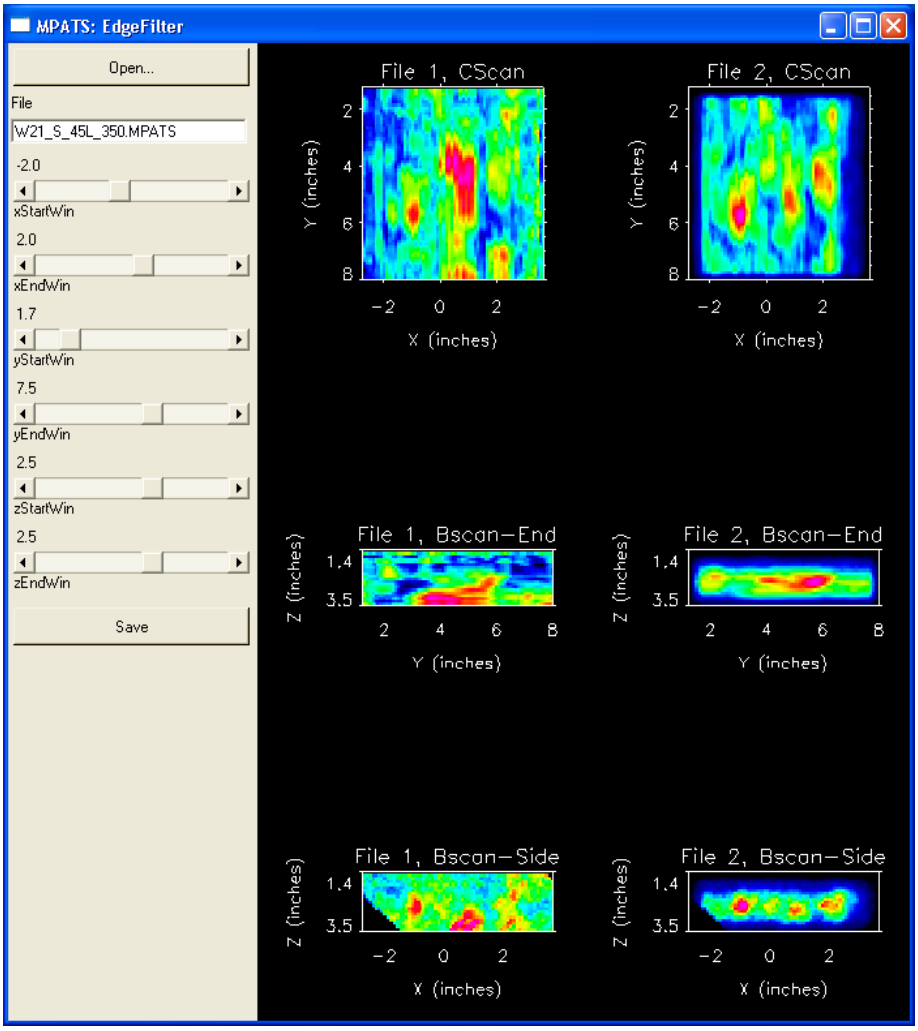

Figure 5.4. Application Window and Controls for the MPATS *Edge Filter* Tool

5.4 Data Fusion

We completed three data fusion MPATS tools. The *ViewAll* tool puts all available LF/SAFT data on the computer screen for a selected component. The *FuseTwo* tool allows the user to prepare data for data fusion and select a data fusion mode. The *FuseAll* tool shows a completed data fusion result for a selected component.

Figure 5.5 shows the application window and controls for the *ViewAll* MPATS tool. The tool allows the user to open all LF/SAFT files that are available from the inspection of a component. It displays the top view of up to 21 inspections in a fixed format with 450 kHz data in the top row, 350 kHz data in the middle row, and 250 kHz data in bottom row. The left-hand column of top views shows that there is no

data for 60°L waves from the statically cast elbow side. The second and third columns show the top views of inspection data for the 45°L and 30°L inspections from the statically cast elbow side.

Normal beam data is shown in the fourth column and two of the panes are blank because only 350 kHz data was acquired in normal beam mode. In a similar way, the data from the centrifugally cast pipe side is shown in columns five through seven. The user can use the mouse to select an inspection for display in magnified form by clicking on the top view of that inspection. These magnified top, end, and side views are shown on the right of the *ViewAll* MPATS tool's application window.

The *ViewAll* tool controls, shown in the gray control pane, include two sets of radio buttons. The first set allows the user to display the data with the elbow side as negative X, the pipe side as negative X, or display the data as scanned with no reversal applied. The second set of radio buttons allows the user to display the normal beam data with or without X-axis reversal. The application window and controls for the *FuseTwo* MPATS tool is shown in Figure 5.6. The tool allows the user to open two LF/SAFT files and display a fused result. It displays the first file in the left column, the second file in the middle column, and the fused result in the right column.

The *FuseTwo* tool's controls are shown in two gray control panes on the left-hand side of the tool. The first pane allows the user to select the two files and choose the data fusion mode. The second pane allows the user to review the filter settings and change the SAA detection thresholds.

Data fusion can be defined as the process of combining data or information to estimate or predict entity state. For us entity state includes characterization of the material as cracked or blank. The extent of the degradation is also part of entity state. There are three categories of data fusion: fusion of individual data values into a new data value, fusion of objects into a new object, and fusion of inferences into a new inference. The top set of radio buttons in the data fusion control pane allows the user to select one of these three modes. Figure 5.7 shows the application window and controls for the *FuseAll* MPATS tool. The tool allows the user to open all LF/SAFT files for a component and display a fused result. *FuseAll* used the same file layout as *ViewAll* and the same data fusion control set as *FuseTwo*.

We have demonstrated by way of the data fusion tools that the analysis of LF/SAFT data can be made fast and economical. The outcome of work is reported in Section 6.0 of this report and provides a quantification of how well the data fusion tools distinguish cracks from grain boundaries.

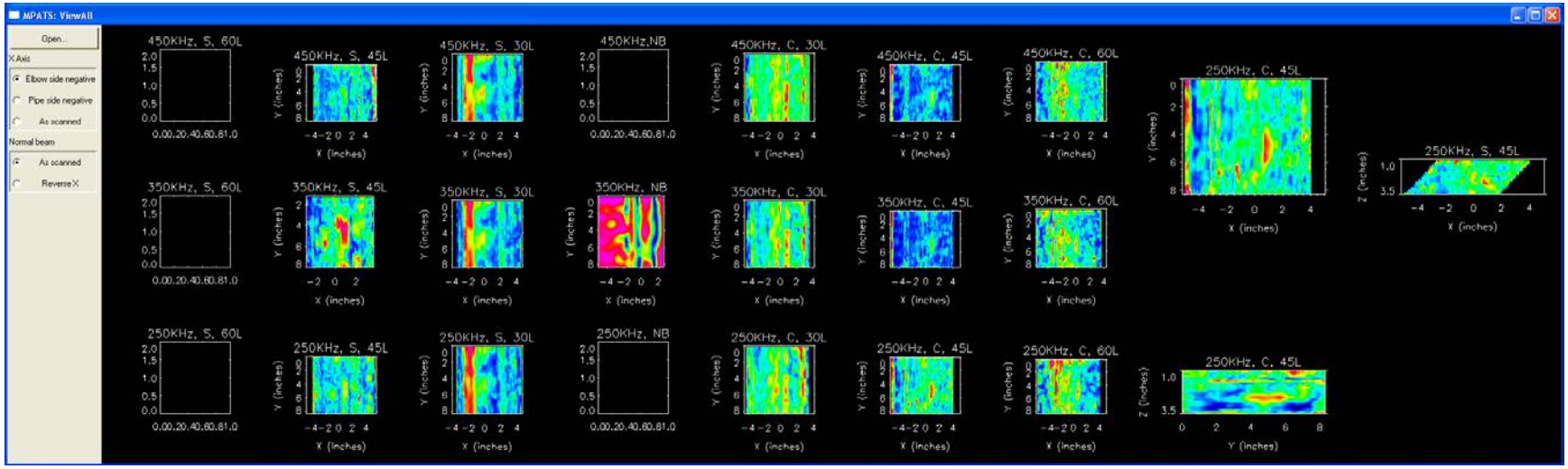

Figure 5.5. Application Window and Controls for the *ViewAll* MPATS Tool

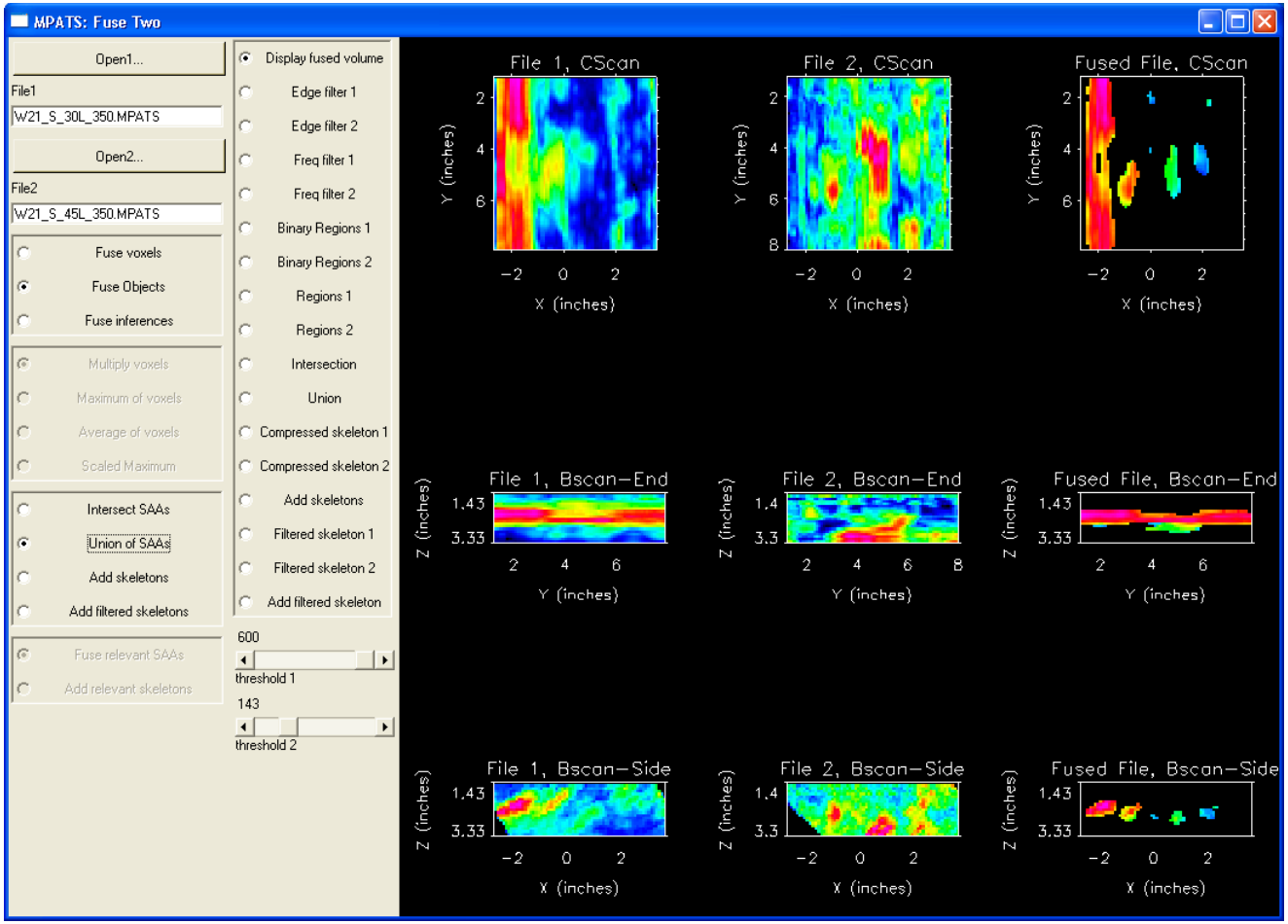

Figure 5.6. Application Window and Controls for the *FuseTwo* MPATS Tool

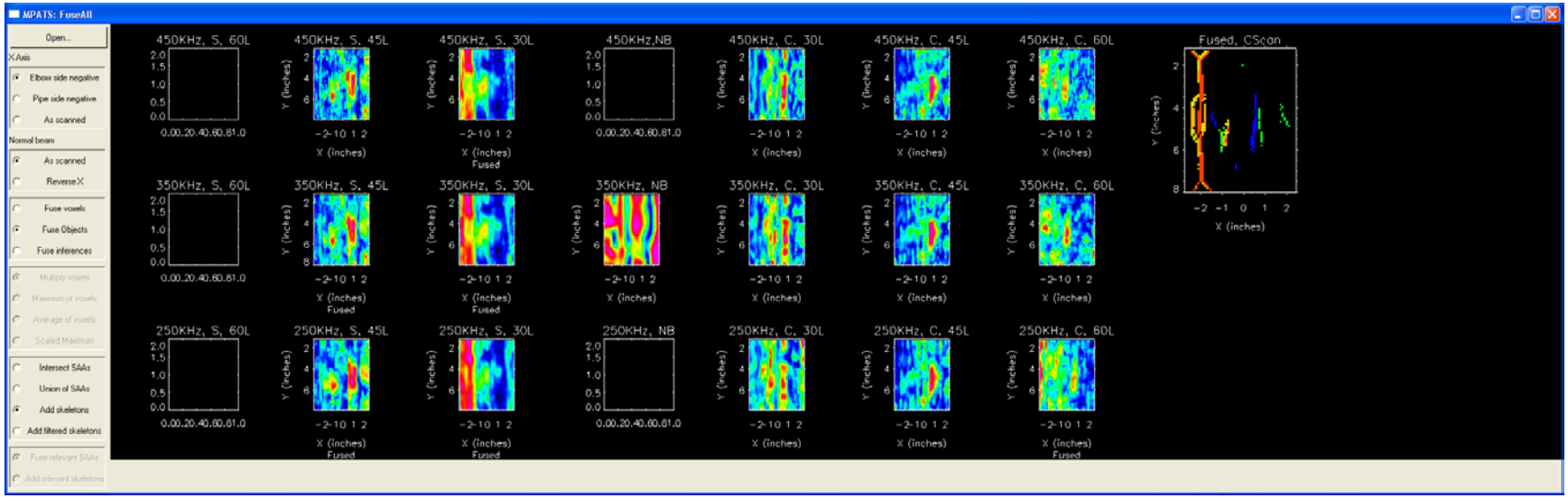

Figure 5.7. Application Window and Controls for the *FuseAll* MPATS Tool

6.0 MPATS Evaluation and Assessment

A procedure for data analysis was developed using the MPATS software on the data files for specimens A, B, and C. These three data sets formed the training data for the procedure and are discussed first. Specimen D is the test data set and its analysis follows later. All of the data files acquired for specimens A–D are listed in Table 6.1. Length and location of the flaw in each specimen was determined in the analysis.

Table 6.1. Low-Frequency Data Sets Acquired for Each Specimen Evaluated in This Study

		0°	30°L			45°L			60°L		
Sample	Side*	350 MHz	250 MHz	350 MHz	450 MHz	250 MHz	350 MHz	450 MHz	250 MHz	350 MHz	450 MHz
A	C	x	x	x		x	x		x	x	
	S	x	x	x		x	x				
B	C	x	x	x	x	x	x	x	x	x	x
	S		x	x	x	x	x	x			
C	C	x	x	x		x	x		x	x	
	S	x	x	x		x, A	x, A				
D	C	x	x	x		x	x		x	x	
	S	x	x	x		x, A	x, A				

*Inspection Side: C = centrifugally cast or pipe side
S = statically cast or elbow side

"A" denotes a re-take of the original data.

6.1 Data Preparation

Figure 6.1 shows a flow chart of the steps required in the MPATS analysis of the low-frequency data. Each section of this flow chart will be discussed.

Each SAFT data file was converted from 8-bit data to 16-bit data for increased dynamic range. The 16-bit data files were SAFT processed with a 25° aperture angle and the no skip option as was previously selected in the 1997 analysis.[(a)] Next, the top 2.54 cm (1.0 in.) of data in the depth or Z dimension was removed to avoid the near surface saturated signals typically recorded in the data. The final step was to create a MPATS text file with pertinent data acquisition parameters for the MPATS software.

6.2 Edge Filter

The MPATS analysis begins with edge filtering each data file. In doing so the Y-axis edge effects are removed and the near-edge counterbore signals at the Y-axis extremes are diminished in amplitude. The purpose is to highlight any potential flaw signals.

The edge-filtered data for Specimen B is shown in Appendix A. From left to right in the MPATS display in the figures are the filter controls, the input data, and the filtered or output data. A color bar is also displayed. The 'Cxx' data represents data acquired from the centrifugally cast or pipe side of the weld at

(a) Diaz AA, RV Harris Jr. and SR Doctor. 2008. *Field Evaluation of Low-Frequency SAFT-UT on Cast Stainless Steel and Dissimilar Metal Weld Components*. NUREG/CR-6984, PNNL-14374, U.S. Nuclear Regulatory Commission, Washington, D.C. This report was completed in 2003 but not published until 2008.

angle xx. The ‘Sxx’ data represent data acquired from the statically cast or elbow side of the weld at angle xx. The inspection frequency in kHz is also noted in the figure caption.

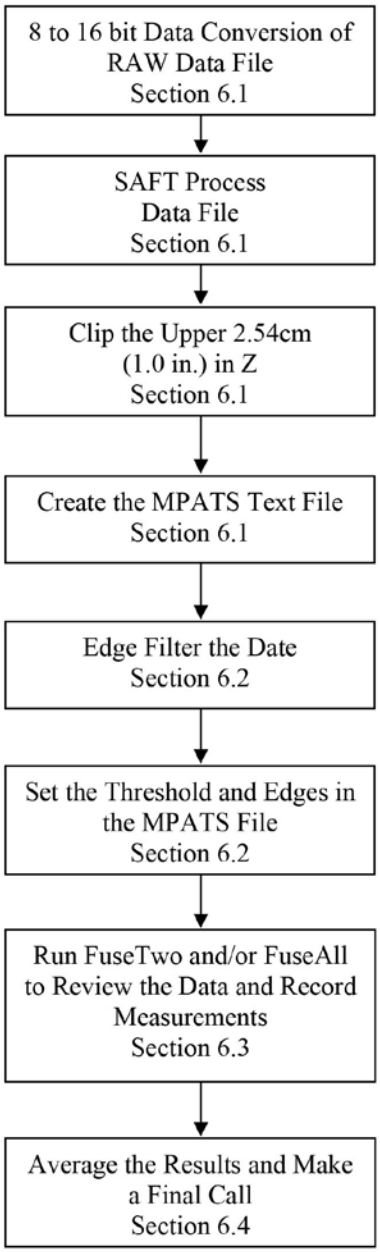

Figure 6.1. MPATS Analysis Flow Chart

The B-scan side views on the bottom of the figures show a back-surface overlay (black line on the image). This overlay was determined from notes on the specimen geometry and from the data itself. The overlay was not always well enough defined to add value to the image. As in the previous analysis,[(a)] the region of interest is in the volumetric space between the top two counterbore edges and including the

(a) Diaz AA, RV Harris Jr. and SR Doctor. 2008. *Field Evaluation of Low-Frequency SAFT-UT on Cast Stainless Steel and Dissimilar Metal Weld Components*. NUREG/CR-6984, PNNL-14374, U.S. Nuclear Regulatory Commission, Washington, D.C. This report was completed in 2003 but not published until 2008.

weld root. So it is important to identify the counterbore signals in the image if they are present. Figures A.2–A.4, at a 30° inspection from the pipe side show a counterbore signal that is intermittent and does not run the entire circumferential length, Y. Figures A.11–A.13 show the 30° inspection data from the elbow, S, side. Strong counterbore signals are evident for most of the circumferential length. These signals assist the operator in selecting the region for further MPATS signal analysis.

The edge filter routine is additionally used to determine the maximum amplitude of the signal or group of signals of interest. A threshold level of 3 dB below this maximum amplitude is recorded in the MPATS text file for the next phase of analysis. This −3 dB clip is consistent with the process used at the EPRI NDE Center in 1997.

6.3 *FuseTwo*, *FuseAll*

The *FuseTwo* routine operates on two input data files and provides a means for comparing and quantifying the data sets, one or two at a time. Appendix B shows the results from a *FuseTwo* analysis on the 250 and 350 kHz data from Specimen B. The top two figures in B.1–B.10 show the edge filtered C-scan and B-scan side views of the data. The lower left image is the thresholded (at the –3 dB level) C-scan image and the lower right is the skeleton of the thresholded image. Clicking on the skeleton image at appropriate points provides X and Y coordinate information at that location. Flaw length and location are determined from these X and Y values.

Also displayed in the C-scan images is the true-state information for the crack (red line). This red line feature can be turned off or on and was only used in this training phase of the MPATS analysis.

Appendix B shows the skeleton for the data one file at a time. The *FuseTwo* routine allows the addition of two skeletons and *FuseAll* permits the addition of all possible combinations of skeletons from a specimen. This feature assists the operator in viewing the data and determining which inspection angles and frequencies are contributing to the crack call. For example, Figure 6.2 shows the skeleton from five inspections at 250 kHz. The S45 (light green) data has an offset in the X direction of 2.54 cm (1.0 in.) as was determined by the location of its counterbore signals. This data is corrected by a shift to the right. It is uncorrected in Figure 6.2. The skeletons show the counterbore signals at −2.5 and 2.3 cm (−1 and 0.9 inch) in X with the flaw signal at approximately 0.5 cm (0.2 in.). The shifted S45 and S30, and C30 data contribute significant information about the flaw while C45 data does not. The C60 data contributes slightly to the flaw.

6.4 Evaluation Results

The start and stop locations of the indications from the skeletonized images of Specimens A, B, and C were recorded. Figures C.1–C.3 show the results. The average value of length and X position from the one significant cluster of indications from each specimen was determined. Spot-like indications were discounted. If these potentially numerous and small indications are included in the flaw determination, the false call rate tends to increase. Figure 6.3 shows a correlation between the number of SAAs and the length of the SAA for this training data set. These small SAAs can be attributed to grain boundaries, component geometry, irregular surface conditions, and the like. Both a low-pass filter of the data and threshold setting help eliminate these small insignificant indications.

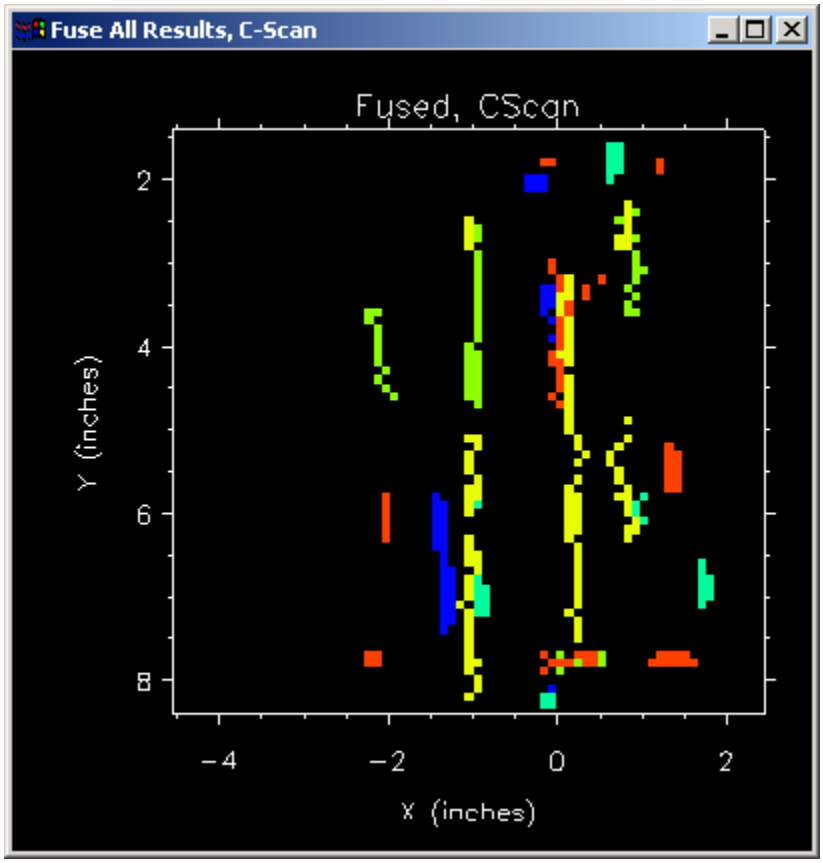

Figure 6.2. Skeleton from Specimen B, at 250 kHz for Inspections S45 (light green), S30 (red), C30 (yellow), C45 (cyan), and C60 (blue)

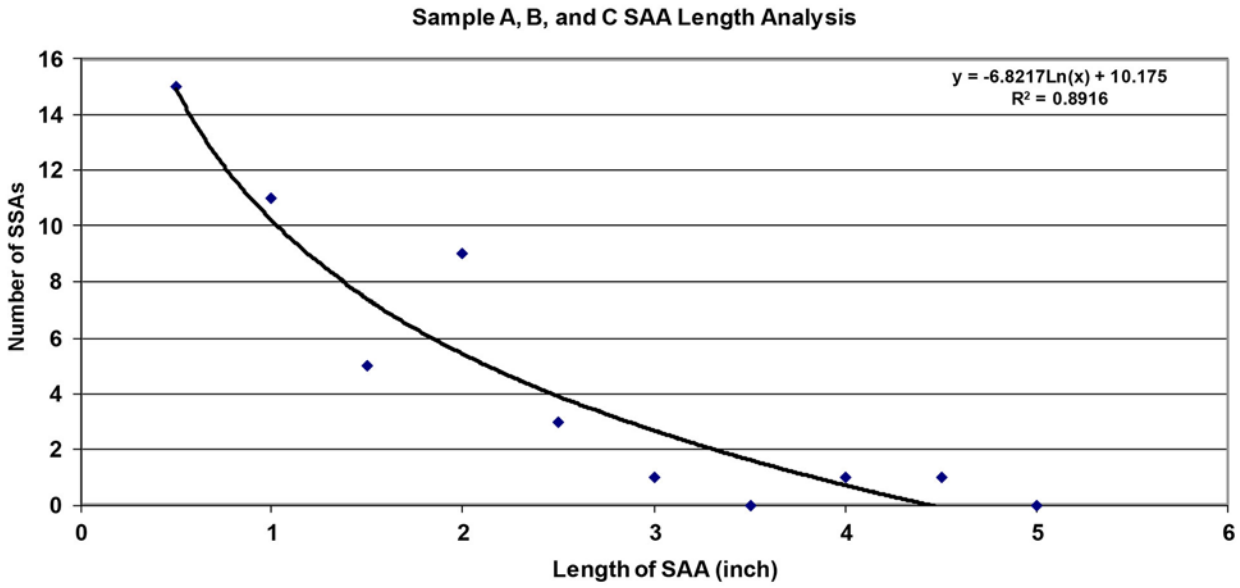

Figure 6.3. Correlation of the Number of Signal Amplitude Anomalies to the Length of the Anomaly

The final call on Specimens A, B, and C is shown in Figures C.4–C.6 along with the true state and the 1997 call.[(a)] The MPATS analysis produced similar or better results in Specimens A and B but worse in C. A limiting factor in the C data set was the data itself. Data was acquired in the X or axial direction over a range of 23.4 cm (9.2 in.) for Specimen A, 24.4 cm (9.6 in.) for Specimen B, and only 19.6 cm (7.7 in.) for Specimen C on average. With this shorter X range in the C specimen data, the counterbore signals were typically not well represented. This could lead to error in the sub-volume selection of data for the MPATS analysis. This limitation is caused by the OD surface condition on Specimen C which prevented acquisition of data in a longer axial, X, direction. Additionally, a possible irregular surface could cause error in the beam angle, further compromising data integrity.

In summary a procedure was formed for discriminating between coherent ultrasonic energy from grain boundaries and from cracks in coarse-grained steel components. The signal and image processing tools that were developed in the PV-Wave environment made the analysis timely. Further automation will improve the process consistency. The procedure was developed and proven on Specimens A, B, and C.

6.5 Testing Results

As an independent and semi-blind test to evaluate and to get a preliminary sense of the performance of the MPATS software, the primary user of the LF/SAFT inspection system performed data analysis on Specimen D using the latest version of MPATS. Without the true-state data readily available, the NDE engineer was trained in the use of the MPATS software and conducted an independent assessment of the utility of the tools, the ease-of-use, and the general functionality of the software for improving the analysis procedures from the process used in 1997. Since over 6 years had elapsed since the NDE engineer had conducted the initial analysis of Specimen D, this activity was defined as a “semi-blind” assessment where the focus was aimed at evaluating the MPATS software rather than attempting to duplicate previous results.

The NDE engineer was trained in the use of the MPATS software and then began an independent analysis of the Specimen D data. The initial MPATS configuration file for this data set (previously SAFT processed) was already generated, and the assessment started with the utility of the *EdgeFilter*. Employing specific criteria defined earlier in this document, the individual data files were edge filtered to reduce reflected signal responses from the beveled edges of the specimen and to reduce SAAs outside the established area of interest. The edge filter was also used to reduce the high-amplitude responses from the counterbore geometry that could potentially mask scattered ultrasonic energy from nearby cracks located between the weld root and the top edge of the counterbore. This tool was also used to establish an amplitude threshold (3 dB clip) for SAAs, essentially increasing or reducing the amplitude of specific SAAs identified by the analyst, while superimposing the back-surface overlay to better account for axial and depth positioning of the indications.

Typically, the 30° inspection angle is used for detection and localization of the counterbore, and this helps to define the zone of interest relative to the other scans and relative to any SAAs that exist between the counterbores and the weld root. Used as positional markers, the edge filter can then be used to reduce the high-amplitude counterbore responses, thereby highlighting lower-amplitude SAAs and allowing for more accurate positional determinations of other SAAs.

(a) Diaz AA, RV Harris Jr. and SR Doctor. 2008. *Field Evaluation of Low-Frequency SAFT-UT on Cast Stainless Steel and Dissimilar Metal Weld Components.* NUREG/CR-6984, PNNL-14374, U.S. Nuclear Regulatory Commission, Washington, D.C. This report was completed in 2003 but not published until 2008.

Next, the *FuseTwo* tool was invoked to compare and contrast pairs of data files, typically matching inspection angles from opposite sides. This allows the analyst the ability to identify SAAs that illustrate redundancy and also provides a means to determine the amount of offset (difference in registration) between various data sets. As the files are processed by the *FuseTwo* tool, the skeleton function allows the analyst the capability of mapping the coordinates of particular SAAs of interest that exhibit characteristics called out in the criteria discussed previously. From this, the *FuseAll* tool is then used to analyze redundancy from the various inspection angles, frequencies, and scan orientations. In a very short time, the analyst is now capable of potentially reviewing all 19 scans and visually comparing and contrasting the images with only the SAAs of interest based on specific criteria, thresholding, position, and a host of other pertinent parameters. In the *FuseAll* tool, the analyst then tabulates the start and stop locations (X and Y coordinates) of the pertinent skeletonized SAAs, and from this data, the averaged positional value of the cluster of pertinent SAAs is computed as a final-call for the suite of scans analyzed.

This comprehensive approach provides the analyst with a very powerful tool for analysis, data reduction, application of detection and sizing criteria, the impact of redundancy, and the ability to acquire final-call information much more effectively than in the past. The NDE engineer was trained in the initial utility of the MPATS software in approximately 2 hours, and the independent data analysis activity was approximately 2 hours in duration. The actual procedures for the analysis described here could take a trained user less than an hour to complete, where the manual analyses of these data sets would have taken over 10 hours of time previously. The resultant savings in time alone is nearly an order of magnitude.

7.0 Conclusions

This effort was directed at meeting the deliverables defined in the Operating Plan milestone described earlier, specifically addressing enhancements to the capabilities and functionality of the low-frequency/SAFT analysis process. The OP milestone is two-fold, requiring PNNL staff to address issues of improving the capability to more consistently and reliably discriminate between ultrasonic responses attributed to grain boundaries and those from cracks, and to improve the speed and effectiveness of the multi-scan-angle-frequency analyses.

The work reported here describes PNNL's multi-phased approach to meet this OP milestone by focusing on development and testing of software and analysis tools, and quantifying the performance of the software tools on actual LF/SAFT data acquired from coarse-grained cast stainless steel components. The multi-parameter analysis tool set (MPATS), has been shown to provide enhanced capabilities and functionality for use in analysis of LF/SAFT data, and illustrates the flexibility, utility, time savings, and ease-of-use for addressing the challenges associated with the previous analysis protocol. The interactive capabilities and enhanced functionality of the MPATS is based on PV-Wave software for data analysis and fusion operations. PV-Wave is a 3D data analysis platform and has many signal and imaging processing functions built in. This work demonstrates that PV-Wave is well-suited for the analysis operations required, and is shown here to provide a streamlined and powerful foundation for the development of MPATS for enhanced discrimination and crack identification in coarse-grained material.

The utility of MPATS was demonstrated on four piping specimens in this study. Results from the analysis of Specimens A, B, C, and D (previously examined in field trials at the EPRI NDE Center in 1997) using MPATS show very encouraging results compared to the true-state data of the piping specimens examined, and also correlate well with the previous manual analysis results. A review of Figures C.4, C.5, C.6, and C.8 in Appendix C illustrates the final-call data from the manual analysis performed in 1997 compared to the MPATS analysis results and the true-state conditions of the specimens examined. Since the results of the MPATS analysis for Specimens A, B, and C were not conducted in a blind fashion (the true-state data were available and used for learning, development, and testing purposes), only the data associated with Specimen D can be viewed as meaningfully quantitative. In reviewing the final-call data from an analysis of Specimen A, there is a high degree of agreement between the true-state and both the 1997 and 2003 results, with the MPATS analysis resulting in oversizing the crack length and a very accurate representation of the axial position of the crack. For Specimen B, final-call results indicate that the MPATS analysis provides a more accurate axial position of the crack than the 1997 results, but like the previous results, only approximately 50% of the crack is detected. For Specimen C, it is shown that the 1997 final-call results more accurately represent the true-state axial position and length of the crack than the MPATS analysis, where both manual and automated methods were shown to undersize the circumferential extent of the crack. For Specimen D, a semi-blind and independent MPATS analysis provided very accurate axial positioning of the crack but only detected approximately 50% of the true flaw length. Previous manual analyses in 1997 provided a more accurate representation of the crack length, but showed the crack to be located on the elbow side of the specimen rather than the pipe side (where the true-state indicates the crack is located). The axial difference between the final-call results of the two analyses was less than 0.5 cm (0.2 in.).

The evaluation of Specimen D provided more confidence in the utility of the tools and the ability of the MPATS to more consistently and reliably duplicate the manual analysis using the specific set of criteria applied to the data sets for detection, discrimination, localization, and sizing tasks. Use of the MPATS software for analysis of Specimen D allowed the analyst to simultaneously view the pertinent scans that provided the most useful data based on redundant SAAs, identification of positional markers along the ID, and other features that piece the puzzle together for a more effective final-call determination. The

final-call data for Specimen D can be found in Appendix C. Figure C.7 depicts the various indications (SAAs) evaluated prior to computing the final-call for this suite of data. Figure C.8 illustrates the true-state of Specimen D compared with the final-call from 1997 using manual techniques and the full complement of criteria and the final-call from the MPATS analysis in 2003. With only one true data point, it is evident that more work needs to be done to quantify the MPATS analysis performance. A more detailed performance evaluation can be conducted when large blank CSS specimens become available for further data acquisition, and when the full suite of criteria, tools, and functionality are fully implemented in the MPATS platform.

Although the MPATS software is not complete, this effort focused on the development, testing, and assessment of the most significant tools and applied criteria that could be accomplished within the schedule and scope of this effort. This working version of the MPATS software in its present form addresses the technical challenges defined in the OP milestone, and provides the necessary improvements to the analysis protocol as requested by the NRC.

8.0 Recommendations

Recommendations are considered in three categories—acquisition of new low-frequency/SAFT data sets, construction of more MPATS tools, and integration of image processing and data fusion into SAFT-UT.

The work conducted to date using this new technique demonstrates the potential for useful crack detection in CSS and DMW materials using low-frequency ultrasound. Specifically, the LF ultrasonic inspection technique coupled with SAFT signal processing, utilizing the full complement of examination angles (0°, 30°, 45°, and 60° from both sides of the weld) in the longitudinal wave mode, in a pitch-catch configuration at frequencies ranging from 250 to 450 kHz has demonstrated promising improvements in the POD for fatigue cracking (of larger dimensions) in coarse-grained stainless steels. Utilization of this technique in the field has provided positive results with respect to detection, localization, and length sizing. However, these results do not represent data from a statistically large number of field-representative CSS specimens. To date, approximately 20 CSS specimens (PNNL and EPRI-WOG specimens) have been examined using this inspection and analysis protocol.

Presently, this technique allows for discrimination of cracks from other features, if cracking is present. However, we do not yet have a baseline for determining whether a specimen contains a crack. This is due to the extreme variability in sound transmission through different specimens, so that it is difficult to establish amplitude criteria. The resolution of this will require inspection of many more specimens, including base material with no cracking present, and recording amplitudes and indication characteristics from geometric, metallurgical, and crack-like reflectors. Target motion criteria are difficult to use because of the low resolution at sub-megahertz frequencies. PNNL still requires further testing and refinement of the crack identification criteria for eliminating the geometric reflections (based on variation of amplitude as a function of angle and frequency) so that cracks can be more reliably detected. This work will provide the necessary data for generating meaningful POD curves to better understand the relative improvements and performance of the inspection methodology coupled with the utility of MPATS.

The portion of MPATS that was constructed has demonstrated enhanced utility and improved capabilities for discrimination of ultrasonic responses from grain boundaries and cracks in coarse-grained metals, and improving the analytical effectiveness in both time and cost to the project. The reported analysis indicates that the approach of building small image processing tools can discover the computing sequences that distinguish cracks from grain boundaries. With a well-defined scope and limited resources, the development effort focused on a ranked and prioritized list of automated functions, tools, and additional capabilities for the MPATS software. Since further development and testing is required to fully automate the entire set of criteria and detection/discrimination capabilities, completion of the MPATS is recommended. Thus, the construction of the MPATS should be addressed next FY. After the basic sequences of filtering, registration, segmentation, and data fusion are discovered, large PV-Wave applications can be built to deploy and control these sequences and automatically distinguish cracks from grain boundaries.

In working with the MPATS software, a list of detailed recommendations for future MPATS software enhancements, development of additional functionality and capabilities, and improved utility were generated. This list includes tool fabrication and other modifications/enhancements that will provide the analyst with the capability to apply a weighting scheme to the data, automate various procedures that are still manually entered or invoked, and further refine the consistency and accuracy of the resultant final-call determination.

PV-Wave technologies can be added to SAFT-2004 to form integrated data fusion and scientific imaging capability. MPATS is extensible to other experiments by designing menus to load data based on the experiment type. The tool set will permit growth to encompass new data fusion problems in the inspection of coarse-grained materials. For example, the ultrasonic and eddy current inspections from the inside of the pipes will want to be fused with each other and with ultrasonic inspections from the outside surface of the pipe.

9.0 References

Bankman IN. 2000. *Handbook of Medical Imaging, Processing, and Analysis*, Academic Press, New York.

Diaz AA, SR Doctor, BP Hildebrand, FA Simonen, GJ Schuster, ES Andersen, GP McDonald and RD Hasse. 1998. *Evaluation of Ultrasonic Inspection Techniques for Coarse Grained Materials*. NUREG/CR-6594, PNNL-11171, U.S. Nuclear Regulatory Commission, Washington, D.C. ADAMS Accession No. ML14071A001.

Hall DL and J Llinas. 2001. *Handbook of Multisensor Data Fusion*, CRC Press, New York.

Appendix A

Analysis of Specimen B Inspections Using the Edge Filter

Appendix A

Analysis of Specimen B Inspections Using the Edge Filter

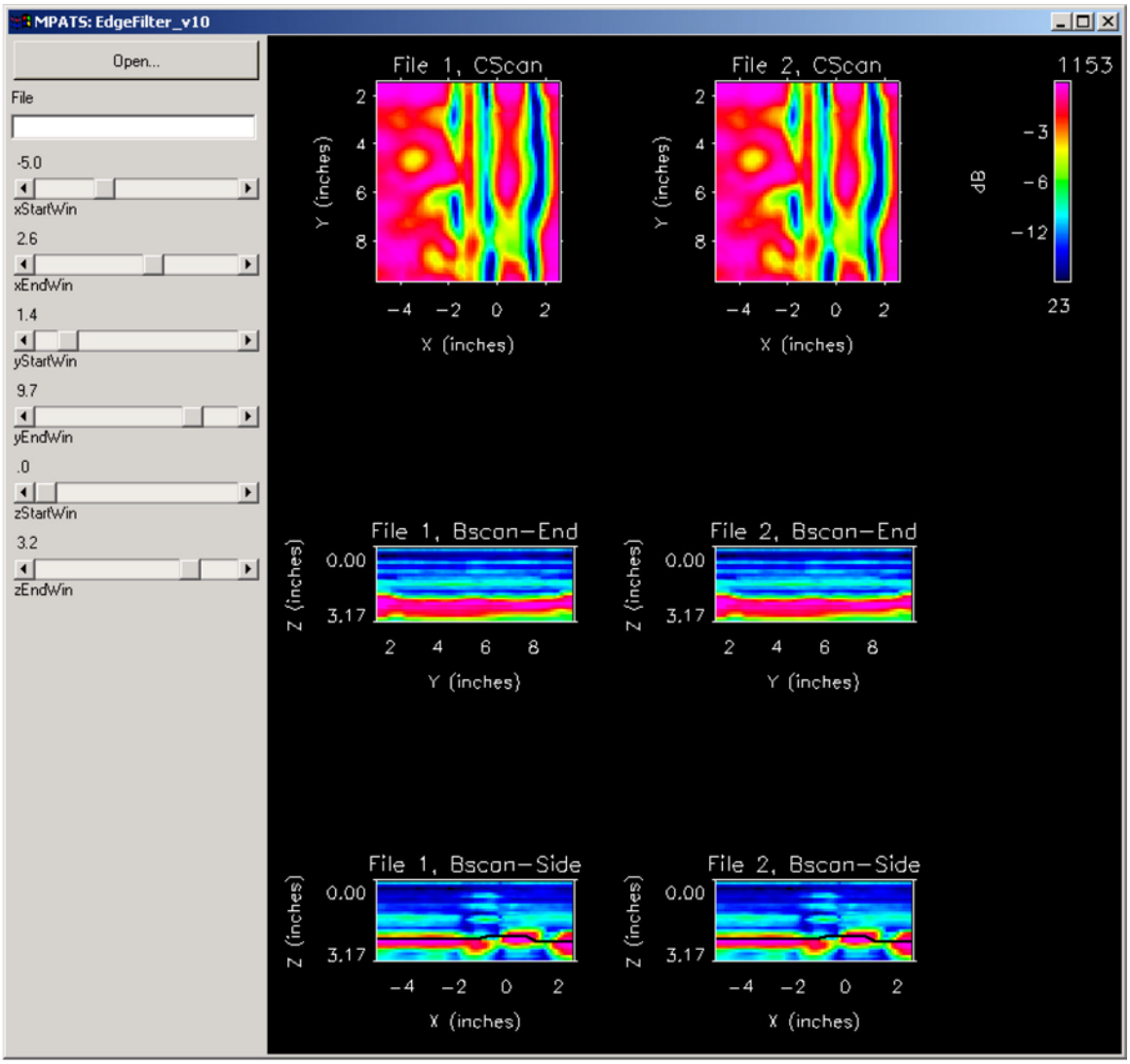

Figure A.1. B, C0 at 350 kHz

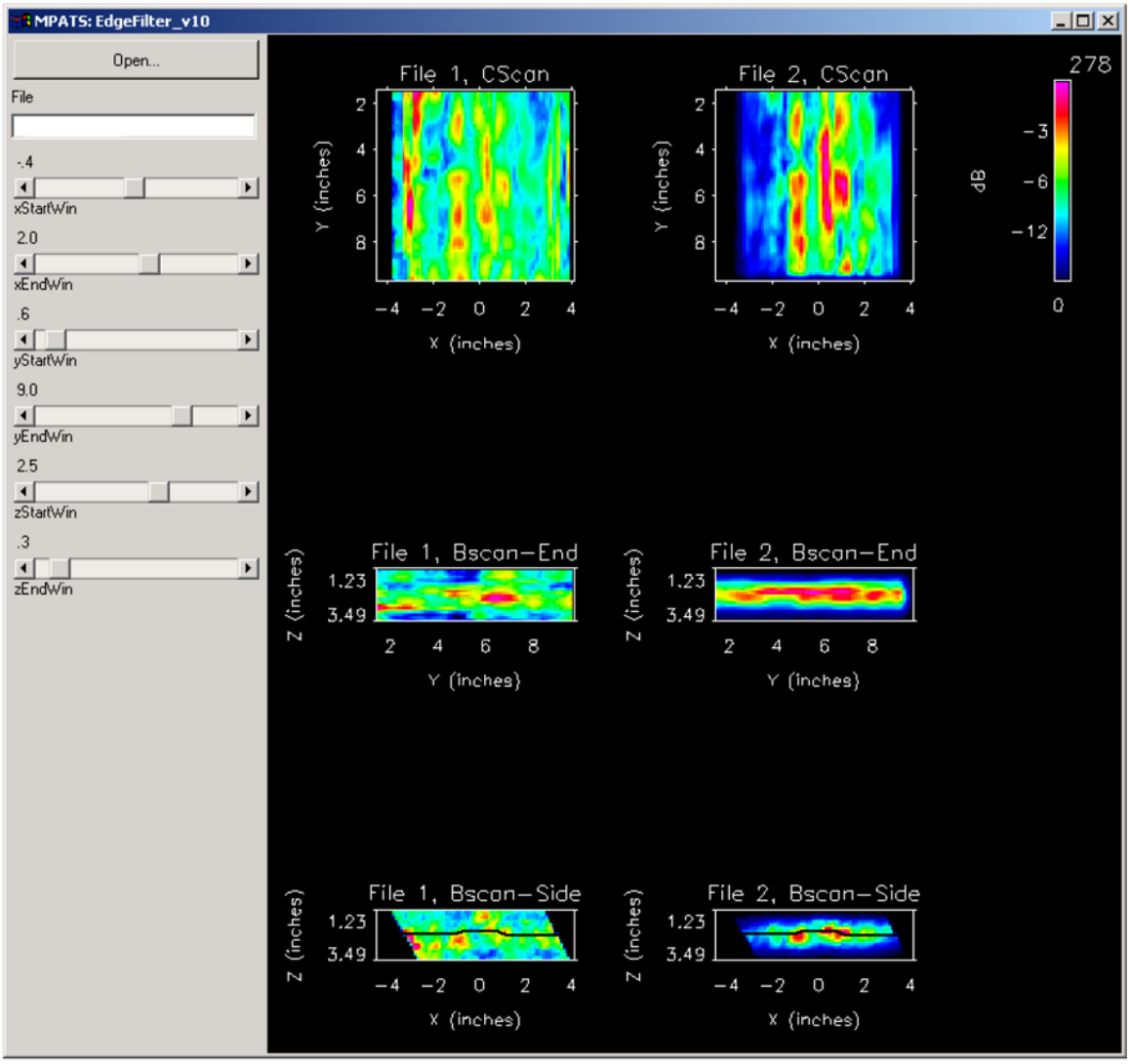

Figure A.2. B, C30 at 250 kHz

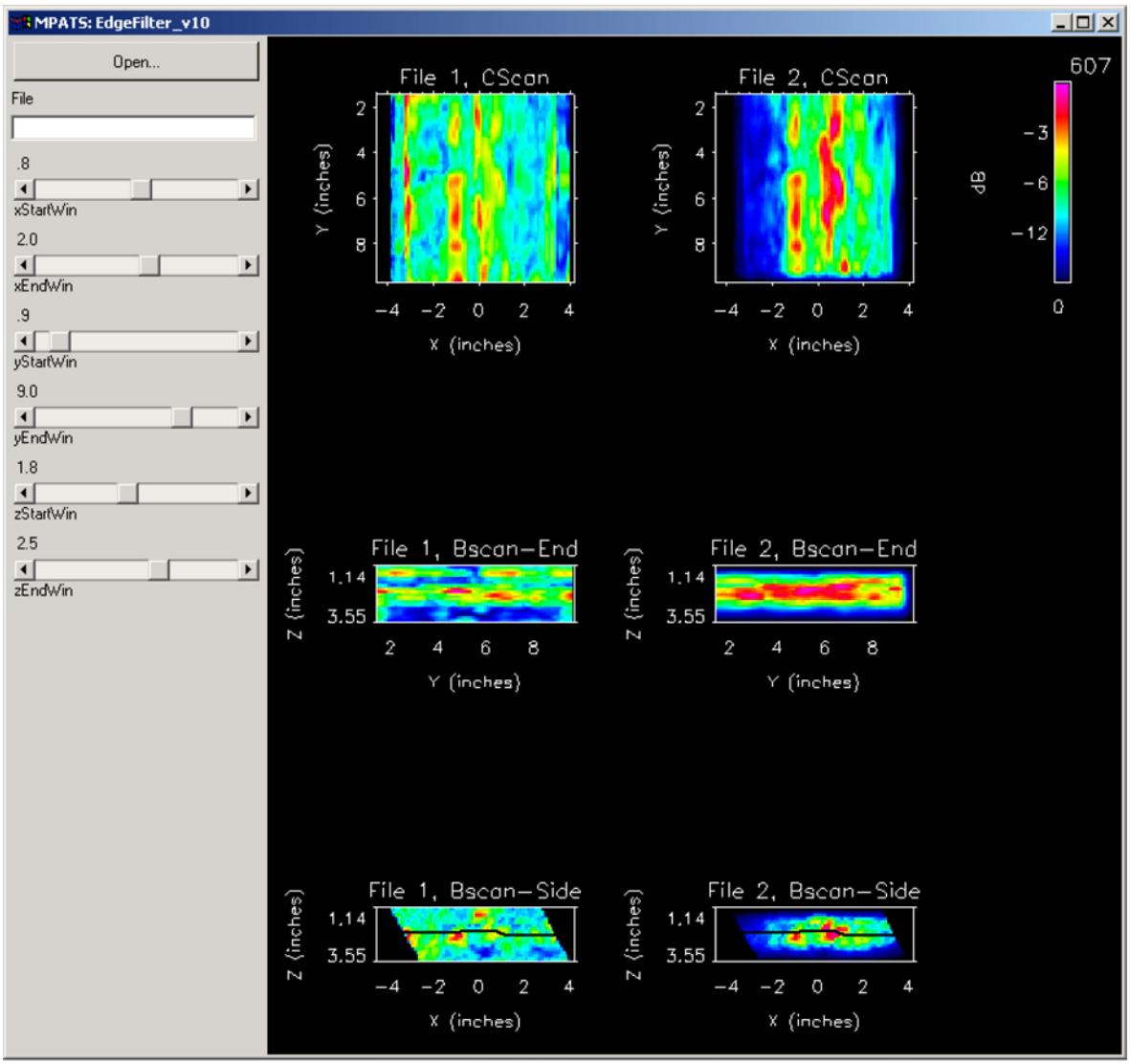

Figure A.3. B, C30 at 350 kHz

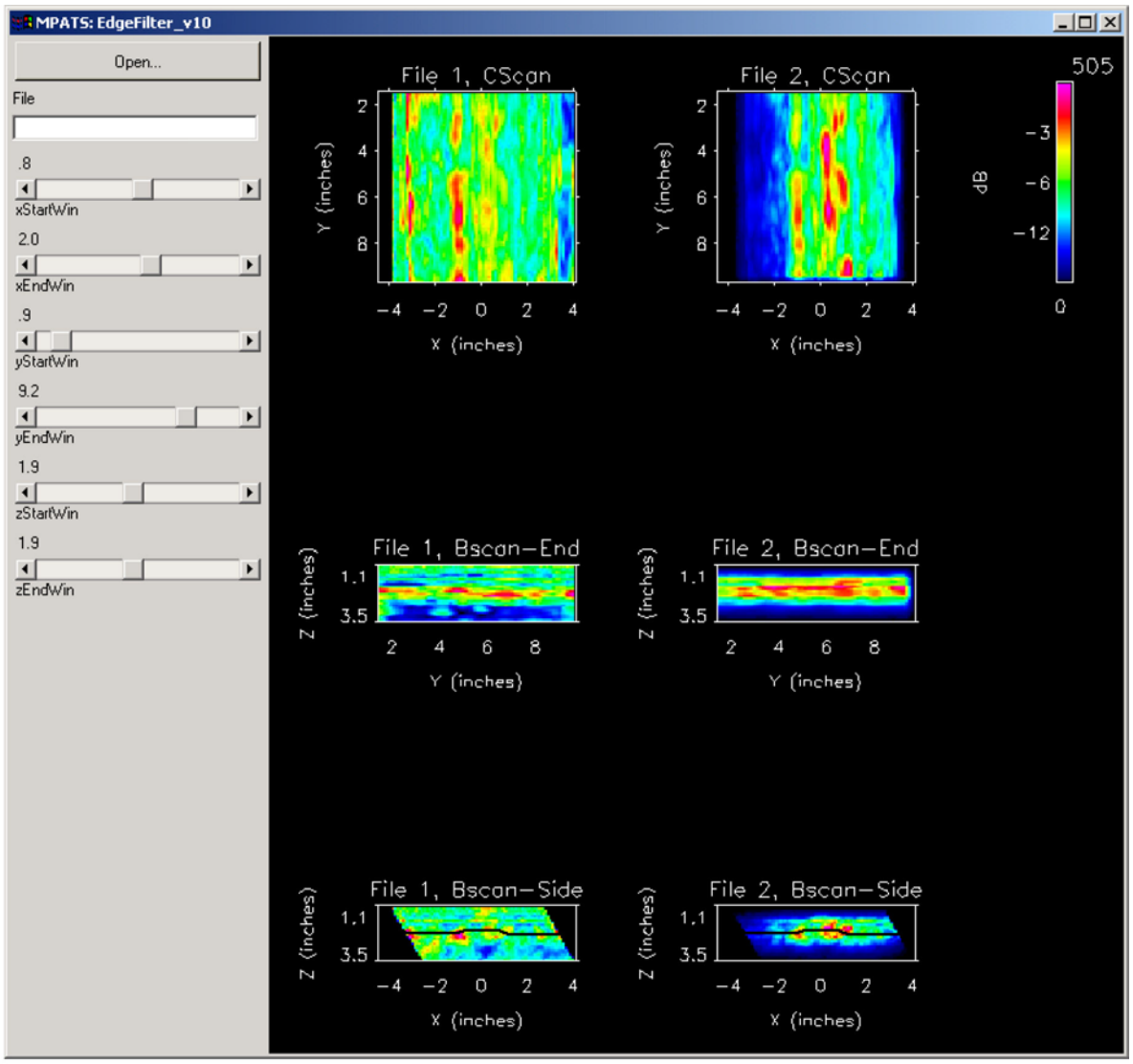

Figure A.4. B, C30 at 450 kHz

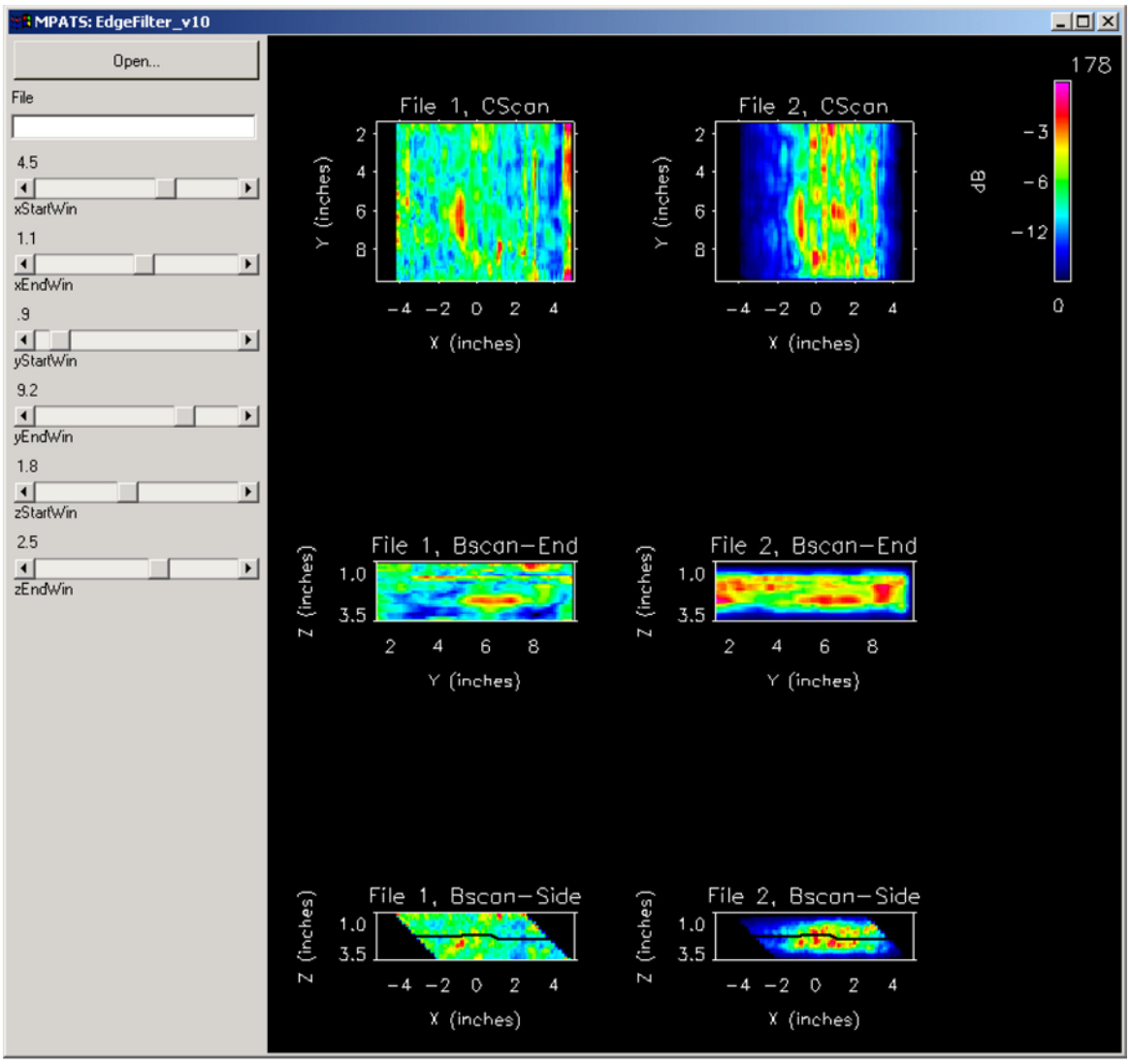

Figure A.5. B, C45 at 250 kHz

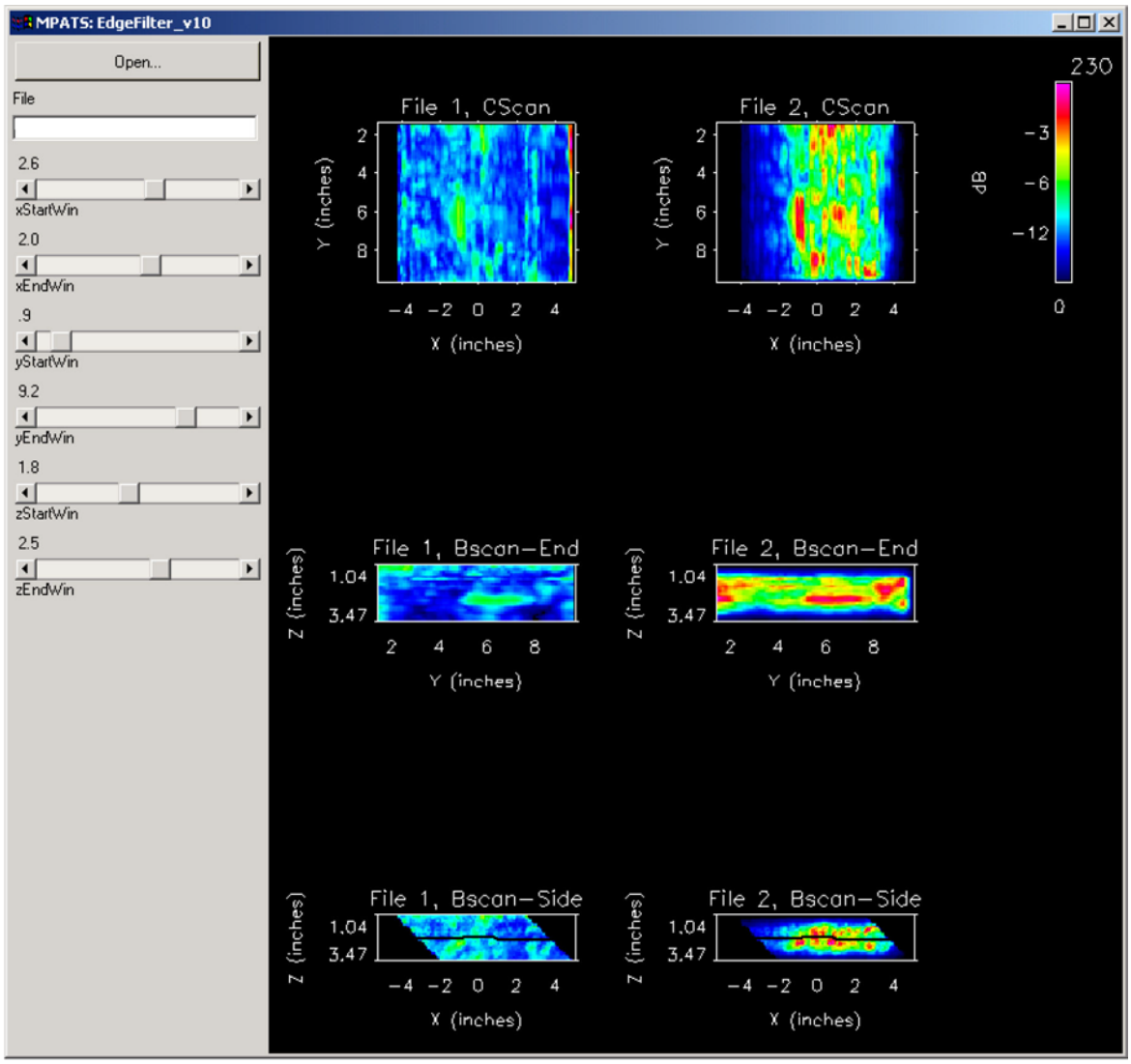

Figure A.6. B, C45 at 350 kHz

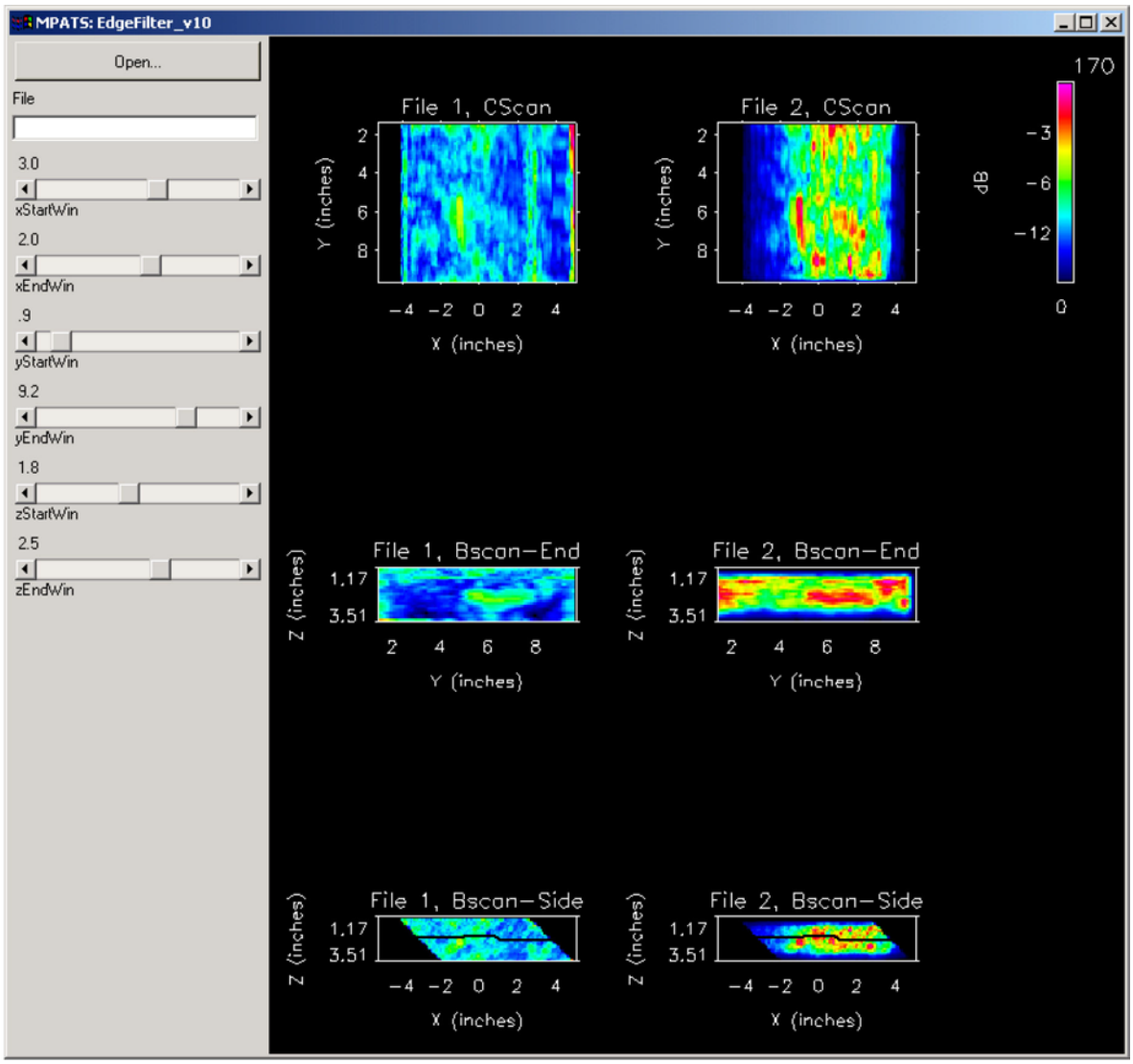

Figure A.7. B, C45 at 450 kHz

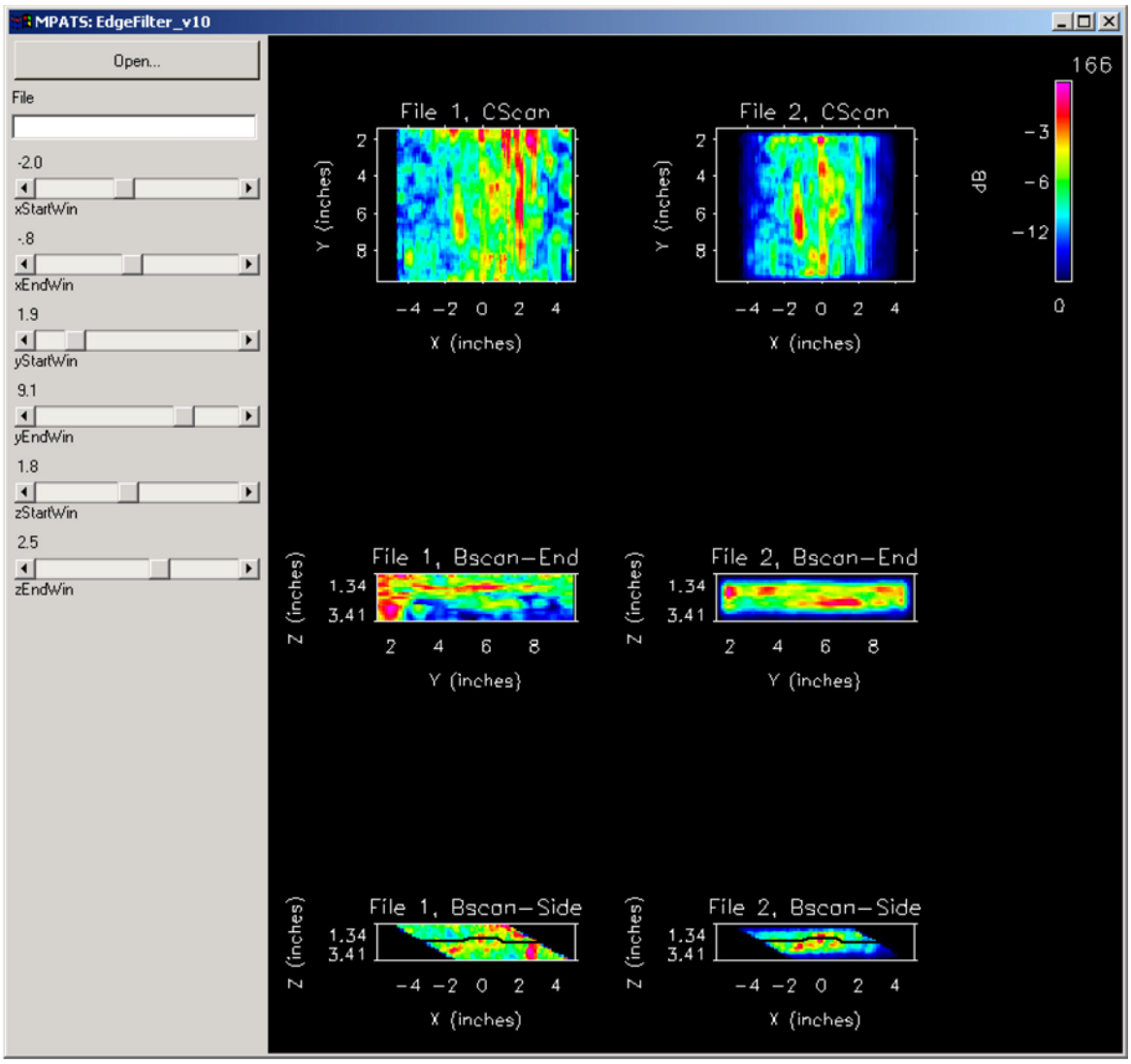

Figure A.8. B, C60 at 250 kHz

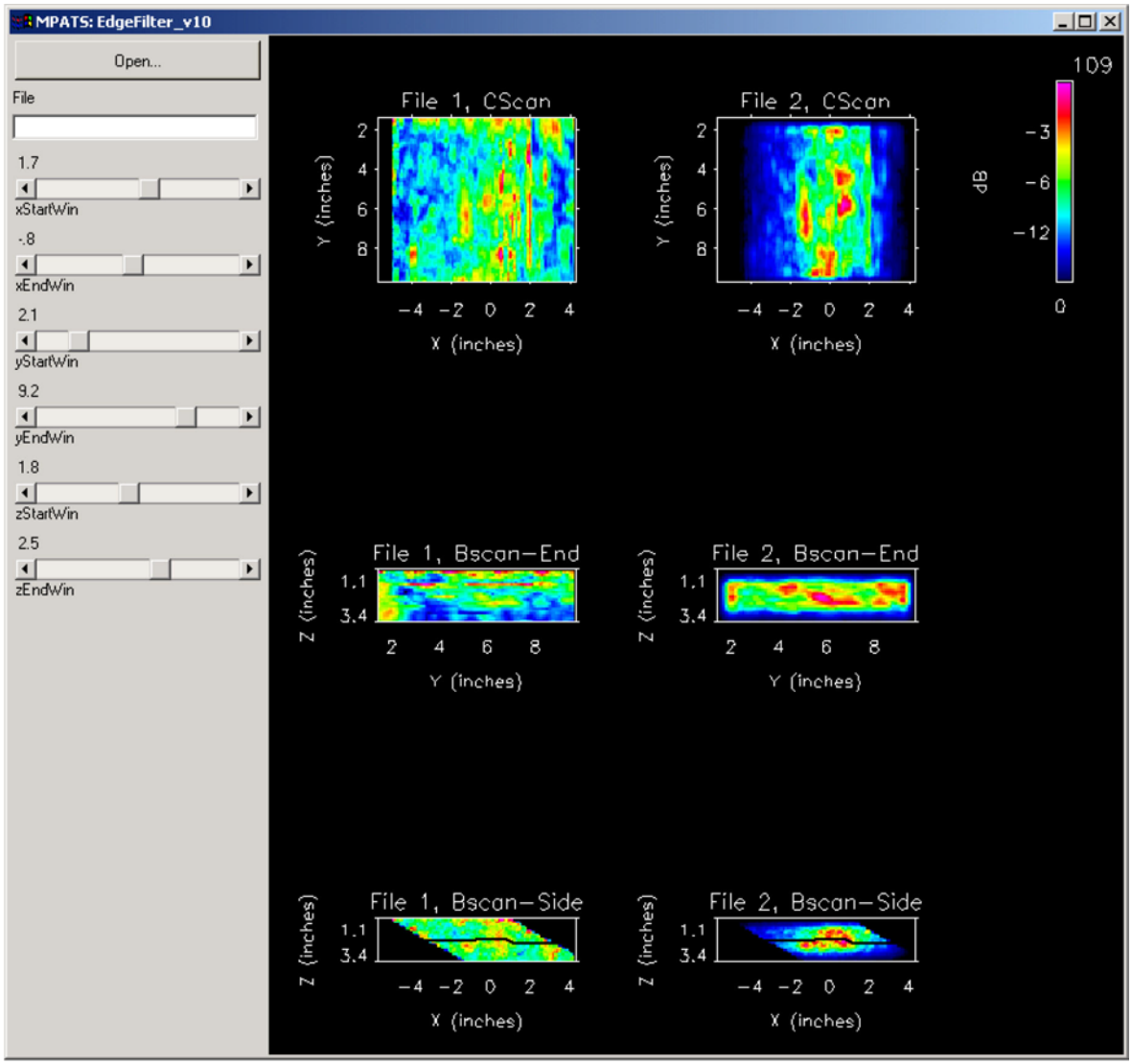

Figure A.9. B, C60 at 350 kHz

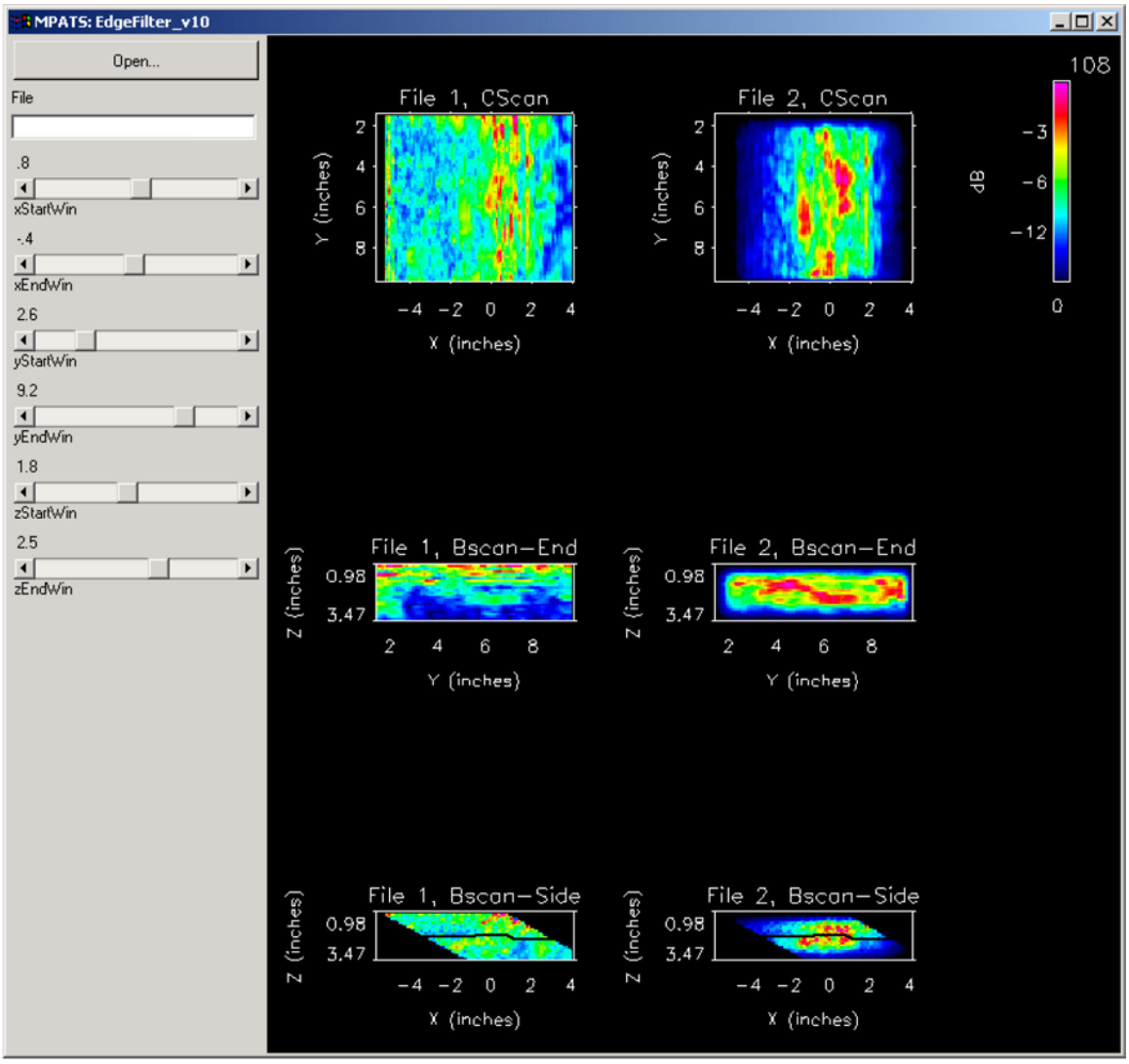

Figure A.10. B, C60 at 450 kHz

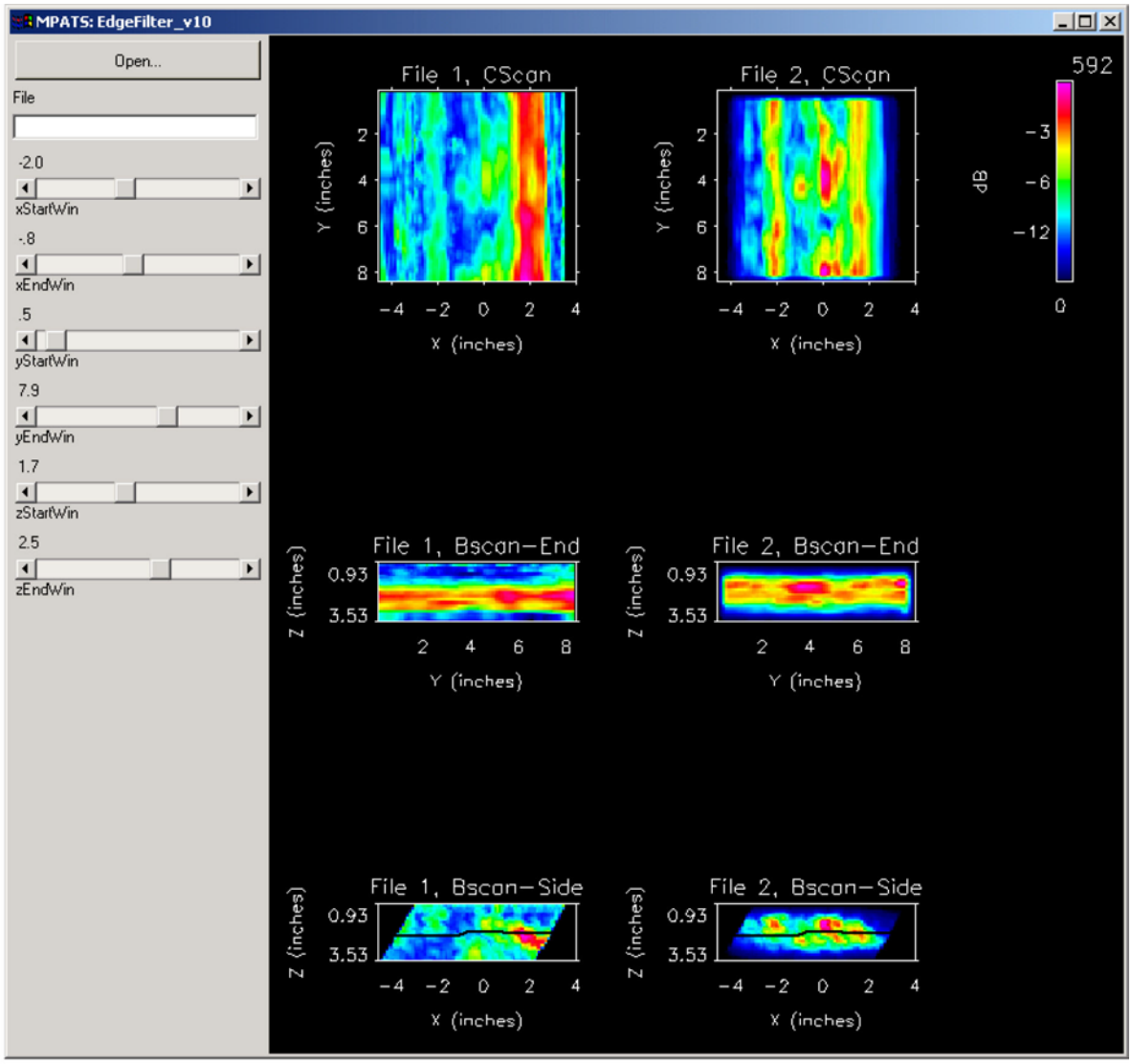

Figure A.11. B, S30 at 250 kHz

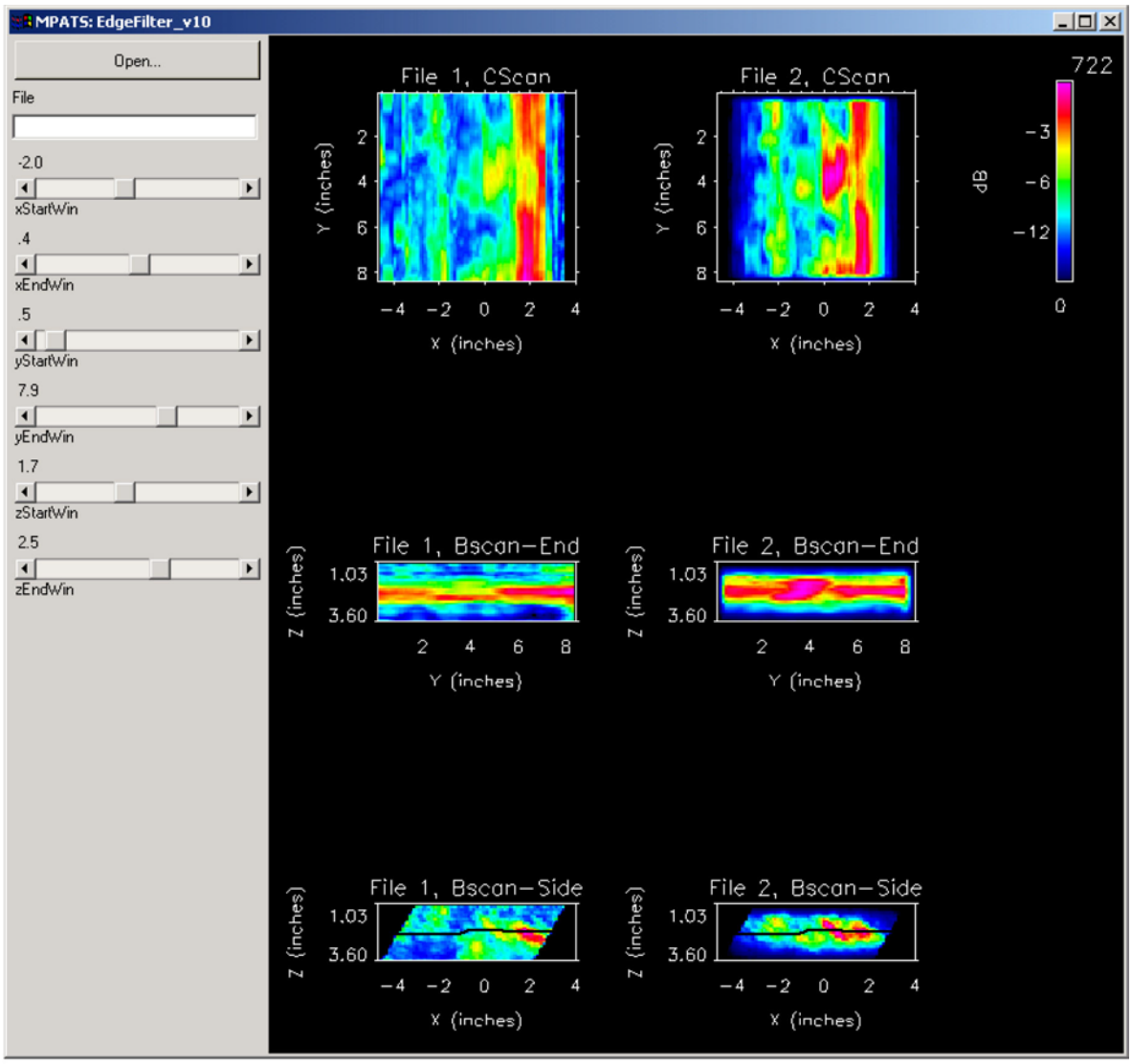

Figure A.12. B, S30 at 350 kHz

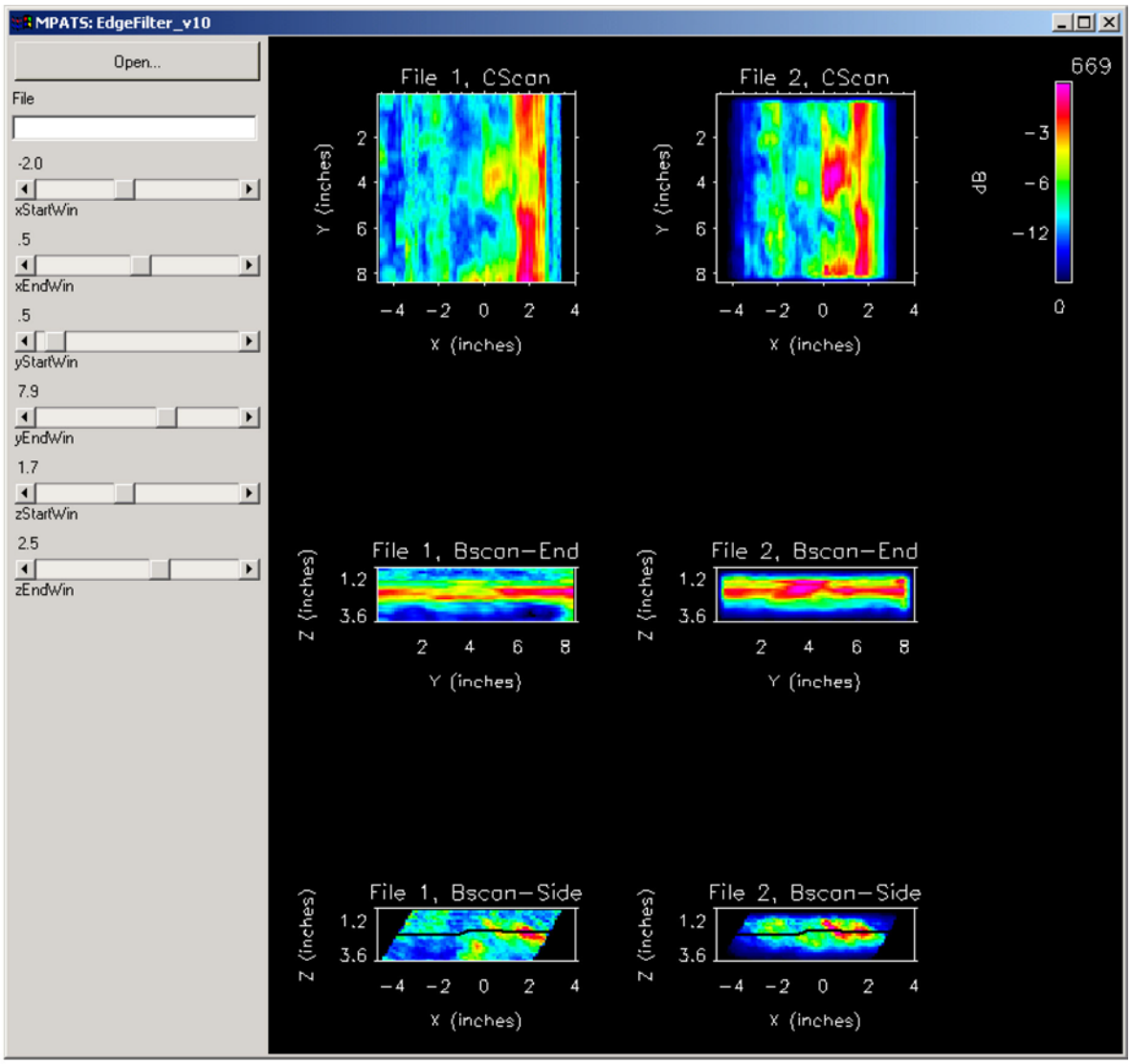

Figure A.13. B, S30 at 450 kHz

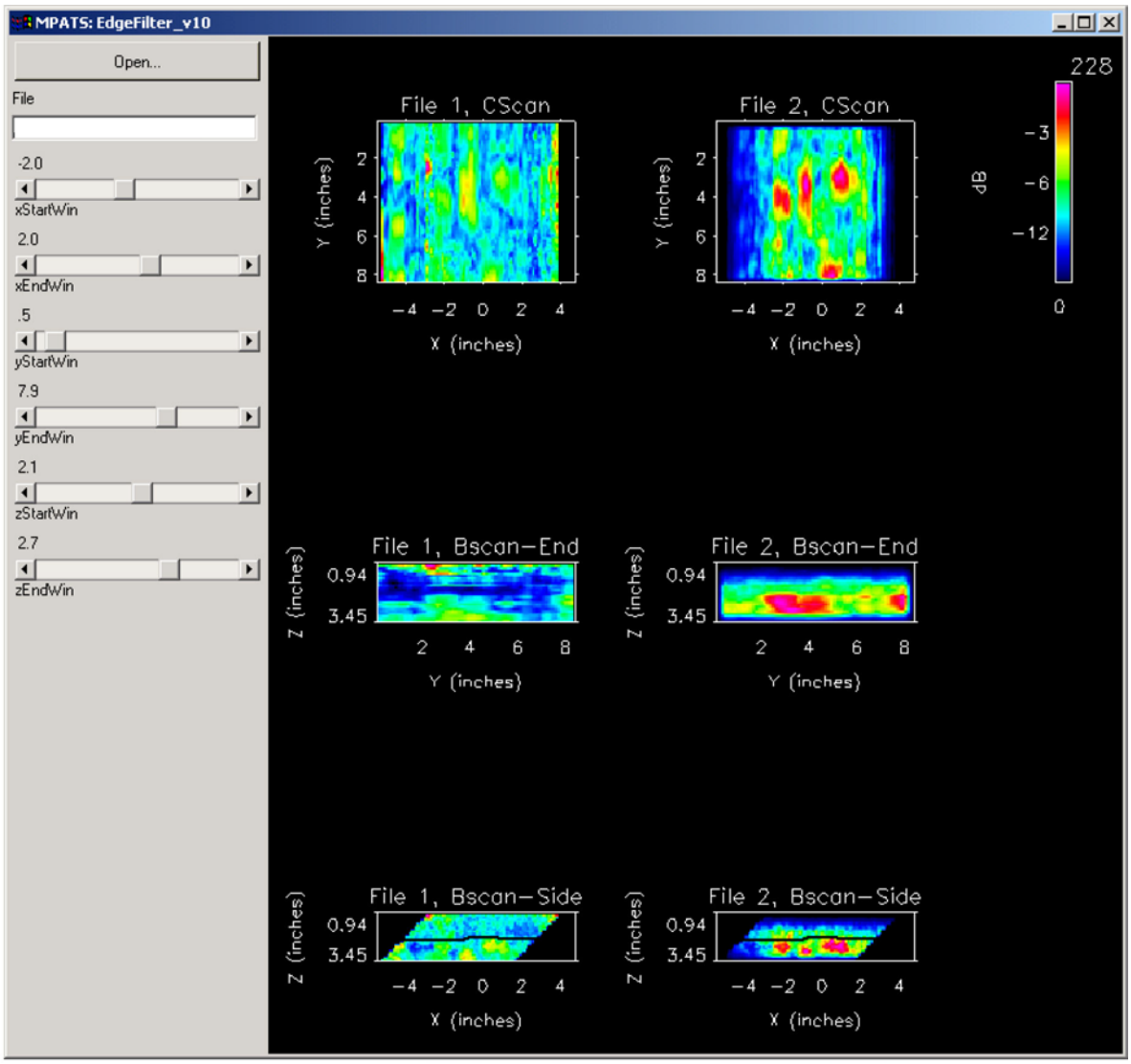

Figure A.14. B, S45 at 250 kHz

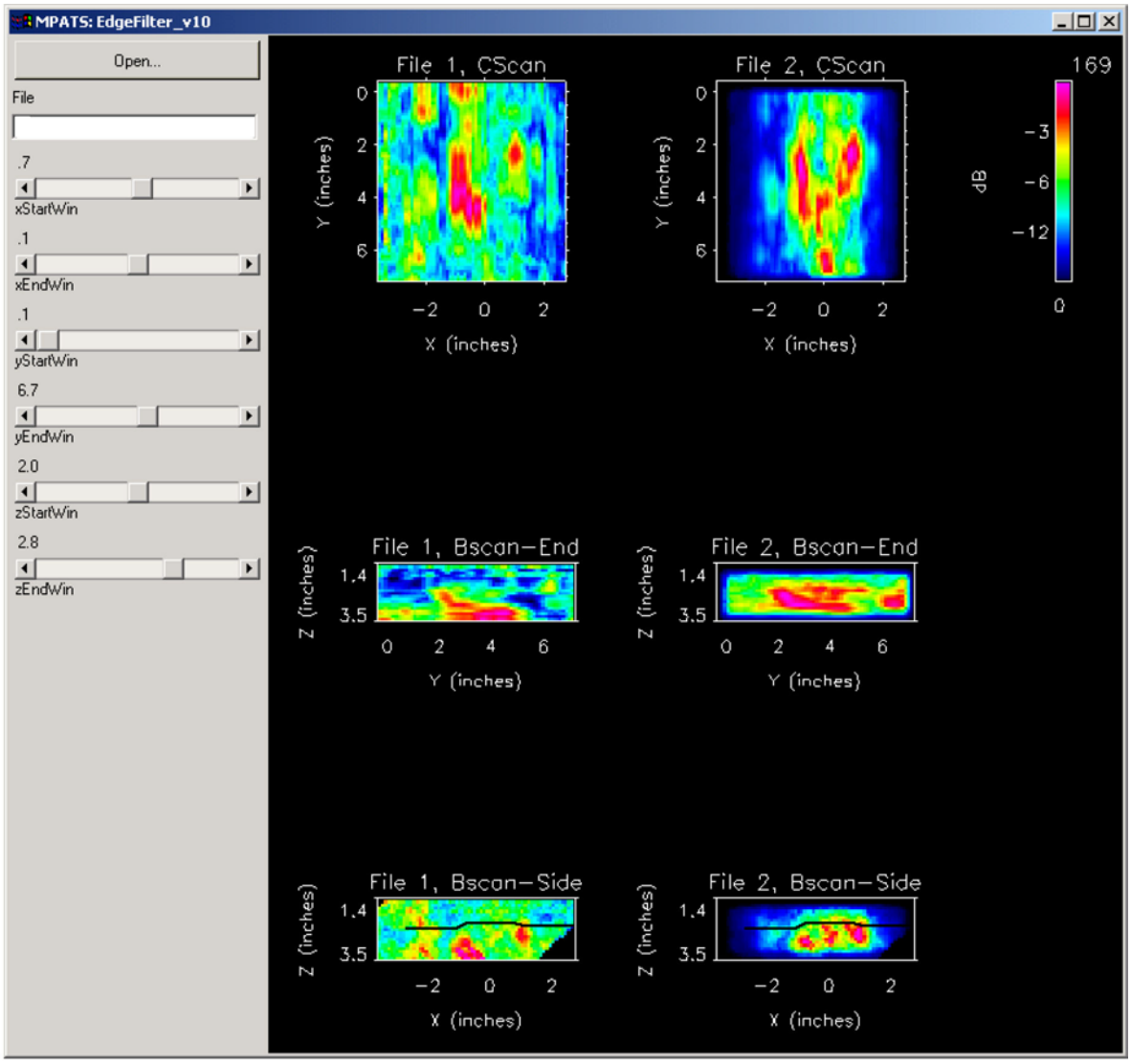

Figure A.15. B, S45 at 350 kHz

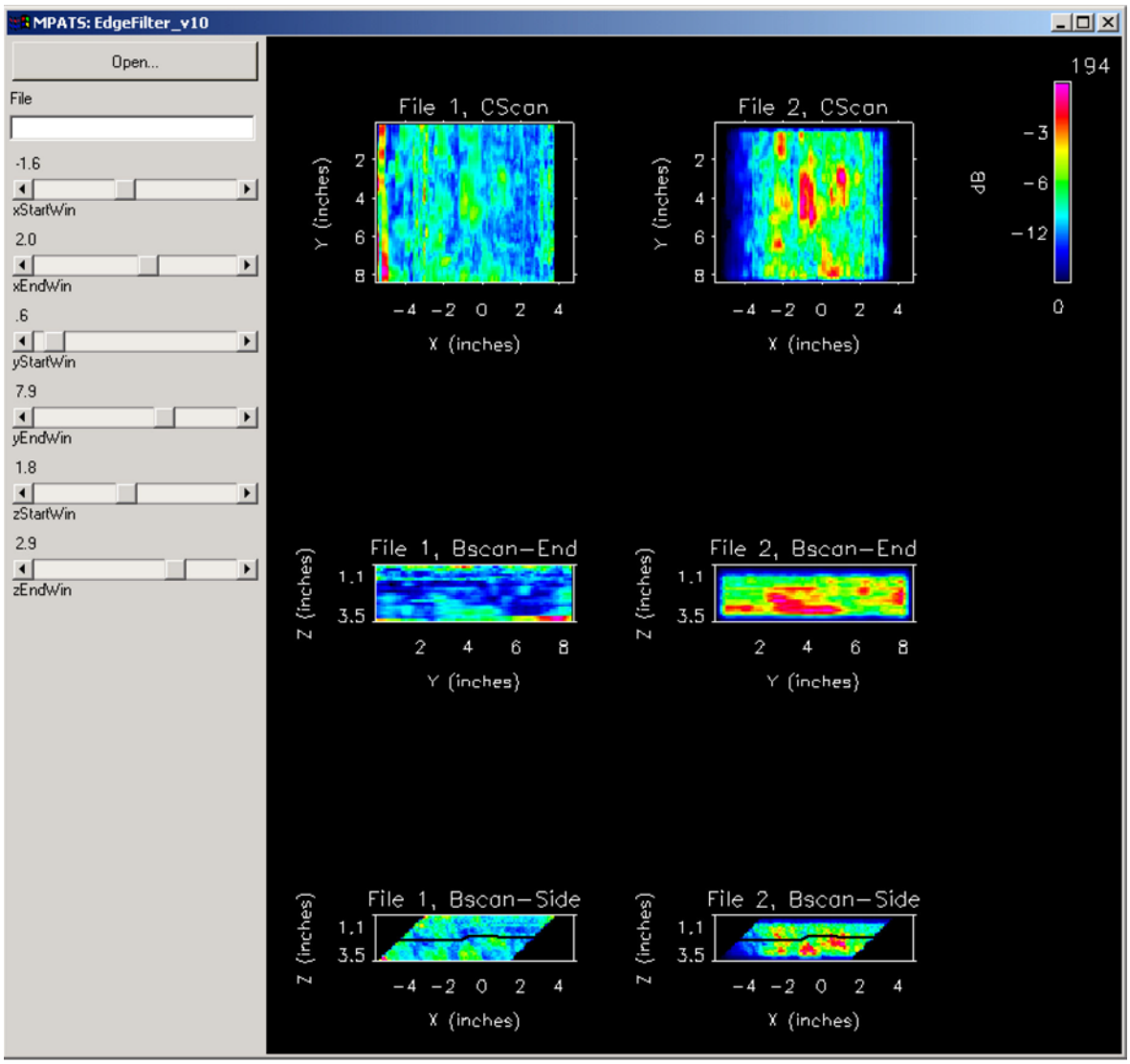

Figure A.16. B, S45 at 450 kHz

Appendix B

Data Fusion of Specimen B Inspections

Appendix B

Data Fusion of Specimen B Inspections

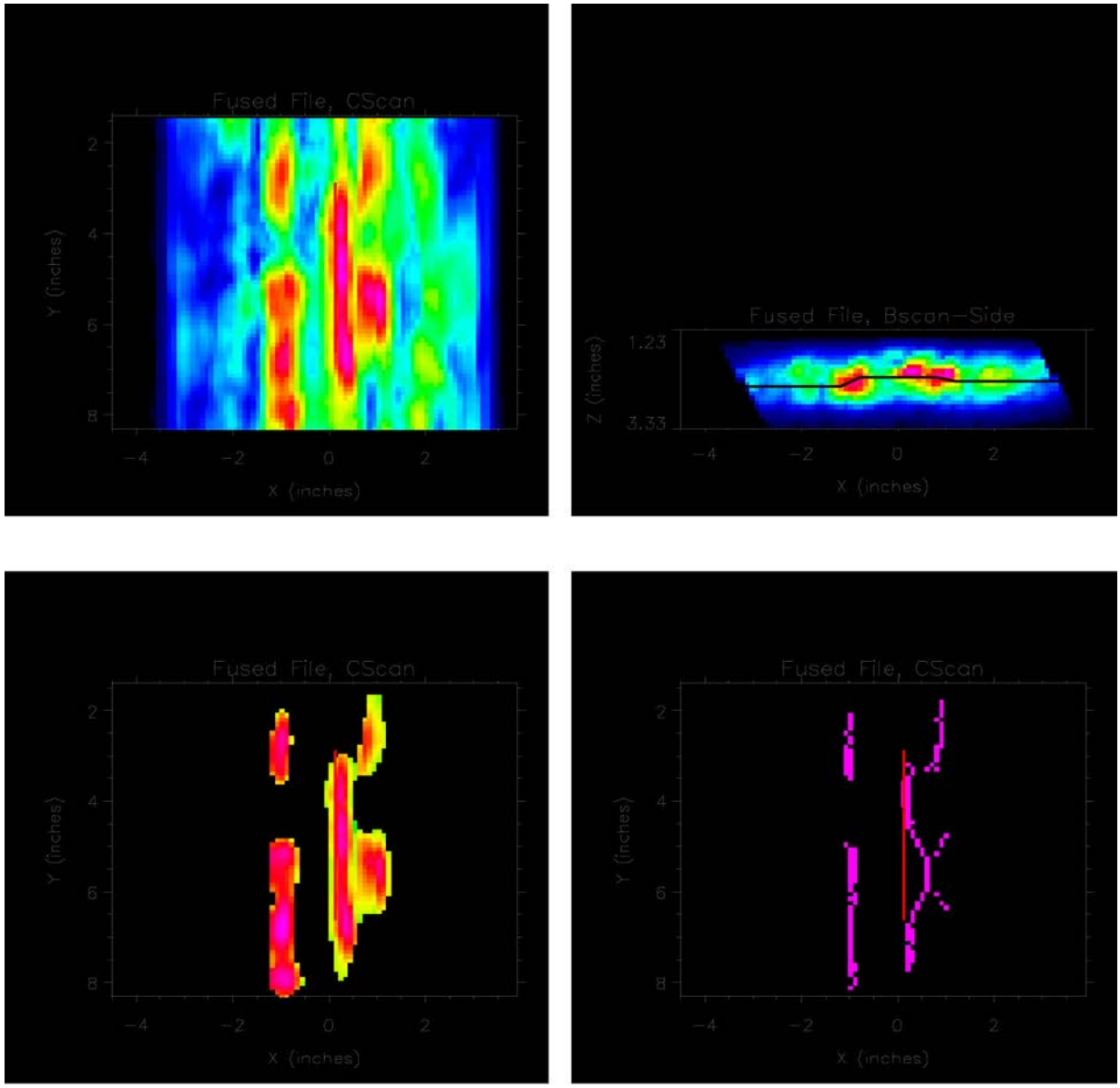

Figure B.1. B, C30 at 250 kHz

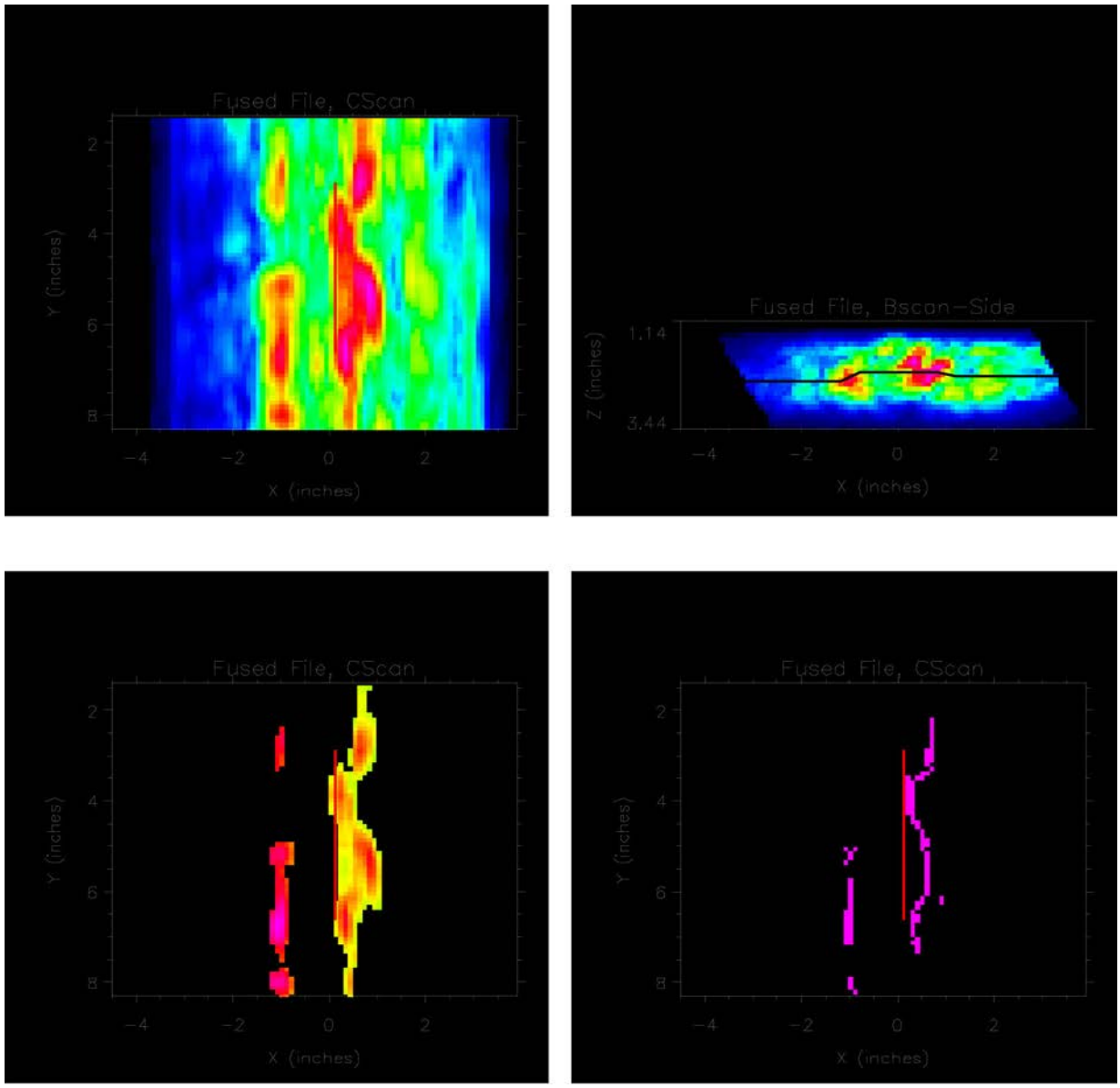

Figure B.2. B, C30 at 350 kHz

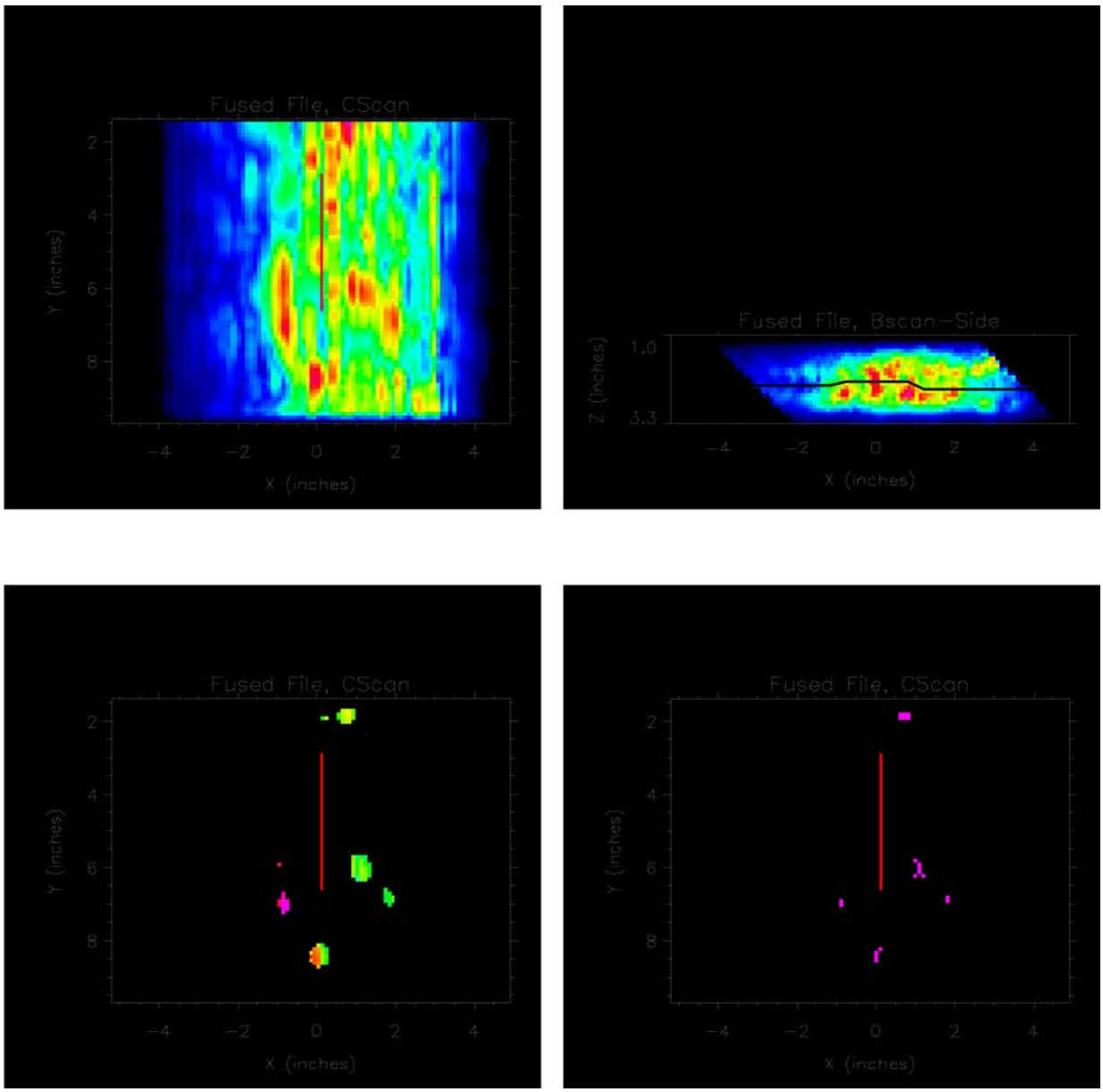

Figure B.3. B, C45 at 250 kHz

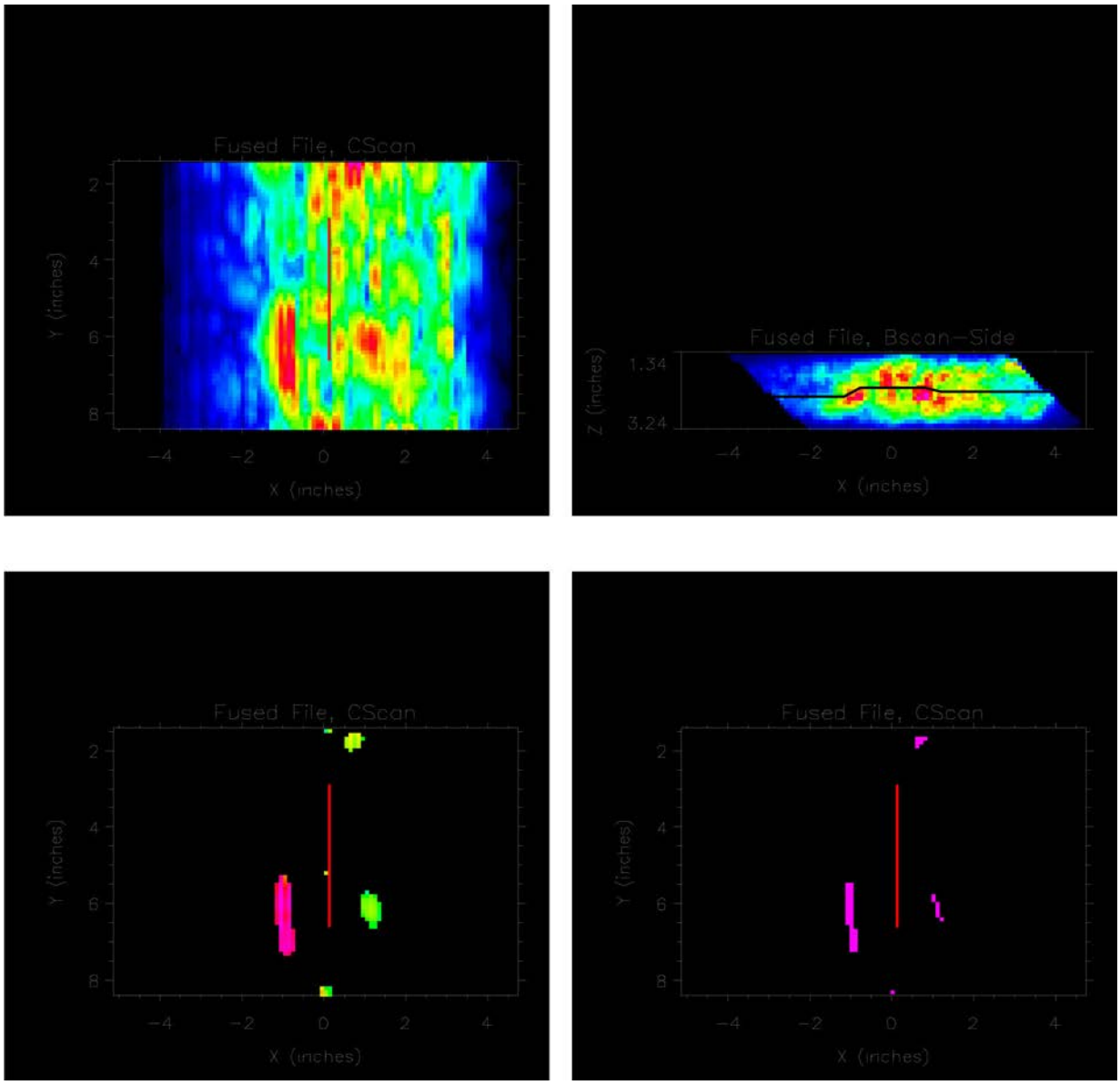

Figure B.4. B, C45 at 350 kHz

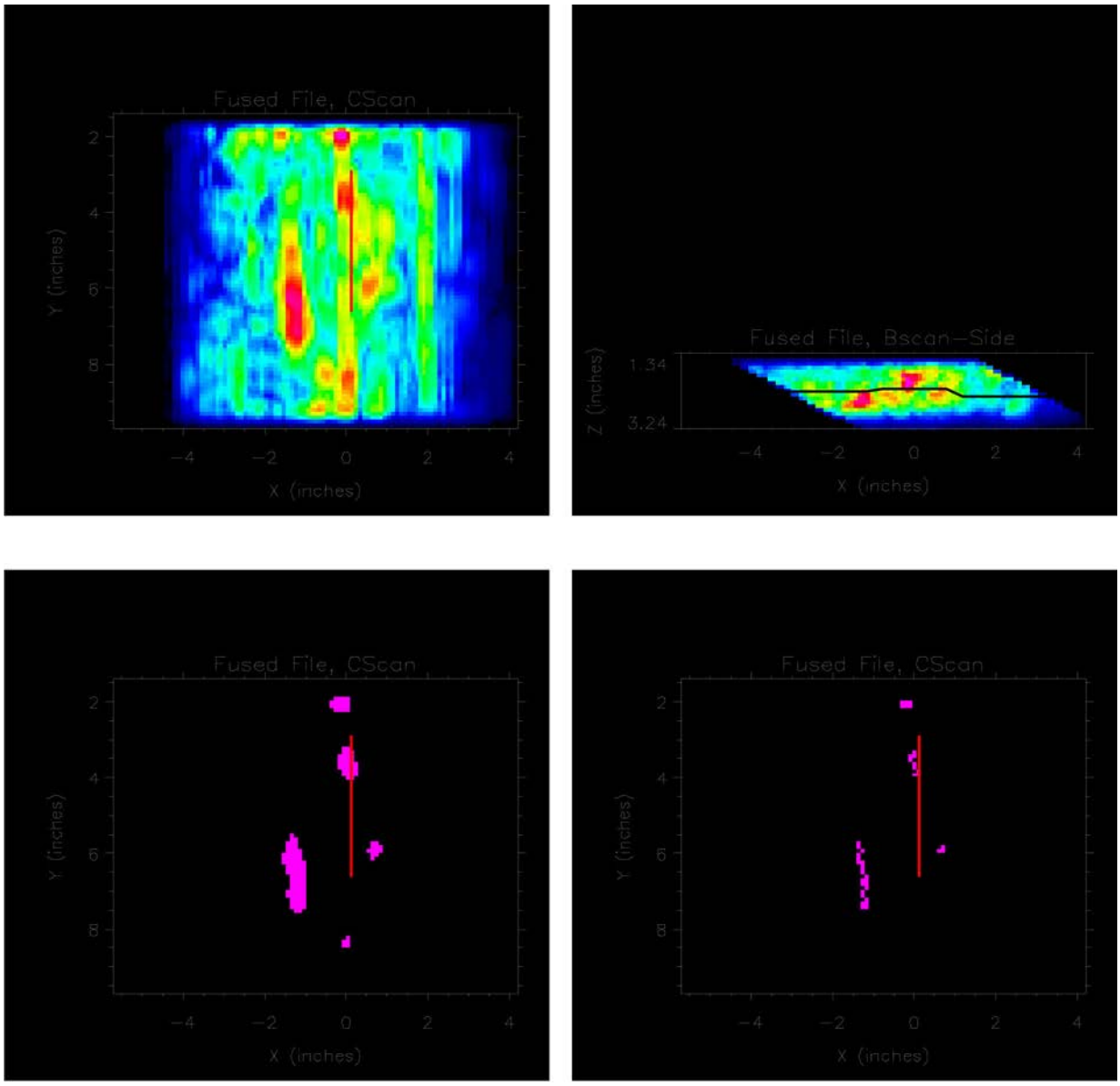

Figure B.5. B, C60 at 250 kHz

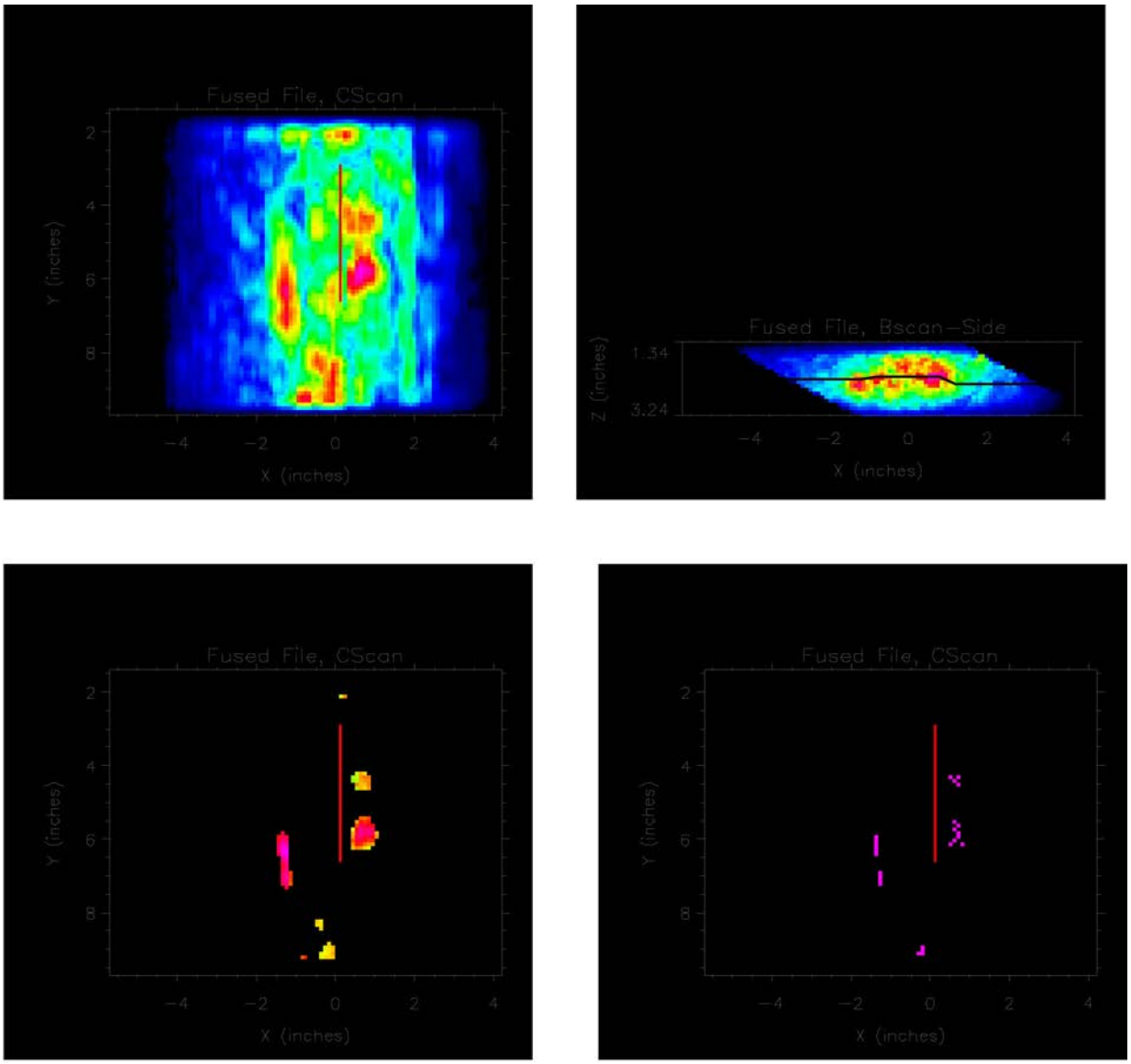

Figure B.6. B, C60 at 350 kHz

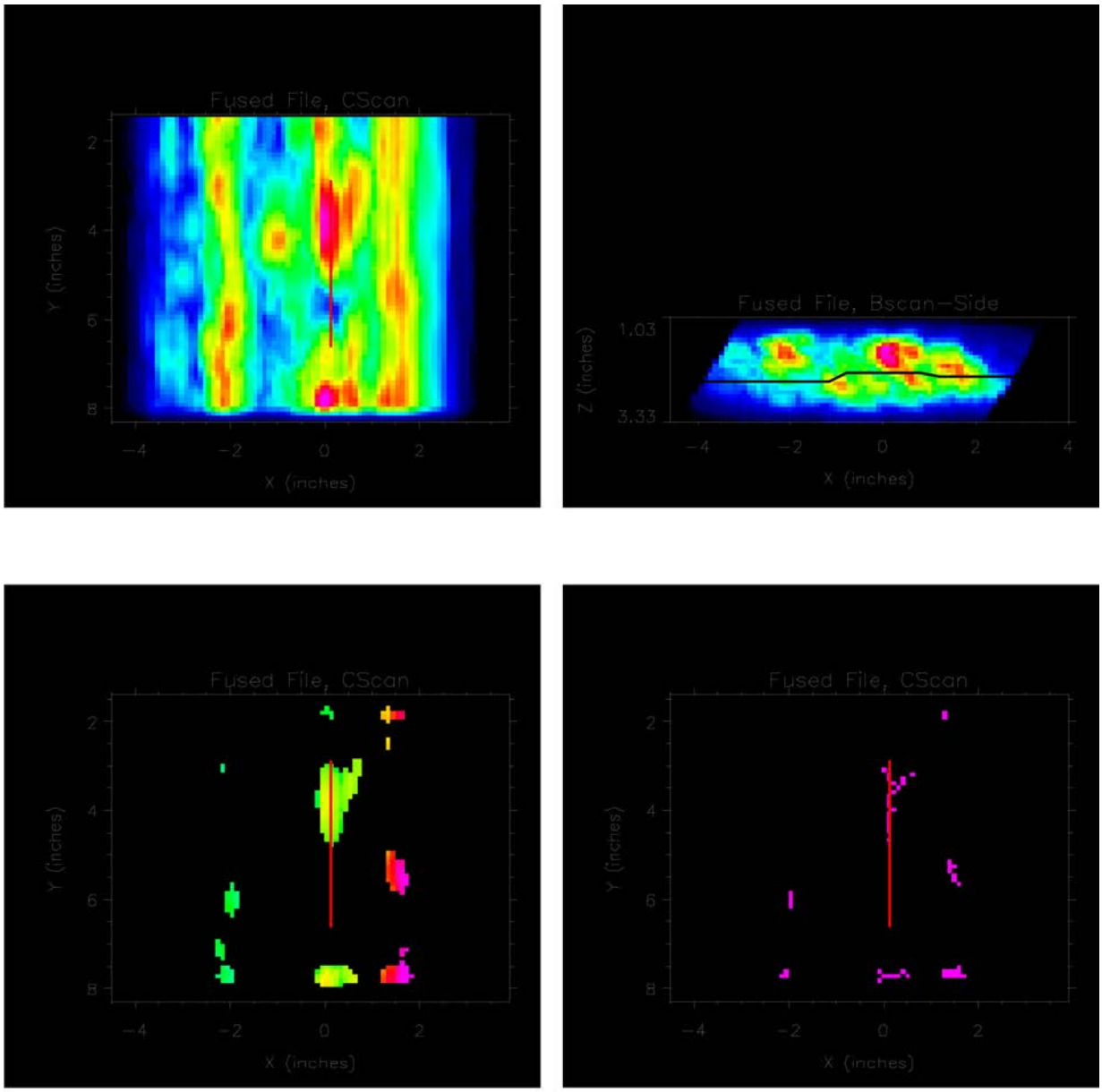

Figure B.7. B, S30 at 250 kHz

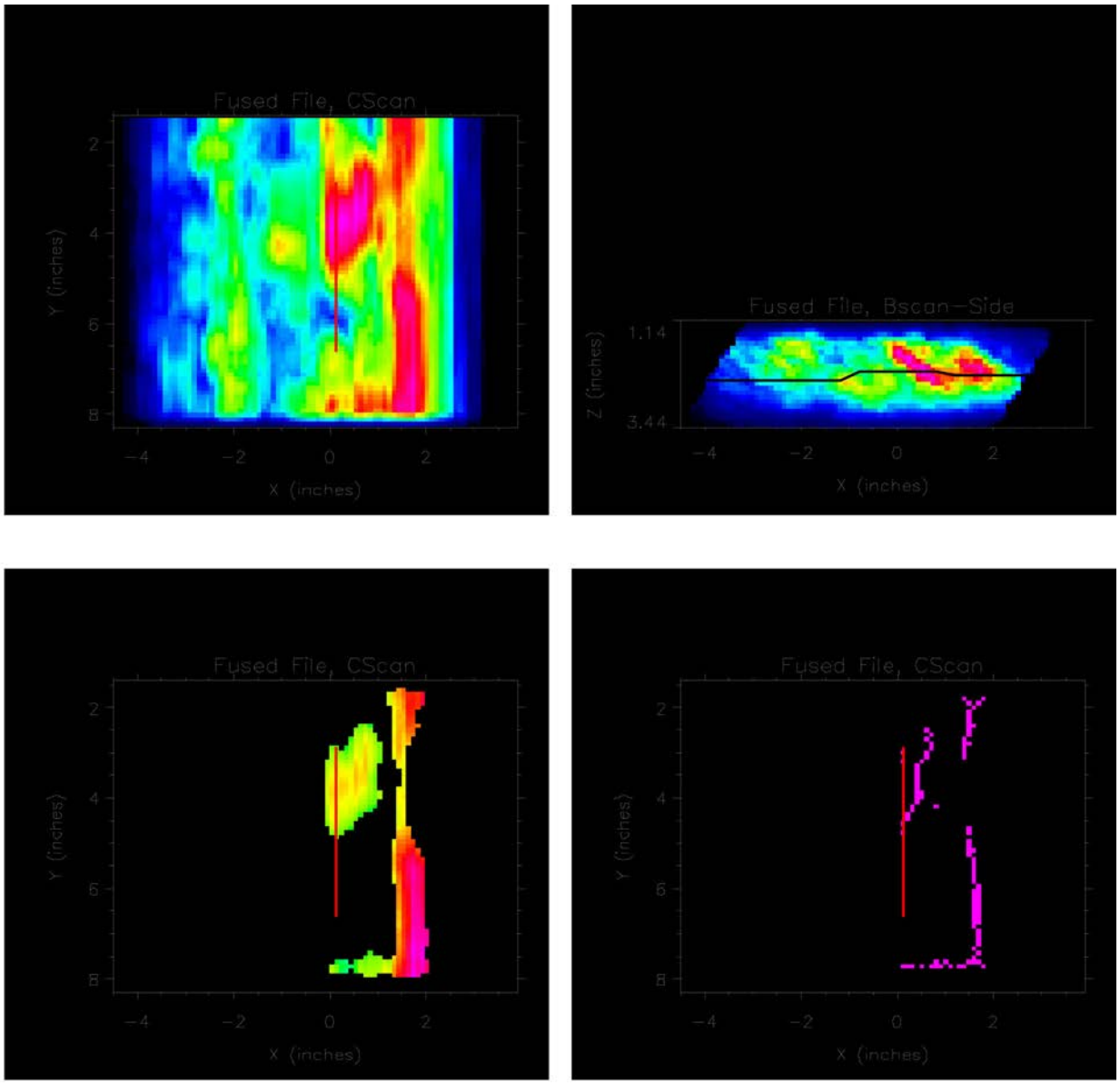

Figure B.8. B, S30 at 350 kHz

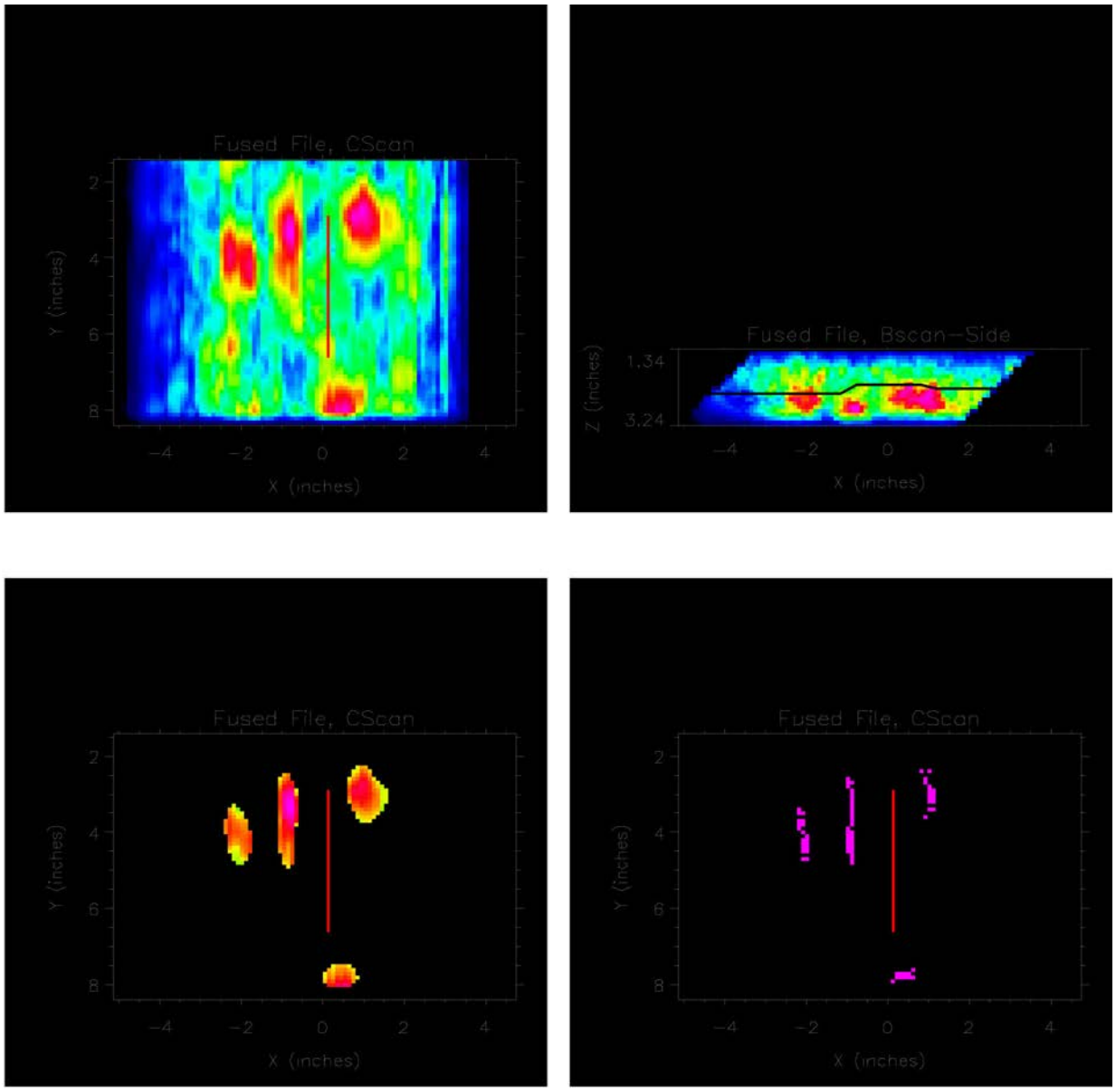

Figure B.9. B, S45 at 250 kHz with an X Offset (x' = x + 1 inch)

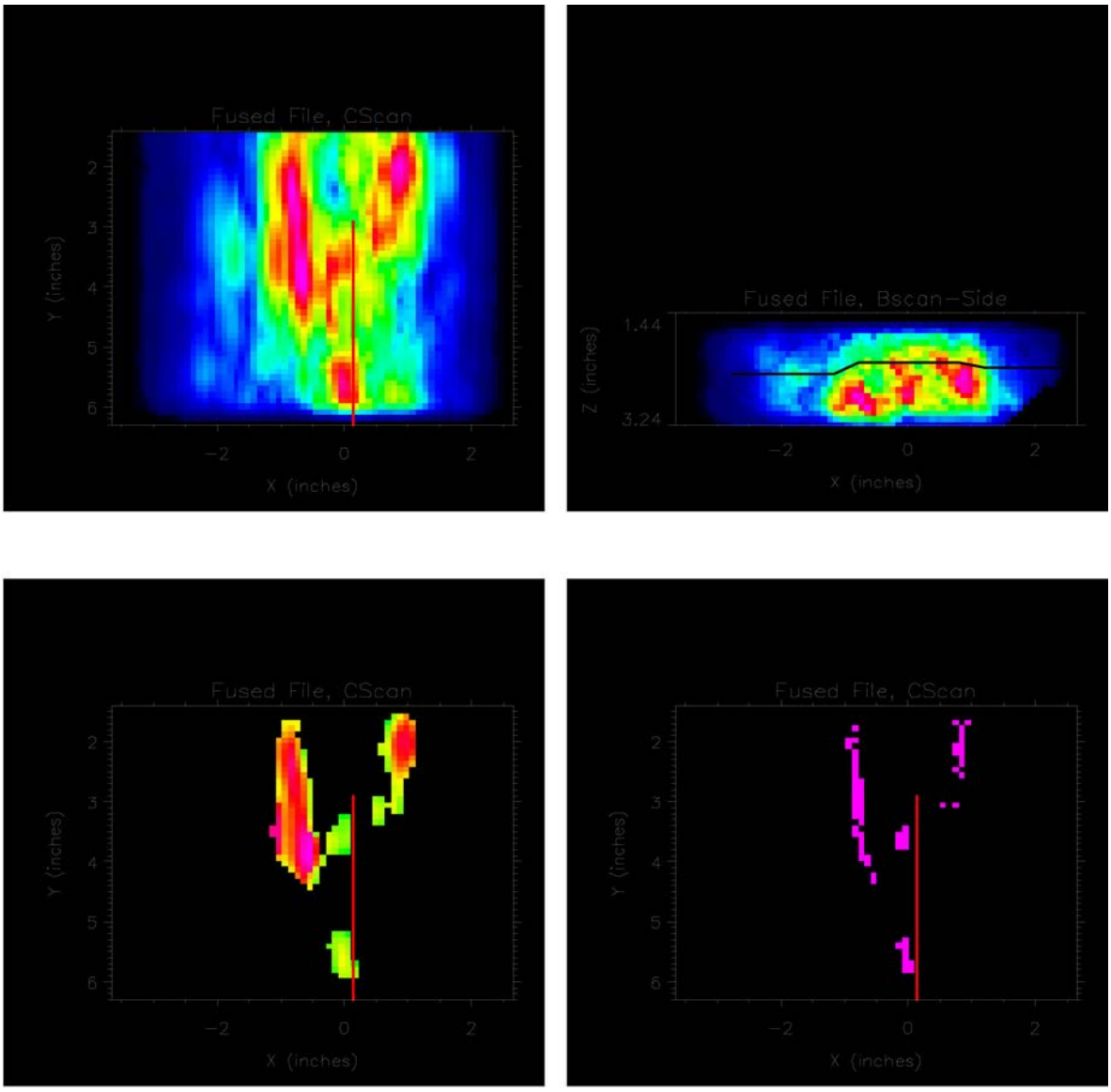

Figure B.10. B, S45 at 350 kHz with an X offset (x' = x + 1 inch)

Appendix C

Plots of Inspection Results for Specimens A, B, C, and D

Appendix C

Plots of Inspection Results for Specimens A, B, C, and D

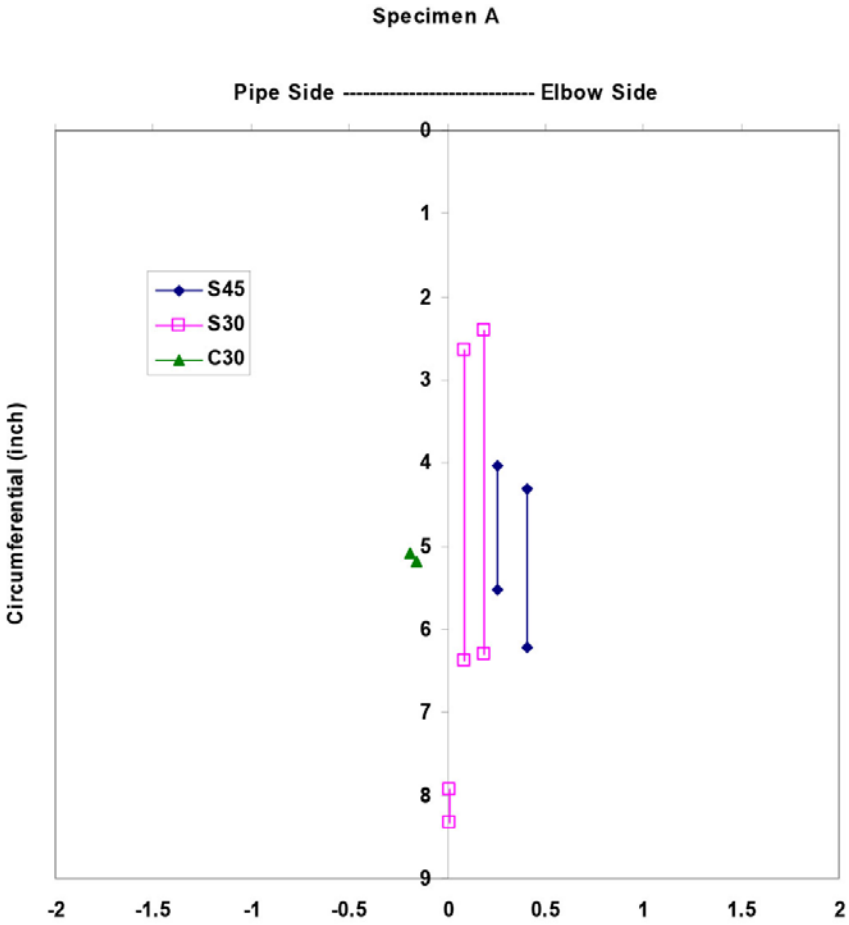

Figure C.1. Indications from Specimen A

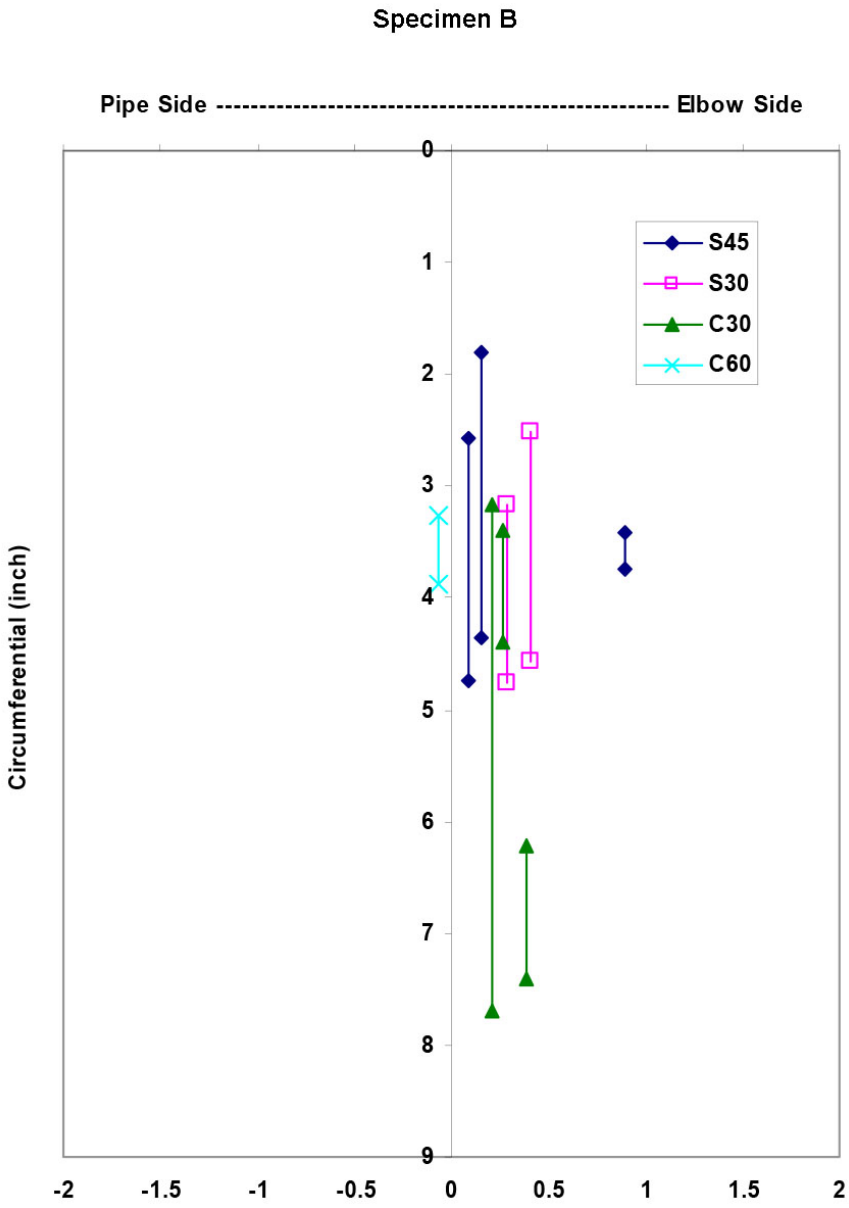

Figure C.2. Indications from Specimen B

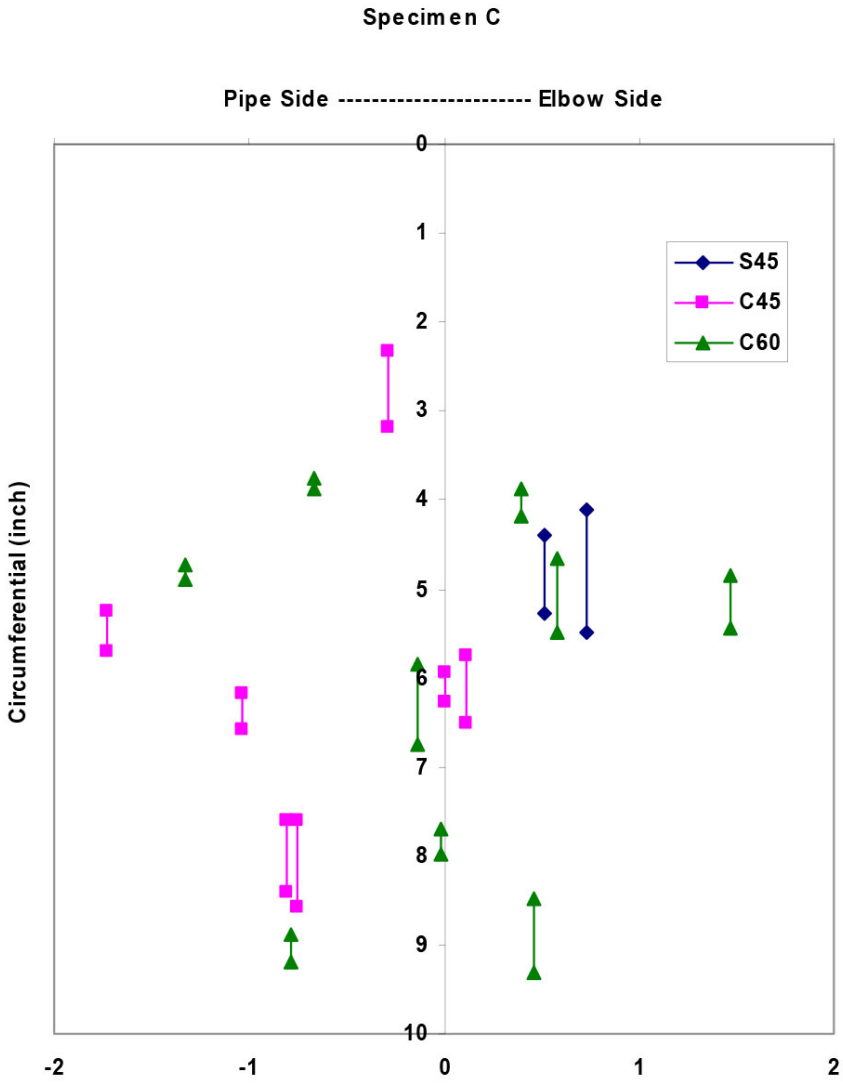

Figure C.3. Indications from Specimen C

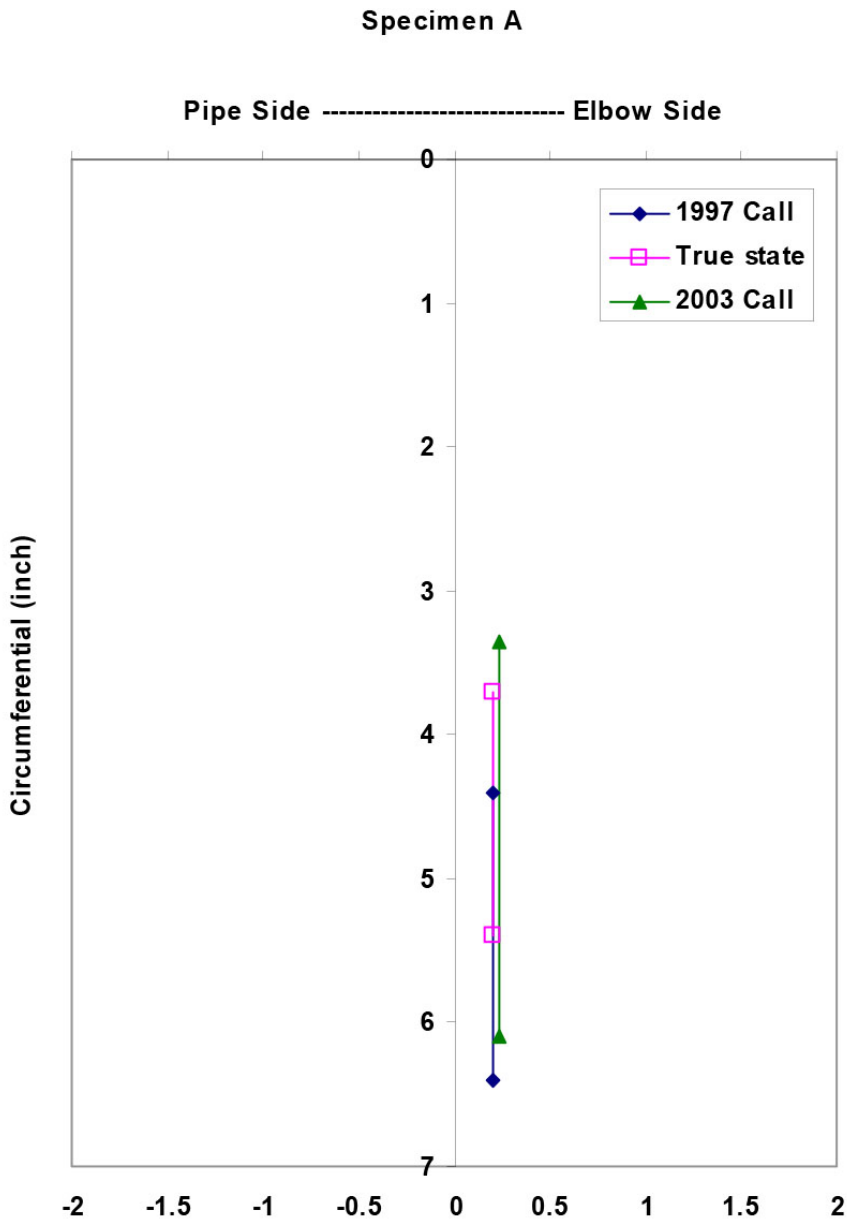

Figure C.4. True State from Specimen A Compared to the 1997 and 2003 Call

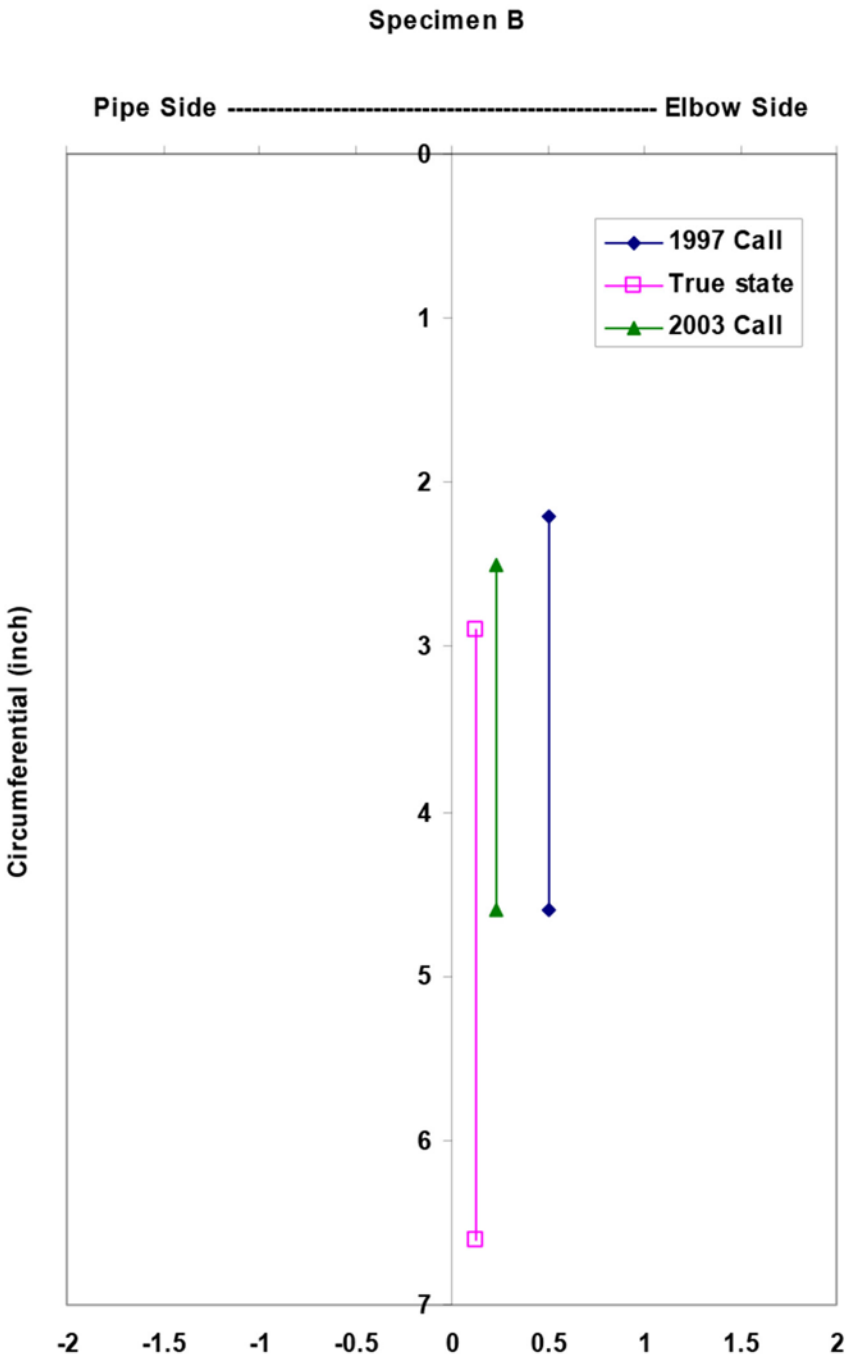

Figure C.5. True State from Specimen B Compared to the 1997 and 2003 Call

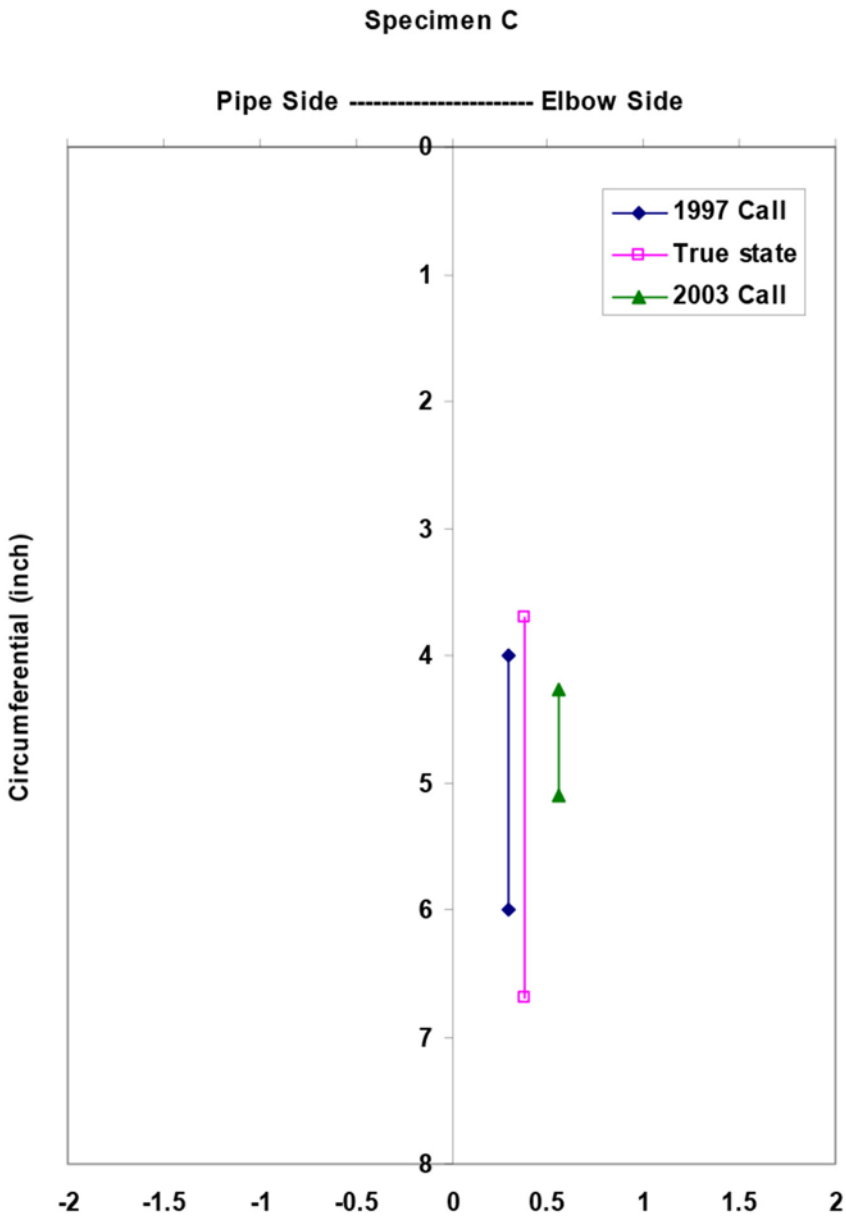

Figure C.6. True State from Specimen C Compared to the 1997 and 2003 Call

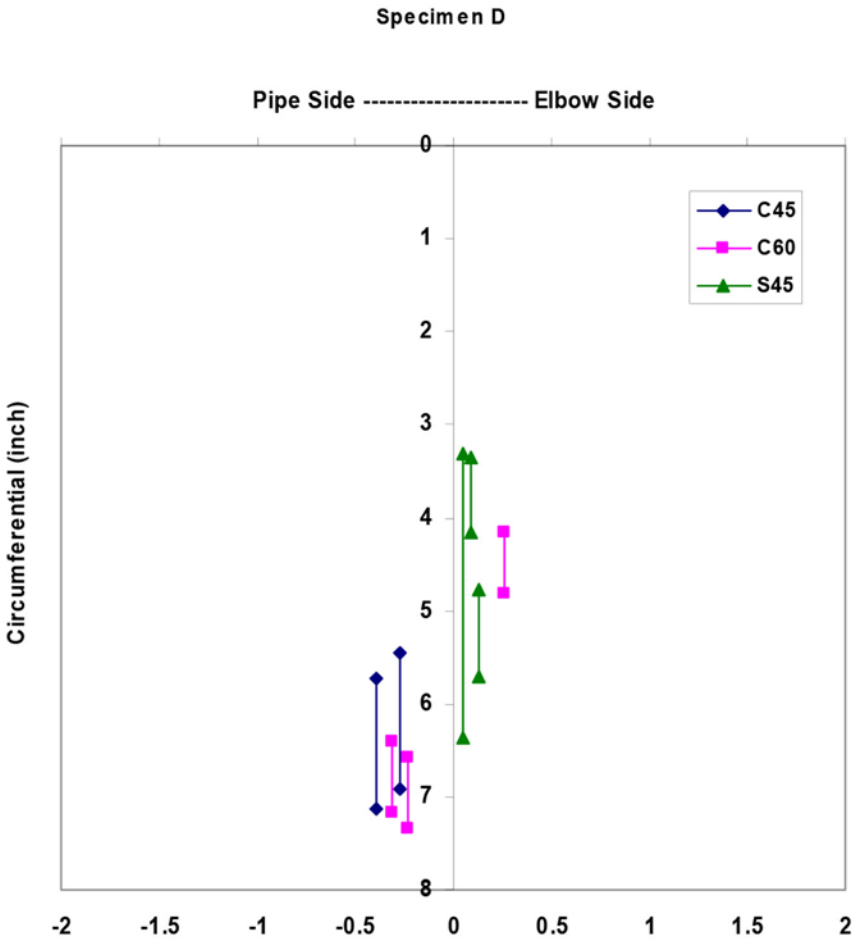

Figure C.7. Indications from Specimen D

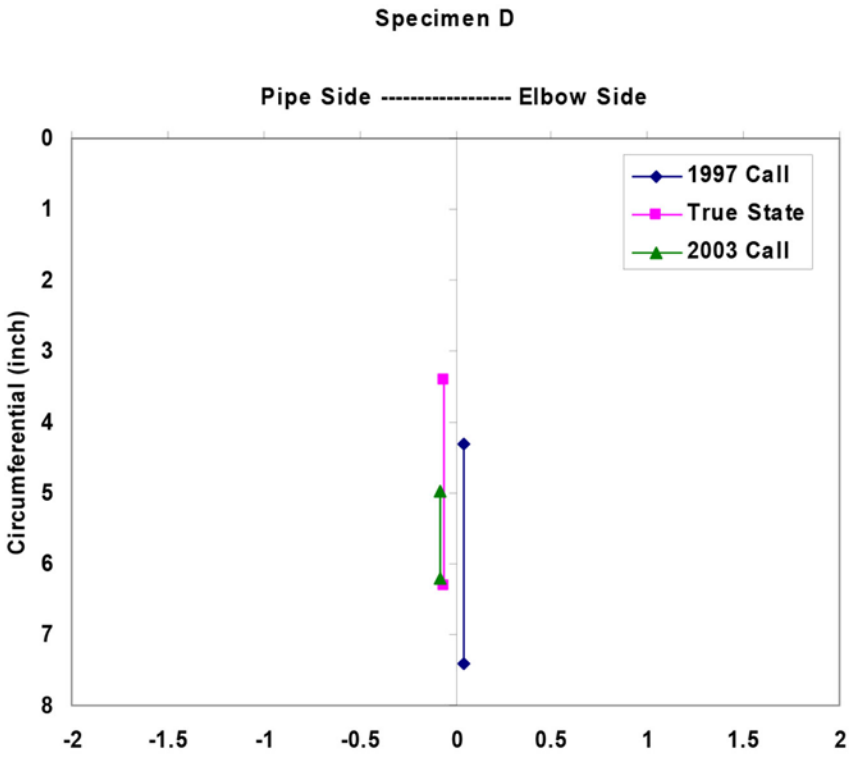

Figure C.8. True State from Specimen D Compared to the 1997 and 2003 Call